Brain morphometry of HIV-infected children on early antiretroviral therapy (ART) from age 5 to 9 years

By
Emmanuel. C. Nwosu

Thesis presented for the degree of Doctor of Philosophy in Biomedical Engineering

Faculty of Health Sciences
University of Cape Town

Date of Submission: November 2019
Supervisor: Dr. Frances Robertson
Co-supervisor: Professor Ernesta Meintjes

Declaration

I, EMMANUEL.C. NWOSU, hereby declare that the work on which this dissertation is based is my original work (except where acknowledgements indicate otherwise) and that neither the whole work nor any part of it has been, is being, or is to be submitted for another degree in this or any other university.

I authorise the University to reproduce for the purpose of research either the whole or any portion of the contents in any manner whatsoever.

Signature: Signed by candidate

Date: 19th November 2019

Dedication

This thesis is dedicated to the blessed memory of my Dad – Samuel Nwosu – who gave it all during his lifetime and opened doors of opportunities for the younger generation. You will forever be in our hearts.

Acknowledgement

Completing a piece of research project like this won't be possible without the generous support from a lot of people. First, I would like to thank Dr. Frances Robertson, my supervisor, for holding me by the hand and walking this journey with me while it lasted. Thank you for your support, guidance, insight and painstakingly giving positive critical feedback. Thanks to Professor Ernesta Meintjes, my co-supervisor, for the generous financial support and mentorship, guidance and painstakingly providing positive critical feedback in the course of the project. Thanks also to Dr. Martha Holmes for her generous input, providing resources and data, as well as being the third eye and giving feedback to some of the thesis chapters and manuscripts written for publication. Thanks to my PhD colleague, Steven Randall, for providing the initial expert training on manual segmentation of brain volume.

I also wish to appreciate the help of Dr. Barbara Laughton, Professor Mark Cotton and the entire team at the Family Clinical Research Unit (FAMCRU), Department of Paediatrics & Child Health, Tygerberg Children's Hospital and Faculty of Health Sciences, Stellenbosch University, for providing clinical, demographic and neuropsychological data for this study. I appreciate the valuable feedback provided for chapters in the thesis. A huge thanks to Professor Andre van der Kouwe and his research group at A.A. Martinos Centre for Biomedical Imaging, Department of Radiology, Massachusetts General Hospital, USA for providing useful technical support in processing participants MRI scans with FreeSurfer's longitudinal stream as well as troubleshooting most of the automated segmentation issues during this project. I am also grateful to the staff of Cape Universities Brain Imaging Centre (CUBIC) for performing the MRI scans of study participants. Thanks to the study participants from the Cape Town arm of the Children with HIV Early antiretroviral therapy (CHER) clinical trial and their caregivers for consenting to participate in this neuroimaging follow-up study. Thanks to the members of the UCT medical imaging research unit for being great friends and for all the various supports they provided me throughout the period of my PhD journey. A special thanks to the Writing Lab Team of the Faculty of Health Sciences, UCT led by Dr. Natashia Muna. Working with you and as a writing consultant helped tremendously in my development and in improving my academic writing skills. Thanks to the UCT Postgraduate Funding Office for providing me with seed funding for this research.

My undying gratitude goes to my family, my wife – Dr. Sinesipho Nwosu – for always understanding my passion for this work and being willing to make any sacrifice to support me. Your prayers, support, and genuine care did a lot. To my mum – Mrs. Mabel Nwosu – you gave us a chance to follow our hearts and pursue our ambitions. To my Siblings Amaka (Adanne), Ozioma (Ozy), Chisom (Som) and Uche (Uc) you made me realise that I can be a scientist and still have a life by balancing both well. Thanks to my Brother-in-law, Francis Okorie and my nieces, you made me know I can be part of a family outside the biological one. To the Professor Monica Jojo family, you gave me one gift that I will be eternally grateful for, because of that gift my life is complete.

Finally, Thanks to the Father unlimited – God – who because of Him, life is now meaningful. You have taken care of me in the most amazing way. I owe you everything.

Abstract

As of 2017, 1.8 – 2.1 million children vertically infected with HIV were living in sub-Saharan Africa, of whom an estimated 320, 000 were in South Africa. Since implementation of the prevention of mother to child transmission (PMTCT) strategy, the infection rate has been substantially reduced. More recently, the World Health Organisation's (WHO) recommendation of early antiretroviral therapy (ART) initiation for children with perinatal HIV infection has considerably decreased the immediate effects of perinatal HIV infection, including mortality and morbidity. Despite this, not much is known about the long-term outcome of continued ART on early-treated, perinatally HIV-infected children.

Early HIV invasion of the developing brain is associated with neurodevelopmental delays and neurocognitive deficits including encephalopathy, slower processing speed, language impairment, lack of concentration and attentiveness, and psychomotor slowing. Alterations in the neurodevelopmental trajectories of brain morphology, including cortical thickness and folding (gyrification) and sub-cortical volumes may be related to the observed neurocognitive deficits during a critical period of brain development spanning from mid-childhood into early adolescence (age 5 -13 years). The effects may be studied using structural magnetic resonance imaging (MRI) and automated segmentation software. FreeSurfer (https://surfer.nmr.mgh.harvard.edu/) is a valuable tool for investigating brain morphology but was not originally designed for segmenting pediatric brains. In this study we therefore first validate the latest FreeSurfer version 6.0.0 against manual segmentation for the study of pediatric HIV. We then assessed the long-term effects of perinatal HIV infection, early ART initiation as well as clinically designed ART interruption, HIV-related encephalopathy, disease severity at ART initiation and immune health measures on the developmental trajectories of cortical thickness and folding (gyrification) over the period from 5-9 years.

Study participants were 141 children (75 HIV+, 66 uninfected controls; 72 male) from the Cape Town arm of the children with HIV early antiretroviral therapy (CHER) clinical trial. HIV+ children were randomized at age 6 -12 weeks to receive either immediate limited ART for 40 or 96 weeks, to be restarted when clinical and/or immunological criteria were met, or to start ART only when they developed HIV symptoms or CD4 percentage dropped below 20% (25% in the first year) as per guidelines at the time. Uninfected controls comprised children born to HIV+ mothers (HIV-exposed uninfected (HEU)) or uninfected mothers (HIV-unexposed (HU)) and were recruited from an interlinking vaccine trial. MRI scans were performed at time points around their 5th, 7th and 9th birthdays, in accordance with protocols approved by the human research ethics committees of the Universities of Stellenbosch and Cape Town and voluntary informed consent was received from either participants or their guardians.

Both automated and manual methods were used to segment brain regions from high-resolution structural MRI scans. In addition, FreeSurfer was used to examine cross-sectional differences in cortical thickness and gyrification over the cortical surface at age 5. Linear mixed-effects models were used in conjunction with FreeSurfer's longitudinal processing stream to calculate and compare the annual rate of change in cortical thickness and gyrification between ages 5 and 9 in HIV+ children and controls.

Results showed that automated FreeSurfer segmentation tended to overestimate volumes of all structures relative to manual segmentation, except the left caudate nucleus. Consistency and agreement between methods were highest for the putamen (Consistency: right ICC=0.89, left ICC=0.90; agreement: right ICC=0.84, left ICC=0.83) and lowest for the corpus callosum (consistency ICC=0.64, agreement ICC=0.26). There were no subcortical volume differences between HIV+ children and controls, except the globus pallidus which was smaller in HIV+ children using both manual and automated segmentation.

Subsequent cross-sectional FreeSurfer analyses showed widespread regional increases in cortical thickness and decreases in gyrification at age 5 years, related to the effects of perinatal HIV-infection and early ART initiation. Clinically designed interruption led to thicker cortex in the left rostral middle frontal and right insula regions and, lower left precuneus and right superior frontal, as well as higher lateral occipital gyrification compared to HIV- controls. There were significant regional differences due to HIV severity based on CDC classification and viral burden at enrolment both in cortical thickness and gyrification compared to controls. Cortical thickness was not associated with immune health parameters, while gyrification was negatively associated with immune health measures. However, the linear rate of change of cortical thickness and gyrification from age 5 to 9 in the HIV+ children was not different from that of uninfected controls, nor was it different between controls and children on interrupted or continuous ART. Children with HIV-related encephalopathy showed a decrease in gyrification with age during this period, in contrast to controls who showed stable gyrification except in frontal regions where gyrification increased with age.

Children with perinatal HIV infection display alterations in cortical development due to ART interruption and disease severity at age 5 years, despite starting ART early in life. Our results suggest that cortical gyrification is more sensitive than cortical thickness to effects of perinatal HIV infection. ART interruption and disease severity at ART initiation affect cortical morphometry development at age 5 years in a perinatally infected, early-treated pediatric cohort. However, on continued ART the cortical developmental trajectory is no different from that of uninfected controls. Any structural defects resulting from ART interruption appear to normalise by age 9, except in children with HIV-related encephalopathy, who show an altered trajectory of gyrification development.

Table of Contents

List of Figures

Figure 4.2: Colour maps showing parameter estimates for group (ART-Interrupted or Continuous ART vs. HIV- controls) from vertex-wise regression of (a) cortical thickness (CT) and (b, c) local gyrification indices (LGIs), controlling for sex, age and ethnicity. Positive regression coefficients (red/yellow) indicate ART-Interrupted/Continuous ART > controls, and negative coefficients (cyan/blue) indicate ART-Interrupted/ Continuous ART < controls. The colour bar scale applies to both lateral (top) and medial (bottom) views. N=75 (21 ART-Interrupted, 25 Continuous ART, 29 HIV- controls). Results reported at a threshold of $p<0.05$, with a cluster size corrected threshold of $p<0.05$.

a) The left superior / rostral middle frontal region and right insula outlined in black show where ART-Interrupted children have thicker cortex compared to HIV- control children.

b) The left precuneus and right rostral and caudal anterior cingulate regions outlined in black show where ART-Interrupted children have lower gyrification compared to HIV- control children, while higher gyrification is observed in a right lateral occipital region (indicated with a white arrow).

c) The posterior right superior frontal and superior parietal lobule (indicated with a white arrow) regions outlined in black show where Continuous ART children have lower gyrification compared to HIV- control children, while higher gyrification is observed in the left fusiform, right rostral middle frontal / pars triangularis / pars orbitalis (indicated with a white arrow) and lateral occipital regions.

Figure 4.3: Colour maps of parameter estimates for group (CDC-mild or CDC-severe vs. HIV- controls) from vertex-wise regressions of (a, c) cortical thickness (CT) and (b, d) local gyrification indices (LGIs), controlling for sex, age at scan and ethnicity. Positive regression coefficients (red/yellow) indicate CDC-mild/CDC-severe > controls, and negative coefficients (cyan/blue) indicate CDC-mild/CDC-severe < controls. The colour bar scale applies to both lateral (top) and medial (bottom) views. N=73 (12 CDC-mild, 32 CDC-severe, 29 HIV- controls). Results reported at a threshold of $p<0.05$, with a cluster size corrected threshold of $p<0.05$.

a) The right medial frontal region outlined in black shows where CDC-mild children have thicker cortex compared to HIV- control children.

b) The left fronto-temporal-insular and inferior temporal, and right fusiform and lingual regions outlined in black show where CDC-mild children have higher gyrification compared to HIV- control children.

c) The left fusiform and right insula regions outlined in black show where CDC-severe children have thicker cortex compared to HIV- control children.

d) The right superior parietal lobule and fusiform regions outlined in black show where CDC-severe children have lower and higher gyrification, respectively, compared to HIV- control children.

Figure 4.4: Colour maps of parameter estimates for group (HVL or LVL vs. HIV- controls) from vertex-wise regressions of (a, c) cortical thickness (CT) and (b) local gyrification indices (LGIs), controlling for sex, age at scan and ethnicity. Positive regression coefficients (red/yellow) indicate HVL/LVL > controls, and negative coefficients (cyan/blue) indicate HVL/LVL < controls. The colour

bar scale applies to both lateral (top) and medial (bottom) views. N=73 (25 HVL, 21 LVL, 29 HIV- controls). Results reported at a threshold of $p<0.05$, with a cluster size corrected threshold of $p<0.05$.

a) The right caudal anterior cingulate/superior frontal region outlined in black shows where HVL children have thicker cortex compared to HIV- control children.

b) The right fusiform and postcentral regions outlined in black show where HVL children have higher gyrification compared to HIV- control children.

c) The left insula region extending into the inferior frontal gyrus and anterior portion of the superior temporal gyrus where LVL children have thicker cortex compared to HIV- control children.

Figure 4.5: (a) Colour map of regression coefficients for LGI at age 5 years on CD4 percentage at enrolment. Clusters outlined in black show the regions indicated in Table 4 where lower CD4 percentage was associated with greater LGI, after controlling for sex and age at scan.

(b - d) Plots of mean LGI at age 5 years as functions of CD4 percent at enrolment in the left fronto-parieto-temporal, superior parietal and rostral middle frontal regions.

Figure 5.1: Colour map of regression coefficients for a) cortical thickness and b) local gyrification indices (LGIs) showing rate of change through time points of age 5, 7 and 9 years in HIV-uninfected (HIV-) children controlling for sex. Positive regression coefficients (red/yellow) indicate increases with age, and negative coefficients (cyan/blue) indicate decreases with age. The colour bar scale in each figure applies to both lateral (top) and medial (bottom) views. (N = 66)

Figure 5.2: a) Plots of change with age (5 – 9 years) in cortical thickness and gyrification in regions where HIV+ differed from HIV- children in cross-sectional comparisons at ages 5 and 7 years respectively. b) Clusters outlined in black and shown with yellow arrow are regions where HIV+ differed from HIV- children in cross-sectional comparisons.

Figure 5.3: Colour map of regression coefficients for local gyrification indices (LGIs) showing differences in rate of change through time points of age 5, 7 and 9 years between HIV-uninfected children (HIV-) and children diagnosed with HIV-related encephalopathy (HIVE) controlling for sex. Positive regression coefficients (red/yellow) indicate HIV- children > HIVE children, and negative coefficients (cyan/blue) indicate HIV- children < HIVE children. The colour bar scale applies to both lateral (top) and medial (bottom) views. (HIV- = 66, HIVE = 12).

a) Bilateral rostral middle frontal regions where rate of change in gyrification differed between HIVE and HIV-. Left hemisphere regions outlined in blue are where the difference is significant at a threshold of $p<0.05$, with a cluster size corrected threshold of $p<0.05$

b) Plot showing the difference in rate of change (between age 5 and 9 years) in gyrification between HIVE and HIV- (left) and spaghetti plot of individual trajectories for rate of change with time (right) in the rostral middle frontal region.

List of Tables

List of Abbreviations

3TC – Lamivudine

A

ADC – AIDS dementia complex

AIDS – Acquired immune deficiency syndrome

ANI – Asymptotic neurocognitive impairment

ANCOVA – Analysis of covariance

ANOVA – Analysis of variance

ART – Antiretroviral therapy

ARV – Antiretroviral drugs

AVERT – AVERTing HIV and AIDS

AZT – Zidovudine

B

BBB – Blood brain barrier

C

CD4 – Cluster of differentiation 4 (a glycoprotein on the surface of immune cells)

CD8 – Cluster of differentiation 8 (a glycoprotein acting as a co-receptor for the T-cell receptor)

CHER – Children with HIV Early Anti-retroviral Therapy

CNS – Central nervous system

CSF – cerebrospinal fluid

D

DICOM - Digital Imaging and Communications in Medicine

DNA – Deoxyribonucleic acid

E

ELS – Early Life Stress

F

fMRI – functional MRI

FI – Fusion inhibitors

G

GUI – Graphic User Interface

H

HAART – Highly active antiretroviral therapy

HAD – HIV-associated dementia

HAND – HIV-associated neurocognitive disorder

HIV – Human immunodeficiency virus

HIVE – HIV-related encephalopathy

I

IQ – Intelligence quotient

ISTI – Integrase strand-transfer inhibitors

L

LGI – Local gyrification index

M

MEMPRAGE - Multiecho magnetisation prepared rapid gradient echo

MND – Mild neurocognitive disorder

MPRAGE - Magnetisation prepared rapid gradient echo

MRI – Magnetic resonance imaging

MTCT – Mother-to-child transmission

N

NMR – Nuclear magnetic resonance

NRTI – Nucleoside reverse transcriptase inhibitor

NNRTI – Non-nucleoside reverse transcriptase inhibitors

P

PHE – Progressive HIV encephalopathy

PI – Protease inhibitors

PML – Progressive multiple leukoencephalopathy

Q

QDEC – Query, design, estimate, contrast

R

ROI – Region of interest

S

SA – South Africa

SNR – Signal – to – noise ratio

SSA – Sub-saharan Africa

T

TE – Echo time

TR – Repetition time

U

UNAIDS - Joint United Nations Programme on HIV/AIDS

V

VBR – Ventricular brain ratio

W

WHO – World health organisation

Glossary

Astrocytes – star-shaped specialized glial cells that respond to any form of insult to the central nervous system.

Basal ganglia – group of subcortical nuclei (caudate nucleus, putamen, substantia nigra, globus pallidus, nucleus accumbens, subthalamic nucleus) that modulate and refine nerve impulse to the cerebral cortex and primarily are involved in motor learning and control**.**

BrainVoyager – brain imaging research tool for analysing and visualising functional and structural MRI data.

Calcification – neurological disorder that is characterised by deposition of calcium in brain regions that control motor activities of the body.

CD4 count – absolute count of helper T-Helper cells (a type of lymphocyte or white blood cell) per cubic millimetre of blood to determine health of the immune system. It fluctuates under conditions like ill-health, time of the day, etc.

CD4 percentage – total number (percentage) of blood lymphocytes that are CD4 cells which also represent the state of health of the immune system. It is a more consistent measure of body immune system than CD4 count.

CD8 count – absolute count of T-lymphocytes (CD8 cells) per cubic millimetre of blood. CD8 cells help in fighting neoplastic cells. It is often linked with inflammation due to microglial/macrophage activation in the brain

CD4/CD8 ratio – compares the ratio of the two major blood lymphocytes, usually used to check for reduction of body immune system (CD4 cell) in comparison to CD8 cell. It is a complementary measure of health of immune system.

Cerebral Haemorrhage – bleeding within brain tissue instead of outside which is caused by rupture of blood vessels or vessel networks that supply the affected brain tissue. This is usually preceded by formation of a blood clot (aneurysm) in blood vessels.

Choroid plexus – network of nerves that projects from the lateral ventricle and produces cerebrospinal fluid (CSF). They are usually among the first tissues attacked by the HIV virus

Cortical thickness – measure of thickness of layers of the cerebral cortex in human brain, measured either locally or by taking average global thickness. Cortical thickening usually positively correlates with cognitive ability.

Corpus callosum – large c-shaped collection of white matter nerve fibres that connects the right and left hemispheres of the brain.

Cytokines – large group of proteins, peptides or glycoproteins secreted by specific cells of the immune system that are important in cell signalling

Dementia – category of brain diseases that affect mental abilities such as memory loss, impaired judgement or language skills, etc. Most commonly linked with disease conditions of old age and adult HIV infection.

Efavirenz – non-nucleoside reverse transcriptase inhibitor class of antiretroviral drugs which prevents nucleoside transcriptase enzyme from working, thereby preventing HIV from multiplying.

Endothelial cells – thin layer of cells that line the interior of the blood vessel and filter biochemical substances that cross through the vessel. These cells are attacked by the HIV virus.

Encephalopathy – condition of brain malfunction or damage that leads to the slowing down, or completely halting of developmental processes, functions or structures controlled by the affected brain region(s). It is often linked with brain viral infections especially HIV infection.

FreeSurfer – neuroimaging software tool used in this study to perform morphometric analyses of T1 MRI scans of study participants' brains. It is designed and developed at the Martinos centre for biomedical and computational neuroimaging analyses.

Freeview – recent GUI and visualization tool developed for FreeSurfer, similar in functionality to tkmedit, tksurfer. It differs from tkmedit in that it can load multiple volumes at once and can be used to visualize high resolution (100um) data as well as tractography splines.

Gp120 – glycoprotein on HIV envelope that enters the host cell by binding on the CD4 cell receptor of the host, then fusing the viral membrane with the host cell membrane.

Gyrification – the process that involves the changing of brain morphology to generate the gyral and sulcal regions on cerebral cortex, it is also a measure of numeric value of gyral convolution in brain imaging analyses.

Gyrus – convolutions on both brain hemispheres due to infolding of the cerebral cortex, they are surrounded by grooves known as sulci. (Plural: gyri)

Hepatic steatosis – condition, also known as fatty liver disease, where fat accumulates in the liver

Hypercholesterolaemia – inability of the liver to metabolize and remove cholesterol or lipoproprotein leading to their accumulation in the liver and a high cholesterol level in the blood

Hypertriglyceridaemia – condition where the level of triglyceride in the blood is higher than normal. It can be caused by genetic or non-genetic factors.

Intracranial volume – in context of the FreeSurfer reconstruction algorithm, it is all the volume within the cranium including the brain, meninges and CSF

In utero – function(s), process (es) or action (s) that occur in the womb or before birth

IsiXhosa – language spoken by a group of tribes that live at the south-eastern part of South Africa. Some of the children that participated in this study reported speaking home language of the isiXhosa tribe.

Lymphocytes – immune cells that fight bacteria, toxins and neoplasmic cells and act as the body's defence mechanism against foreign and harmful organisms and substances. CD4 and CD8 cells are types of lymphocytes.

Macrophages – specialized white blood cells that play the important immune system role of detecting, ingesting and neutralizing bacteria, dead cells and other harmful organisms.

Meningitis – inflammation of the meninges – the three membranes that cover the brain and spinal cord – due to bacterial or viral infection.

Microcephaly – condition of drastic reduction in brain volume or non-attainment of normal brain size, usually due to neuronal atrophy associated with viral infections especially HIV infection.

Microglia – type of neuronal support cell (neuroglia) that acts as the first and main form of active immune defence in the central nervous system.

Monocytes – type of undifferentiated white blood cell that plays an important role in destroying invaders as well as being involved in healing and repair processes.

Morphometry – measurement of structural landmark, dimension and external shape of the whole organism, tissue, organ of a living organism, for example the brain – brain morphometry.

mri_glmfit – FreeSurfer program that performs general linear model analyses in the surface or volume brain models by making statistical estimation and inferences.

MultiTracer – Java-based 3D visualization tool for anatomical delineation and quantification of volumetric grayscale images.

Myelination – process of growing an electric insulating, myelin sheath around neurones to improve fast transmission of signals along neurones.

Neuroimaging – the part of medical imaging that is associated with the investigation of the nervous system.

Neuronal atrophy – terminology that translates to neuronal cell death and usually relates to a decrease in size and loss of connection in neuronal tissue due to loss of cytoplasmic protein. It is observed in cases like microcephaly in pediatric HIV infection.

Neuron – the basic unit of the nervous system that processes and transmits information through the nervous system as chemical or electrical excitations.

Neuropathogenesis – origin and/or development of a disease condition of the nervous system.

Neurotoxins – biochemical substances that are toxic to neurones, nervous system or its peripheral components.

Pancreatitis – acute or chronic inflammation of the pancreas.

Prostaglandins – group of active lipid compounds (eicosanoids) that aid in tissue recovery at the site of damage or injury.

Spastic paraparesis – group of disorders that cause progressive and severe weakness and spasticity of the lower extremities.

Query Design Estimate Contrast (QDEC) – FreeSurfer analysis tool used for group comparison and analyses that run on graphic user interface (GUI) environment, a front-end to the mri_glmfit stream.

Radio frequency – band of pulse frequencies within the range of 10^4 and 10^{12} Hz, usually applied in MRI scan

Rhabdomyolysis – complex condition that involves rapid dissolution of injured or damaged skeletal muscles

Spin – quantum characteristic of elementary particles which is visualized as the rotation of these particles on their axes. It is responsible for measurable angular momentum and magnetic moment

Stavudine – antiretroviral drugs in the class of nucleoside reverse transcriptase inhibitors often used in combination with other anti-HIV drugs

Structural MRI – The modality of MRI scan for examining the structure and pathology of structures of the body, in this case the brain.

Subcortical – regions of the brain inferior to cerebral cortex

Sulcal enlargement – brain structural disorder in which the deep, narrow grooves of sulci and fissures begin to widen and become shallow. This disorder is associated with ventriculomegaly and has been observed as a structural defect in HIV infection.

Sulcus – deep, narrow groove that separates adjacent convolutions of the brain (plural: sulci).

Tat – viral protein that works in efficient HIV transcription as well as in supporting its replication.

Thymidine – nucleoside pyrimidine with a thymine base that is attached to the sugar deoxyribose.

TKMEDIT – program used for visual inspection and editing of voxels in 2D slices of sub-cortical segmented brain MRI scan during reconstruction process in FreeSurfer.

TKSURFER – program interface also used for inspecting voxels of 3D cortical brain MRI scan during reconstruction process in FreeSurfer.

Voxel – basic unit of measurement for 3-dimensional, spatial or graphical or pictorial entity. It is a combination of "volume" and "pixel" – unit of measurement of 2-Dimensional pictorial entity.

Viral load – measure of the amount of viral substance in a host, environment or bloodstream, often used to quantify the amount of HIV virus in infected subjects.

Ventriculomegaly – abnormal dilation of the lateral ventricles of the brain in which the ventricular atrium diameter is 10mm or more. It is associated with hydrocephalus and advanced pediatric HIV infection.

Zidovudine – an antiretroviral drug that belongs to the class of nucleoside reverse-transcriptase inhibitors used to prevent perinatal transmission and prevent infection in newborns.

Chapter 1 - Introduction

The Human Immunodeficiency Virus (HIV) burden in younger cohorts is still high (WHO, 2018; Smith, 2014; UNAID, 2018; AVERT 2018). By mid-2017, 1.8 - 2.1 million children living with HIV were reported globally with 180, 000 new infections in children under 15 years of age, most of them in sub-Saharan Africa (WHO, 2018; UNAID, 2018).

South Africa's HIV profile is high compared to most other countries of the world (Spies et al., 2015; Barron et al., 2013; Smith et al., 2014). Women between the ages of 15 and 24 account for about 25% of new infections and contribute to the large HIV disease burden (AVERT, 2018). Every young woman infected with HIV is a potential mother which increases the likelihood of perinatal HIV infection to her children. Currently, most pediatric HIV infections are acquired through vertical transmission; during pregnancy, birth or through breastfeeding (WHO, 2018; AVERT, 2018). It is expected that the prevalence of HIV infection in pregnant women in South Africa will still be high at least for the next two decades (Barron et al., 2013). Because of the difficulty in accessing antiretroviral therapy (ART), this implies that vertical HIV transmission, from mother-to-child, may still be a major challenge (Le Doare et al., 2012; Barron et al., 2013).

In South Africa in 2017 between 320, 000 – 331, 820 children were estimated to be living with HIV (World Bank, 2016; UNAID, 2017), mostly vertically infected. HIV progresses faster in children than in adults and its effects are more severe and obvious in younger, vertically-infected children, who are not initiated to early ART (Sherr et al., 2014; Le Doare et al., 2012; Wachsler-Felder et al., 2002). HIV infection is associated with developmental and behavioral delays and deficits (Le Doare et al., 2012; Sherr et al., 2014). Cognitive deficits in children typically manifest as failure to reach developmental milestones, or development of these milestones at a slower rate than a typically developing child (Sherr et al., 2014). This affects the ability to engage in scholastic, educational and social activities, and is associated with emotional and behavioral disorders. Neurocognitive defects can be in any or all the domains of language and verbal fluency, executive performance, intellectual processing speed, psychomotor and mental development. Behavioral issues that have been observed in HIV-infected children are poor self-control, apathy, withdrawal syndrome, irritability, depression and personality changes (Sherr et al., 2014; Paul et al., 2002; Rausch et al., 2001; Le Doare et al., 2012).

Neuroimaging studies in adult HIV cohorts have shown that cognitive deficits are associated with specific changes to brain morphology, mostly caused by neural atrophy (Ances et al., 2012; Ellis, 2010). Cortical thinning is a morphometric defect associated with neurocognitive deficits and reduced intellectual skills in HIV infected adults (Thompson et al., 2005a; Kallianpur et al., 2011). Sulcal widening is observed as the enlargement of sulci and reduction in cortical folding of the brain

(Steinbrink et al., 2013; Thurnher et al., 2000). Enlarged lateral ventricular volumes (Paul et al., 2002; Kallianpur et al., 2016), white matter related abnormalities (Underwood et al., 2017; Baker et al., 2017), and regional and total brain volume reduction both at cortical and subcortical levels (Paul et al., 2002; Di Sclafani et al., 1997) are also frequently observed.

These structural abnormalities are the result of HIV and viral toxins penetrating the selectively permeable blood brain barrier (BBB) which protects the brain from harmful foreign substances (Avison et al., 2002; Banks., 1999). Once HIV gains access into the brain tissue, most of the brain's immune system, as well as the BBB, are compromised (Ellis, 2010; Avison et al., 2002; Steinbrink et al., 2013; Banks., 1999). A compromised BBB leads to an increased influx of virus and viral product, while a compromised brain immune system enables viral replication (Steinbrink et al., 2013; Banks, 1999; Avison et al., 2002). This leads to continuous increase in brain viral load and severe damage to the brain tissue (Ellis, 2010; Avison et al., 2002; Banks, 1999). Due to its conducive nature for replication of HI virus and viral product, the brain is a major reservoir for HIV transmission to the periphery (Van Rie et al., 2007; Ellis, 2010; Avison et al., 2002; Banks, 1999). Hence, different treatment strategies have been implemented to mitigate these effects and protect the delicate tissues of the pediatric brain.

Early ART initiation protects children with HIV from neuropsychological defects, and is beneficial to neurodevelopment, at least in the short term (Le Doare et al., 2012; Laughton et al., 2012; Lindsey et al., 2007). Most guidelines recommend that all children born to HIV-infected mothers should be started on ART as soon as possible after birth, regardless of CD4 count, and that all pregnant and breastfeeding women living with HIV should be on ART, regardless of CD4 count or WHO clinical stage (NUNLM, 2019; WHO, 2015a; 2015b; AVERT, 2018). The children with HIV early antiretroviral therapy (CHER) clinical trial (Violari et al. 2008) conducted at the Perinatal HIV Research Unit at Chris Hani Baragwanath Hospital in Soweto, and the Children's Clinical Research Unit at Tygerberg Children's Hospital in Cape Town, found that early ART (at a mean age of 7.2 weeks) reduced infant mortality by 76% and HIV progression by 75% compared to the previous standard of treatment initiation once children became symptomatic or their CD4 percentage dropped lower than a threshold of 25% (WHO, 2015a; 2015b; Violari et al., 2008). Implementation of the early ART guidelines for infants has raised concerns over the long-term effects especially on development of the central nervous system (CNS), with previous studies showing adverse effects of specific antiretroviral drugs (ARV) in the CNS in adults (Shah et al., 2016; Chang et al., 2008; Robertson et al., 2012).

After conclusion of the CHER trial, a longitudinal follow-up study with clinical, neuropsychological and neuroimaging components was designed to investigate the possible long-term effects of perinatal HIV/early ART initiation on neurodevelopment. The neuroimaging sub-study started acquiring magnetic resonance imaging (MRI) scans of children from the Cape Town arm of the CHER cohort in 2010 when the first children reached 5 years of age, which at the time was the youngest age at which it

was considered feasible to acquire MRI data from non-sedated children. Subsequent scans were acquired at 2-year intervals, when the children were 7, 9 and 11 years of age. MRI scans at ages 5 and 7 were obtained using a Siemens 3T Allegra brain scanner, which was decommissioned part way through acquisition of the 9-year MRI scans. Some of the 9-year scans were reacquired on the new 3T Siemens Skyra full body scanner, which was also used to acquire the remainder of the 9-year as well as 11-year scans. The MRI protocol at each age included structural MRI, as well as diffusion tensor imaging (Jankiewicz et al., 2017), single voxel magnetic resonance spectroscopy (Mbugua et al., 2016) and, from 7 years onwards also resting state functional MRI (Toich et al., 2018), some of which data has already been published.

Analysis of structural MRI from this cohort at age 5 focused on manually traced volumes of the basal ganglia and corpus callosum (Randall et al., 2017), finding volume increases in the putamen and decreases in the corpus callosum with HIV (Randall et al., 2017). However, no investigation was performed of the cerebral cortex, which is known to be affected by HIV infection (Thompson et al., 2005[a]). A cross-sectional investigation of cortical morphometry at age 7 years found reduced parietal folding in HIV-infected children and increased frontal cortical folding with later ART initiation (Nwosu et al., 2018). However, no longitudinal analysis was performed to model developmental changes in brain morphometry in HIV-infected children on early ART in comparison to uninfected controls. Longitudinal vertex-wise designs in neuroimaging are more sensitive to alterations than cross-sectional designs and account for subject-related variation (Reuter et al., 2012). The change of scanner at the time of the 9-year scan introduces possible confounding effects on longitudinal analysis, investigation of which is outside the scope of this thesis. However, the time points of 5, 7 and 9 years at which data was acquired from the Siemens 3T Allegra scanner fall within a period from early childhood to adolescence that is critical for brain development (White et al., 2010; Magnotta et al., 1999; Sowell et al., 2003; 2004). To eliminate confounding scanner effects, in the current work we restrict longitudinal analysis to this time period.

Accurate investigation of the development of pediatric HIV brain morphometry can only be achieved using either tools built specifically for children based on a pediatric brain atlas, or robust tools that accommodate pediatric brain morphometry variations through development. Existing automated segmentation tools such as FreeSurfer (https://surfer.nmr.mgh.harvard.edu/) were originally designed and built using adult brain atlases (Sabuncu et al., 2010; Fischl et al., 2002; 2004; Makris et al., 2004). To ensure the accuracy of these tools in children, it is necessary to validate their brain volume outputs against a gold standard method in healthy HIV+ children. Assessing FreeSurfer's reliability and accuracy will make it more useful in the investigation of the combined effects of HIV and early ART in children. A comparison of a previous version (v5.3.0) of FreeSurfer with manual tracing in a pediatric HIV cohort at age 5 years found major discrepancies and lack of agreement between methods (Randall,

2015). The current study aimed to validate the use of the latest FreeSurfer version (v6.0.0 – release date: 23rd January 2017) for investigation of pediatric HIV.

The goal of this study is to fill in gaps in knowledge about brain structural alterations in HIV from our ongoing longitudinal neuroimaging study of perinatally HIV-infected children from the CHER cohort (see Ackermann et al., 2016; Mbugua et al., 2016; Toich et al., 2018; Jankiewicz et al., 2017; Randall et al., 2017; Nwosu et al., 2018). To achieve this, we aim firstly to validate FreeSurfer's accuracy for investigating pediatric subcortical morphometry and secondly, to investigate cortical morphometry and its development in these children between 5 and 9 years. Morphometric measures of interest are those previously associated with HIV infection which include; cortical thickness – a measure associated with neurocognitive deficits (Dubois et al., 2008; Shaw et al., 2006; Wilke et al., 2003), gyrification index – a measure that quantifies the amount of cortex buried within the sulcal folds (Schaer et al., 2008; White et al., 2010; Treble et al., 2013), and volumes of subcortical brain regions including the basal ganglia (caudate nucleus, nucleus accumbens, putamen and globus pallidus) and corpus callosum regions.

1.1 Study aim and objectives

The aims of validating FreeSurfer's volumetric measures in children and investigating the development of pediatric morphometry in HIV were divided into specific objectives as follows:

1.1.1 FreeSurfer validation with manual segmentation:

To determine the degree of agreement and consistency between volumes of the caudate nucleus, nucleus accumbens, putamen, globus pallidus and corpus callosum obtained using manual tracing and automated FreeSurfer segmentation in 7-year-old children, and to investigate the effect of HIV on these measures.

1.1.2 Cross-sectional investigation of effects of HIV on cortical morphometry at age 5 years:

To investigate effects of HIV, early ART initiation and interruption, immune health at ART initiation and HIV severity on brain morphometry at an early age using cortical thickness and local gyrification indices (LGI) derived from FreeSurfer's automated processing pipeline.

1.1.3 Longitudinal investigation of the effects of HIV on cortical development:

To evaluate typical longitudinal development of cortical brain morphometry over the period from 5 to 9 years and determine how this may be altered because of perinatal HIV infection, early ART initiation, ART interruption and HIV-related encephalopathy (HIVE).

Table 1.1: Outline of sample sizes, age ranges and comparisons for the study objectives

FreeSurfer validation with manual segmentation		
Sample size	age range (years)	target comparisons
N = 82 (HIV+: 42; HEU: 17; HU: 23)	7.00 -7.84	Sub-cortical: HIV+ vs. HIV-; HU vs. HEU
Cross-sectional investigation of effects of HIV on cortical morphometry at age 5 years		
N = 75 (HIV+ with/without ART interruption: 21/25; HIV+ classified as mild/severe 12/32: HIV+ with high/low viral load at enrolment:25/21; HIV- 29)	4.94 – 6.52	Cortical: HIV+ vs. HIV-; HIV+ grouped by interruption vs. HIV –; HIV+ grouped by early disease severity vs. HIV -; HIV+ grouped by viral load at enrolment vs. HIV -
Longitudinal investigation of the effects of HIV on cortical development from age 5 – 9 years		
N = 144 HIV+: 75; HIV+ with encephalopathy: 12 HIV-: 66)	4.94 – 9.43	Cortical: Rate of change in HIV- children Comparison for rate of change: HIV+ vs. HIV-; HIV+ with encephalopathy vs HIV-
HIV+ = HIV-infected children. HIV- = HIV-uninfected children. HEU= HIV- children exposed to HIV. HU=HIV- children unexposed to HIV		

The key strength of this study is its setting – South Africa, which has rich data on pediatric HIV infection and management. The study has a relatively large (*n*=141: 75 HIV+; 66 HIV-) sample of an early (< 18 months) ART-initiated cohort whose viral suppression was achieved quite early. They have been on a government policy-regulated homogenous ART regimen and have been clinically followed from birth till age 9 years. Furthermore, manually generated brain volume data are rare and to our knowledge no previous study has followed pediatric cortical development in a HIV+ cohort in a longitudinal design.

1.2 Thesis outline

Chapter 1 gives a brief introduction to the background and motivation for the study and its aim and objectives.

Chapter 2 focuses on the background and review of literature in this research area, including description of key concepts required for this study as well as related previous work relevant to neuroimaging in HIV.

Chapter 3 presents in journal article format, the findings on the validation of FreeSurfer's segmentation of basal ganglia and corpus callosum for HIV+ and HIV- children at age 7 years, compared to data obtained via manual segmentation.

Chapter 4 presents in journal article format the findings of cross-sectional vertex-wise analyses of cortical morphometry at 5 years investigating the effects of perinatal HIV infection, early ART initiation, ART interruption, HIV severity and immune health at ART enrolment on cortical thickness and gyrification at age 5 years.

Chapter 5 presents in journal article format the findings from longitudinal investigation of the effects of HIV infection, early ART initiation, ART interruption and HIV encephalopathy on the trajectory of cortical morphometry from age 5 to 9 years.

Chapter 6 provides a general discussion on the implication of the key findings presented in chapters 3, 4, 5 and conclusion of the thesis.

The work presented in this thesis is being prepared for publication. Results from chapters 3 and 4 were presented in the following conference proceedings;

a. 13th International Meeting of the Society of Neuroscientists in Africa (SONA), Entebbe, Uganda as poster and oral presentation. "**Effects of antiretroviral therapy (ART) initiation timing on frontal cortical morphometry at age 5 years**" – June 2017. Poster number:09. Abstract number: MD 11

b. 23rd Annual Meeting of the Organization for Human Brain Mapping (OHBM), Vancouver, Canada as poster presentation. "**Comparison of FreeSurfer longitudinal and cross-sectional streams for children's brain morphometry**" – June 2017. Poster number: 4108

c. 22nd International AIDS Conference (AIDS 2018) in Amsterdam, the Netherlands as oral poster discussion. **"Neuroimaging findings in children from the CHER (Children with HIV early antiretroviral therapy trial) cohort"** – July 2018. Abstract and poster number: TUPDB0103

d. 10th International workshop on HIV PEDIATRICS in Amsterdam, the Netherland as poster presentation. **"Antiretroviral therapy (ART) interruption is associated with reduced cortical structures at age 5 years compared to uninterrupted"** – July 2018. Abstract number: 68

Chapter 2 - Background and literature review

2.1 HIV infection and the human brain

Studies of adult and pediatric HIV infection have shown that the brain is one of its first targets and is severely affected by the virus (Avison et al., 2002; George et al., 2009; Banks., 1999). The brain acts as a reservoir for HIV and its viral products, from where replication, maturation and subsequent dispersion of the virus to various organs of the body commences (Paul et al., 2002; Van Rie et al., 2007; Avison et al., 2002; Ellis, 2010). The process that enables the virus to cross the selectively permeable blood-brain barrier (BBB) and enter the brain to cause the debilitating effects that are often observed in HIV infection is not completely understood.

There are several theories that explain how the virus penetrates through the semi-permeable structure of the BBB. One of these speculates that the virus and viral products flowing in blood vessels stimulate endothelial cells (astrocytes and microglia) of the BBB to release neurotoxins (cytokines, nitric oxides and prostaglandins) and viral gene products (tat and gp 120), which cause neuronal atrophy and allow the influx of free virus and viral products through the compromised BBB into the CSF and brain tissue (Banks, 1999; Steinbrink, 2013). Another theory proposes that brain infection results from trafficking of infected cells of monocyte-macrophage lineage across the BBB or "Trojan Horse" effects during principal infection of activated CD4 + lymphocytes, and infiltration of infected cells through the choroid plexus (Avison et al., 2002; Ellis, 2010).

Most studies accept that HIV enters the CNS within days to weeks after infection and that viral load increases with disease progression (Van Rie et al., 2007; Paul et al., 2002; Persidsky et al., 1999; Banks, 1999). On entering the CNS, HIV neurotoxins and mediator hosts (monocyte-macrophages cells) destroy neuronal connections (dendrite-synapse linkage) and damage the complex networks, leading to HIV-associated neurocognitive disorders (HAND) (Ellis, 2010; Lindsey et al., 2007; Chriboga et al., 2005). These pathophysiological processes are observed in the brain tissues that are most susceptible to high viral load, including the caudate nucleus, hippocampus, lateral ventricle, putamen, thalamus, corpus callosum, deep white matter and basal ganglia, and affect global grey matter and total brain volume (Paul et al., 2002; Holt et al., 2012).

Alterations in CSF markers of monocyte activation, CNS injury and brain pathology have been detected at autopsy in infected cohorts (Cardenas et al., 2009; Spies et al., 2015). Even after peripheral viral suppression with ART, there may still be residual effects in brain tissue, since some classes of ART are not able to permeate the BBB (Cardenas et al., 2009; Ances et al., 1999; Banks, 1999; Ellis, 2010). In

the ART era, residual minor or severe neurocognitive impairments have also been observed, since many brain injuries that include loss or contraction of the axonal branches or supporting glia cannot be reversed by antiretroviral treatment (Avison et al., 2002; Becker et al., 2011; Chriboga et al., 2005).

Previous studies have associated HIV infection in adults with neurocognitive impairment related to executive functioning, spatial working memory retention, intellectual and learning development, language and verbal learning, psychomotor ability and information processing speed (Vance et al., 2013; McIntosh et al., 2015). Psychomotor abnormality is characterized by disorders of the motor system, such as gait disturbances, pure spastic parapresis, acute meningitis, tremors, fine motor clumsiness, and general leg weakness (Epstein et al., 1986; Rausch et al., 2001; Spudich et al., 2012). Neuropsychological effects of HIV include differences in behaviour compared to uninfected children manifested as apathy, withdrawal syndrome, irritability, depression, and personality changes (Sherr et al., 2014; Le Doare et al., 2012; Mitchell, 2001; McIntosh et al., 2015). There are cases of compromised social skills, and emotional difficulties (Paul et al., 2002; Rausch et al., 2001).

Studies are currently investigating the roles different brain tissues play in the manifestation of these symptoms and their neuropathogenesis, since most symptoms are also linked with comorbid disease conditions and with aging (Paul et al., 2002; Holt et al., 2012).

HIV-associated neurological disorders (HAND) have been re-defined into stages of severity, based on the results of neurocognitive tests. These stages are: Asymptomatic Neurocognitive Impairment (ANI), which is seen at the earliest stage of infection; Mild Neurocognitive Disorder (MND), which occurs as infection progresses; and the most significant and severe case: HIV-Associated Dementia (HAD) (Leon et al., 1986; Rausch et al., 2001; Spudich et al., 2012), which is characterized by loss of concentration, impaired short-term memory loss and general loss of memory (Epstein et al., 1986; Rausch et al., 2001). HAD is linked with AIDS dementia complex (ADC) or sub-acute encephalitis, a syndrome of progressive dementia associated with cognitive, motor and behavioral dysfunction, which is one of the earliest manifestations of AIDS (Navia et al., 1987; Broderick et al., 1993).

Structurally, studies have shown that HIV positive participants have reduced white matter compared to controls (Cardenas et al., 2009; Sarma et al., 2014). Cardenas et al. (2009) reported significant white matter volume loss in the whole brain as well as in the frontal, temporal and parietal lobes, while perinatally HIV-infected youths who started early ART showed reduced white matter volume in bilateral posterior corpus callosum, external capsule, ventral and temporal white matter, mid-cerebral peduncles and basal pons (Sarma et al. 2014). HIV infection in the adult brain is also associated with regional and global brain volume loss, and increased CSF volume due to neuronal atrophy and ventricular enlargement caused by viral proteins and toxins (Cardenas et al., 2009; Ances et al., 2012;

Ellis, 2010; Paul et al., 2002). Individuals at an advanced disease stage, with greater immunocompromise (e.g lower nadir CD4) and viral burden have faster brain tissue loss and greater neurocognitive impairment (Cardenas et al., 2009; Spies et al., 2015; Centers for Disease Control and Prevention, 1993). Major tissue losses and abnormalities are linked with the cerebellum, brainstem, thalamus, caudate nucleus and frontal-striatal brain regions (Ances et al., 2006; Becker at al., 2011; Cardenas et al., 2009; Spies et al., 2015).

2.1.1 Neurodevelopmental implications of HIV in children

About 90 percent of HIV transmission to children is by perinatal means – either before birth (in utero), just after birth (post-partum) or from breastfeeding (Smith, 2014; Sharland & Handforth, 2005; Le Doare et al., 2012). It is estimated that without treatment, the chance of perinatal transmission from mother-to-child (MTCT) is between 15 and 45 percent, but with the recent recommendation of ART for HIV+ expectant mothers and early ART, at least for the first 4-6 weeks after birth in their children, the probability of perinatal HIV transmission has reduced to 5 percent (AVERT, 2018).

Evidence from previous studies has shown that, without ART, HIV infection has a more debilitating effect on younger children than on adults (Epstein et al., 1986; Wachsler-Felder et al., 2002; Rausch et al., 2001). Effects such as severe psychomotor dysfunction, neurological defects, permanent behavioral deficits, learning and intelligence deficiencies, language impairment, progressive loss of executive function/performance, impaired intellectual ability, loss of some life survival skills, memory loss, and impaired performance in both behavioural and emotional spheres are common in pediatric HIV infection (Wachsler-Felder et al., 2002; Rausch et al., 2001; Epstein et al., 1986; Wachsler-Felder et al., 2002; Van Rie et al., 2007; George et al., 2009; Kieck et al., 2004).

One of the most severe neurological effects is progressive HIV-encephalopathy (PHE) – a clinical condition associated with impaired brain growth and delay or loss of developmental milestones which progresses to neurocognitive deterioration, and symmetric motor deficits (Tardieu et al., 2000; Rausch et al., 2001; George et al., 2009; Kieck et al., 2004; Mitchell, 2001: McCoig et al., 2002). Other neurological effects of HIV on the brain include microcephaly (a condition associated with shrinking/reduction of the brain volume due to neuronal atrophy in cortical and subcortical regions), white matter lesions, damage and calcification of the basal ganglia and corpus callosum, cortical thinning, sulcal widening and ventricular enlargement. In addition, progressive multiple leukoencephalopathy (PML), abnormal cerebral vasculature and brain tumours may occur (Van Rie et al., 2007; George et al., 2009; Kieck et al., 2004). The lifelong consequences of these effects and the extent to which they can be reversed by ART are still subjects for investigation (Van Rie et al., 2001; Le Doare et al., 2012; Mitchell, 2001; Wachsler-Felder et al., 2002).

Structural and physiological alterations in children's brains are associated with neuropsychological and cognitive effects in the short term (Sherr et al., 2014; Le Doare et al., 2012; Sharland et al., 2005), but of greater concern is their implication on long term neurodevelopment. With the introduction of early ART for treatment of pediatric HIV (AVERT, 2018; WHO, 2015a; 2015b) there are concerns about; first, the effect of ART exposure on the developing brain; secondly, the effectiveness of early ART to reverse neuropsychological and cognitive effects of HIV and thirdly, the effect of lifelong chronic HIV infection and ART.

2.1.2 Antiretroviral therapy (ART): Benefits and adverse effects

ART drugs are generally designed to slow HIV progression, mostly by preventing viral replication, thus reducing the quantity of virus in the blood of a carrier (WHO, 2015a). By reducing viral load and replication, ART also helps reduce the chances of transmission, especially vertical transmission from mother-to-child either in utero, post-partum or through breastfeeding. Some of the most recent HIV treatment strategies include the use of different classes of ART in combination therapy, to attack different stages of viral replication and growth, preventing viral drug resistance and increasing CD4+ lymphocytes (Ellis, 2010; Lindsey et al., 2007; Avison et al., 2012).

There are several classes of ART medication; **non-nucleoside reverse transcriptase inhibitors (NNRTIs)** are used to directly inhibit the activities of reverse transcriptase, thereby disabling the protein required for the virus to replicate itself in its host. **Nucleoside reverse transcriptase inhibitors (NRTIs)** are pseudo analogues of nucleosides incorporated into HIV DNA, which act as false substrates for reverse transcriptase and thus terminate the proviral DNA chain formation. This class also acts to prevent HIV from replicating itself, thus reducing the amount of HIV in the blood. **Protease inhibitors (PIs)** prevent the HIV protease enzyme from cleaving viral proteins, preventing the replication of immature, non-infectious viral particles (Smith, 2014; Robertson et al., 2012; McCoig et al., 2002; Ellis, 2010). **Integrase strand-transfer inhibitors (ISTIs),** which include the recently introduced dolutegravir and raltegravir, prevent HIV integrase from transporting and attaching proviral DNA to host-cell chromosomes, and subsequent transcription of viral protein and assembling of viral particles by binding metallic ions to the active sites (Hazuda et al., 2000; Dyda et al., 1994). **Fusion inhibitors (FI)** prevent the fusion of HIV and CD4 or other target cells in the extracellular space using various genetic means at the target sites, thereby ensuring that HIV does not bind to the host cells and the immune building blocks are not compromised (Weissenhorn et al., 1997; Chan et al., 1997).

ART has been associated with several adverse outcomes and side effects which affect the brain either directly or indirectly through effects on other organ systems (Cardenas et al., 2009). For example, the NNRTI efavirenz is associated with brain tissue loss (Fortin and Joly, 2004; Shibuyama et al., 2006), while PIs are associated with cardiovascular disease (Hsue et al., 2004), which is linked to the presence of lacunar infarcts and abnormal white matter in the brain (Chui, 2000), as well as metabolic

abnormalities; hypercholesterolaemia, hypertriglyceridaemia and insulin resistance (Smith 2014). Lipodystrophy (fat maldistribution) is reported as a common late complication with ART (Smith, 2014; Robertson et al., 2012; Bartlett and Lane, 2012). Some ISTIs are linked to gastrointestinal effects (nausea and diarrhea), myopathy, rhabdomyolysis, and depression. (Fettiplace et al., 2017; German et al., 2012).

Long-term HAART treatment has been associated with adverse effects like hepatic steatosis, neuropathy, cardiomyopathy, pancreatitis, lactic acidosis, ototoxicity and retinal lesions (Robertson et al., 2012; Bartlett and Lane, 2012). NRTIs can cause mitochondrial dysfunction leading to toxicity which varies with different tissues (Robertson et al, 2012; Kakuda, 2000; Musielak & Fine, 2015). Since early initiation of ART increases the duration of ART exposure, increasing the possibility of adverse effects, there is a need to investigate the long-term effects of ART on the brain (Musielak & Fine, 2015).

2.2 Magnetic resonance imaging (MRI).

Its high spatial resolution and good contrast in soft tissues like the brain make MRI the modality of choice for neuroimaging (Tucker et al., 2004; Du et al., 2012; Spudich et al., 2012). In MRI, different tissue properties are exploited to manipulate contrast, including relaxation times, density of nuclear particles (protons), perfusion, temperature and diffusion. Images generated with these contrasts are useful in clinical research, for studying functional and structural connections, functions of different regions and developmental structure of the brain (Weishaupt et al., 2008; Plewes and Kucharczyk, 2012).

2.2.1 Principles of MRI

MR signal is generated by exploiting the property of spin possessed by elements with an odd atomic mass number (odd protons and/or neutrons) (Khan, 2013). Hydrogen, an element with a single proton is in large supply in water and fat in the human body, and in a strong magnetic field this allows the generation of high spatial resolution images of different tissues of the body (Horowitz, 1989).

At the microscopic level, each proton has mass and charge as well as spin angular momentum, which generates a magnetic dipole moment. Inside the strong magnetic field (B0) of an MR scanner, these proton magnetic dipole moments will tend to align themselves in the direction of the B0 and precess around it at a frequency known as the Larmor frequency, ωL. The Larmor frequency is determined by strength of the external magnetic field B0 as well as the gyromagnetic ratio γ of the nucleus as indicated by the formula:

$$\omega L = \gamma \, . \, \beta 0$$

Bulk magnetisation is created in the direction of the B0 field from the summation of millions of these dipole moments. Application of an alternating magnetic field, B1, perpendicular to B0 and oscillating

at the Larmor frequency, causes the net magnetization to rotate away from the equilibrium position parallel to B0 towards the transverse plane (Horowitz, 1989; Weishaupt et al., 2008). The transverse, time-varying component of the magnetisation can be detected and measured through the current induced in a receiver coil.

At equilibrium, the transverse magnetisation is zero while the longitudinal magnetisation is at its maximum. The decay of the signal to zero as spins dephase and return to their equilibrium position aligned to B0 is known as **relaxation** (Horowitz, 1989; Weishaupt et al., 2008; Plewes and Kucharczyk, 2012; Khan, 2013). There are two main forms of relaxation, the first is T1 relaxation – describing the time in which the net magnetization vector returns to its equilibrium position in the direction of B0 - also known as **spin-lattice relaxation**. The second is T2 relaxation – which describes the rate at which magnetisation in the transverse plane decays because of loss of phase coherence due to interaction with the magnetic fields of other spins, also known as **spin-spin relaxation**.

The key timing parameters that vary contrast in MRI scans are repetition time (TR) and echo time (TE). TR is the time interval between successive radiofrequency (RF) pulses, which controls the T1 contrast of the MR signal. TE is the time in milliseconds between the application of the radiofrequency pulse and the peak of the echo signal (Weishaupt et al., 2008; Plewes and Kucharczyk, 2012) which determines the T2 weighting of the image. Different image contrasts are generated depending on the nuclear spin density and by manipulating the timing variables described above. Since T1 and T2 relaxation times and spin density vary from one tissue type to another (Horowitz, 1989; Weishaupt et al., 2008) these contrasts can differentiate pathologies from normal tissue (Weishaupt et al., 2008; Plewes and Kucharczyk, 2012).

The basic contrasts in MRI are:

1. **T1-weighted contrast**, which is created by using short TR and TE, maximizing contrast arising from differences in T1 between different tissues. T1 contrast is useful for detection of anatomical abnormalities in soft tissues like the brain. In T1-weighted images, tissues with high fat content (like white matter) appear bright and compartments filled with water (like cerebrospinal fluid – CSF) appear dark

2. **T2-weighted contrast**, is created by using long TR and long TE, maximizing contrast due to differences in T2 relaxation time between tissues. T2 weighting is often used in structural imaging and for investigating fluid in the body. With T2-weighted contrast, compartments filled with water (CSF) or fat appear bright.

3. **Proton density-weighted contrast** involves the use of long TR and short TE to reduce the effect of T1 and T2 contrast. Such images are dependent on the density of protons in different

tissue types in the slice or volume of interest. Higher proton density in a given tissue gives a greater magnetisation and brighter signal, while fewer protons generates darker signal.

This study was done with T1-weighted MRI scans, since their contrast is considered optimal for visualising anatomy and for this reason automated segmentation software is usually designed for T1-weighted images.

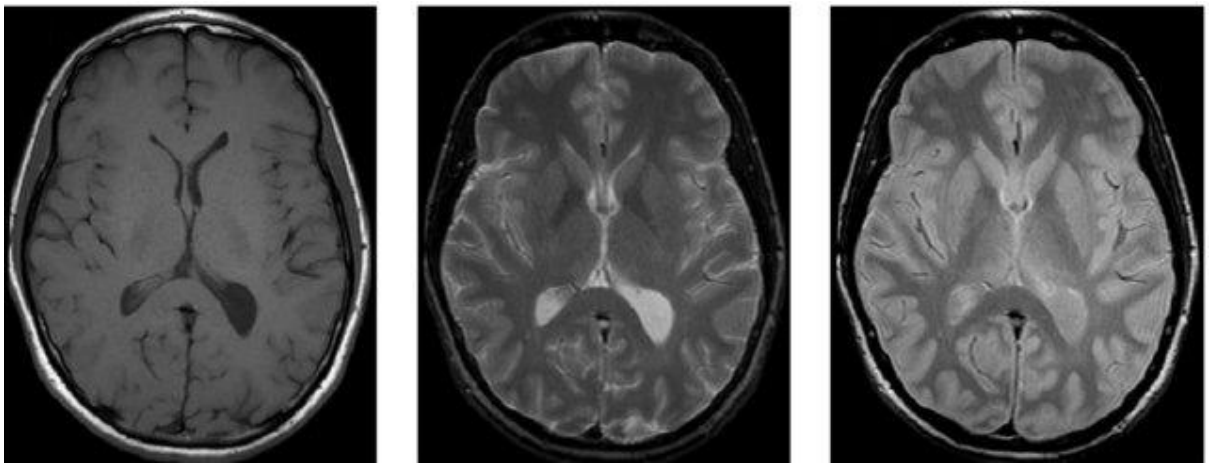

Figure 2.1: **(a) T1-weighted** **(b) T2-weighted** **(c) Proton density-weighted**
Source: Elnakib, 2013

Studies that require multiple scans and contrasts usually produce rapid magnetic signal changes leading to image distortion due to imperfect shimming (Van der Kouwe et al., 2008). The multi-echo magnetisation prepared rapid gradient echo (MEMPRAGE) sequence was designed to reduce B0 distortion while maintaining a high signal-to-noise ratio (SNR) for improving automated brain morphometry analyses. MEMPRAGE images have similar grey matter, white matter and cerebrospinal fluid contrast to MPRAGE, with less distortion and comparable signal/contrast-noise ratio (S/CNR) (Van der Kouwe et al., 2008). The MEMPRAGE sequence is recommended to ensure accurate estimation of intracranial and subcortical volume, as well as cortical thickness. Its bandwidth can also be matched with other multispectral morphometry protocols so that distortion is the same and fine edges of structures are registered accurately across different contrasts (Van der Kouwe et al., 2008).

2.2.2 MRI for studying structural brain development

Structural changes in brain development are investigated by segmenting MRI scans of the brain into anatomical regions and quantifying parameters such as the volume, surface area, and cortical thickness and folding. Segmentation of brain structures can be done using either manual tracing or automated software.

Manual tracing

Manual brain tracing involves freehand delineation of brain structures slice-by-slice on an MRI scan, often on a touch screen device, to create anatomic boundaries (Wood, 2003). It is adjudged the gold standard for segmentation of brain tissues, especially for subcortical structures like the hippocampus

and amygdala, which are associated with several mental and neurological disorders (Wenger et al., 2014; Clerx et al., 2015; Grimm et al., 2015; Morey et al., 2009). However, with certain brain tissues such as the hippocampus it is difficult to establish a clear-cut neuroanatomical landmark and delineate manually especially on T1-weighted images (Grimm et al., 2015). There is no agreement on how manual segmentation represents the actual volume of regions of interest (ROIs), because of inconsistent labelling on different brain slices (Fischl et al., 2002) and lack of agreement on neuroanatomical boundaries for structures such as the ventral striatum (Amunts et al., 2013; Grimm et al., 2015; Wenger et al., 2014). The accuracy of manual segmentation is dependent on the expertise and efficiency of the researcher and the protocol being used. Although it is tedious, time consuming and requires substantial neuroanatomical knowledge and expertise, manual segmentation tools in the hands of an expert neuroanatomist are considered more reliable and accurate than automatic segmentation (Morey et al., 2009; Grimm et al., 2015). There are several tools available in the neuroimaging research community for manual brain segmentation and editing, including MultiTracer.

MultiTracer (http://www.bmap.ucla.edu/portfolio/software/MultiTracer/) is a software tool used for manual anatomic boundary segmentation, to generate volumetric data for regions of interest. It combines a backend algorithm and a graphic user interface (GUI), is written entirely in the Java language and runs on any machine that supports Java 1.3.1 or higher version (Wood, 2003). Files loaded or saved in MultiTracer must be 8- or 16-bit per pixel files and in Analyze Image Compatible format (Wood, 2003; Robb and Hanson, 1991). Usually, the software is downloaded and installed on a tablet computer with a touchscreen and stylus device for tracing. The segmentation process is manually driven and is largely dependent on the knowledge of brain anatomy and manual tracing skills of the user, as well as the tracing protocol being used for the structure of interest. The steps in the manual tracing process used in this study are as follows:

1. DICOM files are first transformed and realigned into the anterior commissure-posterior commissure (AC-PC) plane and rotated for hemispheric symmetry using BrainVoyager QX software (http://www.brainvoyager.com/products/brainvoyagerqx.html) and exported in Analyze compatible format (*.img; *.hdr).

2. MRI scans in Analyze compatible format are then imported into MultiTracer, where a digitizer stylus is used for slice-by-slice manual delineation of regions of interest. Errors in delineation can be corrected and resaved to ensure accuracy.

3. The final segmented structural volume is then computed automatically by MultiTracer's algorithm and the volumetric data can be exported to a spreadsheet for analysis.

Automated segmentation

Several automated brain segmentation tools are available for both surface- and voxel-based analyses. These are replacing time-consuming and labor-intensive manual segmentation (Wenger et al., 2014; Grimm et al., 2015; Morey et al., 2009) since with the large MRI datasets being acquired in modern neuroimaging research come the requirements for consistency and uniformity in segmentation (Grimm et al., 2015; Morey et al., 2009), as well as the efficiency of batch processing of large amounts of MRI data. One of the most versatile automated segmentation tools is FreeSurfer (http://www.freesurfer.net/).

FreeSurfer is an open source tool with reconstruction and analysis functionality for human neuroimaging data (Fischl et al., 2000; Dale et al., 1999), developed and is managed by the Laboratory for Computational Neuroimaging at the Martinos Center for Biomedical Imaging (Fischl, 2012). The latest stable version, FreeSurfer 6.0 runs on 32- or 64-bit Linux machines. From a simple package aimed at constructing cortical surface models of the brain, FreeSurfer has evolved into a tool that can perform automated segmentation of the macroscopic visible structure of the brain from T1-weighted scans (Fischl et al., 1999, 2002; Fischl, 2012). FreeSurfer is primarily used to produce volumetric segmentation and labelling of subcortical brain structures and to create a surface model of the cerebral cortex (Fischl and Dale, 2000; Fischl et al., 2004a), which can be overlaid with fMRI data or used to obtain cortical thickness and folding (gyrification) data (Fischl and Dale, 2000; Fischl et al., 2004a, 2004b, 2008, 2009). Volumetric data of global and regional volumes can be obtained from the subcortical segmentation. Both cortical and subcortical data can be used for cross-sectional and longitudinal studies (Fischl et al., 2004a, 2004b).

FreeSurfer cross-sectional segmentation and reconstruction

Cross-sectionally processed data is useful for performing vertex-wise comparison of morphometric data between subject groups and investigating the relationship of morphometric parameters with clinical variables when there is only one scan per subject. Cross-sectional processing with FreeSurfer involves:

- Conversion of T1 structural MRI scans from DICOM format to FreeSurfer's ". mgz" format.
- Execution of the "recon-all" process to perform reconstruction of brain models in three stages;

  - autorecon1: performs motion correction, conforms resolution to $1mm^3$ as well as Talairach transform computation, intensity normalization and skull stripping.

  - autorecon-2: performs linear volumetric registration, white matter segmentation, smoothing and incorporating of any white and pial matter edits.

- - autorecon-3: performs spherical mapping and registration, maps average curvature to all subjects, performs cortical parcellation and computes statistics, then maps the parcellation mapping to aseg.

- Quality inspection and correction of segmentation errors for reconstructed surfaces on the FREEVIEW visual platform. This involves manual editing including:
    - ❖ Talairach transformation correction.
    - ❖ Skull stripping edits.
    - ❖ Pial and white matter segmentation edits, which involve the correction of inaccurately segmented boundaries between different brain surfaces (pial, white matter and cerebrospinal fluid (CSF) boundaries).

- Repeated reconstruction and inspection after manual editing until the desired output is generated with minimal parcellation and segmentation error.

At this stage, cortical thickness and volumetric data have been generated, but not local gyrification indices (LGIs). To obtain LGI data the recon-all processing stream is rerun on the reconstructed model with the –localGI flag.

The mri_glmfit utility can then be used to perform vertex-wise statistical group comparison on cortical thickness and LGI data. mri_glmfit is more complex than the Query, Design, Estimate and Contrast (QDEC) GUI, but is also more flexible, for example allowing analyses that control for multiple confounding variables. Further statistical analyses of brain volume and cortical surface data can be performed outside FreeSurfer using other statistical software.

FreeSurfer longitudinal segmentation and reconstruction

In longitudinal study designs where there are multiple scans per subject, longitudinal processing and analysis can be used to examine within-subject variation of brain morphology over time. In longitudinal investigations, the effect of inter-subject variation is reduced by using each subject as its own control.

The FreeSurfer longitudinal processing stream relies on the creation of a within-subject template for each subject onto which scans from different time points are mapped (**Figure 2.2**) for reconstruction, segmentations and subsequent longitudinal analysis of morphometric measures (Reuter et al., 2012). The longitudinal pipeline consists of the following three steps:

1. **Cross-sectional reconstruction**: this stage runs the normal cross-sectional processing stream, performing surface reconstruction and image segmentation of all T1 scans for each subject at each time point independently.

2. **Subject base template creation**: the second stage involves the creation of a mean or base template for each subject using information from the different time points (**Figure 2.2**). Segmentation and surface reconstruction are then performed on this unbiased base template.

3. **Longitudinal reconstruction**: the final stage uses information from the previous two stages to reconstruct and create longitudinal data for each subject at each time point, which can then be used in statistical within and between subject comparisons (Reuter et al., 2010; 2011; 2012).

The processes involved include: spatial and non-uniform intensity normalization, Talairach registration, brain mask creation, normalization and atlas registration, subcortical segmentation, surface reconstruction, cortical atlas registration and parcellation (Reuter et al., 2012).

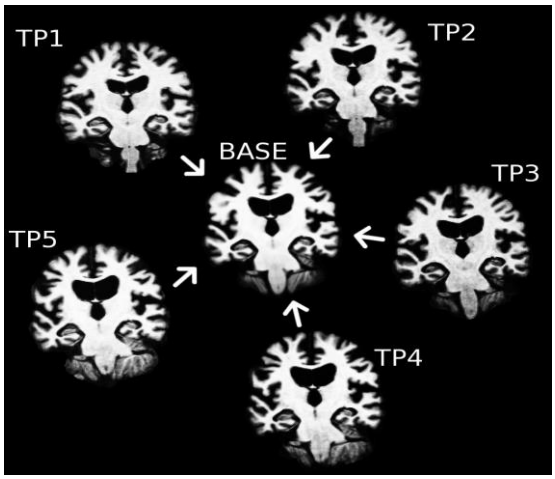

Figure 2.2: Average/base template estimate for a subject and at different time-points – TP1, TP2, TP3, TP4 and TP5. (Reuter et al., 2012)

Automated vs. manual segmentation

Several studies have validated the accuracy and consistency of segmentation outputs from FreeSurfer with manually traced data (Akudjedu et al., 2018; Dewey et al., 2010; Wenger et al., 2014; Morey et al., 2009). Most comparisons between these segmentation techniques have focused on the hippocampus and amygdala, mainly because of their importance in neuropsychiatric investigations and technical challenges involved in their manual segmentation (Morey et al., 2009, Grimm et al., 2015; Wenger et al., 2014). A few other studies have investigated other brain regions, including the caudate nuclei (Akudjedu et al., 2018; Dewey et al., 2010). Studies have reported a strong correlation between automatically and manually segmented region of interest (ROI) volumes (Wenger et al., 2014; Grimm et al., 2015; Morey et al., 2009) but with low agreement between techniques (Grimm et al., 2015;

Wenger et al., 2014). The slight discrepancies observed in correlation were attributed to variations in neuroanatomical atlases used, rather than the algorithm used in automated segmentation (Grimm et al., 2015; Wenger et al., 2014). The systematic and proportional differences between segmentation methods are largely as a result of differences in the definition of anatomic boundaries (Wenger et al., 2014; Morey et al., 2009; Grimm et al., 2015), and depend on the type of automated image processing (surface-based or voxel-based) (Grimm et al., 2015), the brain region concerned and the software version (Wenger et al., 2014) more than the segmentation method used(Grimm et al., 2015).

Unlike manual segmentation, the reliability and accuracy of FreeSurfer have been found to be lower in cases of neurological abnormalities such as severe atrophy, also to vary with age (Sanchez-Benavides et al., 2010; Wenger et al., 2014). FreeSurfer is seen as liberal, including regions beyond the anatomical boundary while manual segmentation may be stricter in delineating boundaries that are difficult to define, especially in the amygdala, entorhinal cortex, lateral ventricle and hippocampus (Wenger et al., 2014; Sanchez-Benavides et al., 2010; Grimm et al., 2015). Manual segmentation may have more sensitivity to detect right-left hemispheric asymmetries than FreeSurfer's automated pipeline (e.g. Sanchez-Benavides et al. 2010, Wenger et al. 2014). However, few studies have validated the accuracy of FreeSurfer in a younger cohort (e.g Lyden et al., 2016; Schoemaker et al., 2016; Bender et al., 2018), and brain regions associated with HIV infection have not been examined in children living with HIV. Validating FreeSurfer's automated volume output against manually traced regional brain volumes in perinatally HIV-infected children will establish the accuracy and reliability of automated segmentation in children at age 7 years, and in conditions like HIV that affect brain structure.

2.3 Pediatric brain involvement in HIV infection

The developing brain is severely affected by HIV infection, especially in cases of perinatal transmission (Ackermann et al., 2014; Chriboga et al., 2005; George et al., 2009; Kieck et al., 2004). The harmful effects of perinatal HIV on brain tissue, possible side effects of ART on the developing brain, as well as the implications to both structural neurodevelopment and neuropsychological performance in the long term are issues for investigation. Previous studies have described specific structural defects resulting from HIV infection in younger cohorts which include; cortical thinning (Yadav et al., 2017; Yu et al., 2019; Lewis-de los Angeles, 2017), alterations in total brain, white and grey matter, and specific subcortical regional volumes (Paul et al., 2018; Sarma et al., 2014; Lewis-de los Angeles et al., 2017; Cohen et al., 2016;), ventricular enlargement and sulcal widening (especially the lateral ventricle proximal to CSF channel) (Van Arnhem et al., 2013; Assefa, 2012), white matter abnormalities/lesions/atrophy (Ackermann et al., 2014; Jankiewicz et al., 2017, Hoare et al., 2015; Van Arnhem et al., 2013; Sarma et al., 2014, Uban et al., 2015) and basal ganglia calcification (Govender et al., 2011). These anatomical deficits were reported to have implications for developmental milestones; intelligence, neurocognition, psychomotor and executive activities, and behavioural and

emotional skills (Sherr et al., 2014; Le Doare et al., 2012; Wachsler-Felder et al., 2002), which motivates the need to investigate brain morphometry measures in this study.

Several recent studies have quantitatively investigated cortical thickness, and ventricular and brain volume differences due to pediatric HIV infection (Lewis-de los Angeles, 2017; Yadav et al., 2017; Van Arnhem et al., 2013; Sarma et al., 2014; Cohen et al., 2016; Paul et al., 2018). Regional decreases in gyrification due to HIV infection have also recently been reported in younger cohorts (Nwosu et al., 2015; Hoare et al., 2018; Lewis-de los Angeles 2017).

Neuroimaging in the CHER cohort at age 5 years showed that early ART initiation was associated with higher levels of choline, glutamate and creatine compared to later ART initiation while baseline CD4/CD8 ratio was observed to predict brain metabolite levels (Mbugua et al., 2016). In contrast, white matter- related abnormalities due to perinatal HIV infection were observed in the corticospinal tracts, despite early ART initiation and viral load suppression (Ackermann et al., 2016). These white matter disruptions persisted at age 7 years in the form of regional lower fractional anisotropy and higher mean diffusivity (Jankiewicz et al., 2017). In addition, poor immune health during infancy was associated with greater functional connection in the somatosensory, salience and basal ganglia networks (Toich et al., 2018). Prior morphometric investigations (Randall et al., 2017, Nwosu et al., 2018), have highlighted the importance of age-specific and longitudinal studies of the development of cortical thickness, gyrification and subcortical volumes for understanding the effects of HIV and ART on the brain. The rest of this section focuses on cortical thickness, cortical folding (gyrification), and global and regional brain volumes since these are the morphometric measures considered in this thesis.

2.3.1 Cortical thickness

The cerebral cortex largely consists of grey matter, which is an aggregation of neuronal cell bodies and is the major point for higher order information analysis and processing. It is highly folded and compact, with an average thickness of 2.5 mm, although it may vary between 1 and 4.5 mm in different regions (Clarkson et al., 2011; Fischl and Dale, 2000). Fischl and Dale (2000) defined cortical thickness as a measure of the distance between the pial surface separating the grey matter from the cerebrospinal fluid, and the grey-white matter interface separating deep white matter from the overlying grey matter (**Figure 2.3**) at every point in the brain. Manual quantification of cortical thickness across the brain is tedious and time consuming, but automated software like FreeSurfer can generate cortical thickness measures at vertices covering the brain surface.

The cortex plays an important role in neurocognition, intellectual ability and other important functions that are highly localised and represented by different regions, including visual processing, language, calculation and executive functions. The thickness of the cerebral cortex is of interest generally because of its continuous changes through development and aging, and its susceptibility to neurodegenerative

diseases (Treble et al., 2013; Sowell et al., 2003; Shaw et al., 2008). Cortical thickness is associated with cognitive and intellectual ability (Haier et al., 2004), especially in developing children (Dubois et al., 2008; Shaw et al., 2006; Wilke et al., 2003), in whom major dynamic and region-specific changes take place. The growth trajectory is roughly an inverted U-shape (Treble at al., 2013; Giedd et al., 1999; Giedd 2004; Gogtay et al., 2004), with different brain lobes peaking at different ages and stages of development (Sowell et al., 2003; 2004; Fischl & Dale, 2000; Gogtay et al., 2004; Epstein., 1986). The initial period of thickness increase peaks during middle childhood (Treble et al., 2013; Gogtay et al., 2004; Shaw et al., 2008), after which there is general cortical thinning into early adulthood, followed by relative stability (Sowell et al., 2003; 2004; Shaw et al., 2008; Raznahan et al., 2011).

Cortical thinning has been reported in previous HIV studies (Masuah et al., 1992; Kallianpur et al., 2011; Thompson et al., 2005). Wiley et al. (1991) attributed cortical neuronal loss and thinning observed at autopsy in HIV encephalitis patients to loss of synaptic density and vacuolation of dendritic processes in the neuropil of the neocortex, suspected to be an indirect effect of HIV infection on the CNS (Wiley et al., 1991). In another study, HIV-related cortical thinning in key nodes for emotional and cognitive processing was significantly correlated with psychomotor speed (Kallianpur et al. (2011). Even in a cohort on ART, cortical thinning of 15 percent in the sensory, motor and premotor cortices was observed, which correlated with immune system deterioration, and cognitive and motor deficits (Thompson et al., 2005).

Although several studies have shown that in adults, HIV infection leads to cortical thinning (Kallianpur et al., 2011; Thompson et al., 2005; Wiley et al., 1991; Masuah et al., 1992), it is not clear what effects HIV and early ART will have on long term neurodevelopment in perinatally-infected children. Studies in HIV+ children have reported region-dependent decreases as well as increases in cortical thickness (Yu et al., 2019; Yadav et al., 2017; Lewis-de los Angeles, 2017). In a previous neuroimaging follow-up study on 7-year-old vertically HIV+ children who received early ART, HIV+ children had thicker cortex than uninfected controls in a small left hemisphere lateral occipital region only (Nwosu et al., 2018). This is consistent with earlier studies that showed the benefit of early ART initiation on neuropsychological performance (Laughton et al., 2012; Lindsey et al., 2007). It remains to be seen whether the longitudinal trajectory cortical thickness is altered in this cohort.

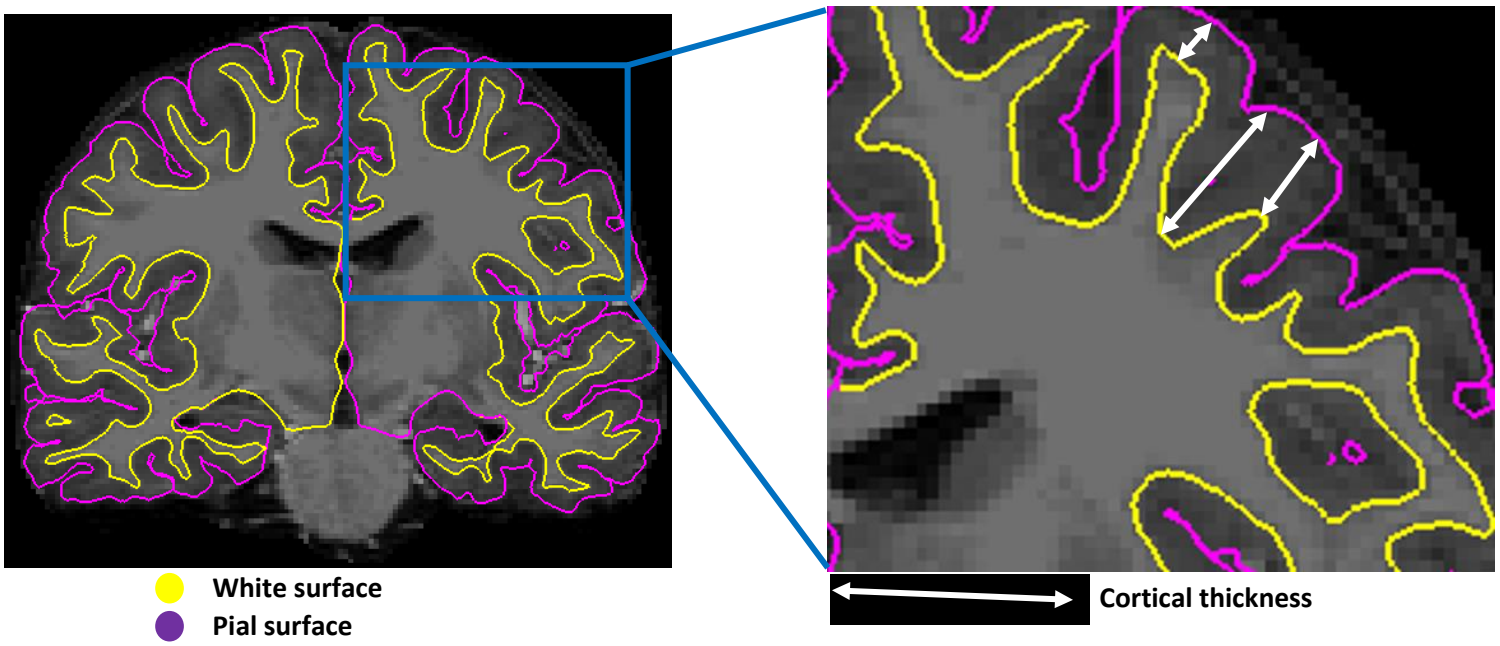

Figure 2.3: Cortical thickness: the distance (indicated by the white line) at each location from the interface between deep white matter and the overlaying grey matter (WM/GM interface – indicated by the yellow line), to the interface between the grey matter and outer CSF space (GM/CSF interface – indicated by the purple line).

2.3.2 Cortical folding (gyrification)

Gyrification is described as the process of evolution of the cortical folding pattern of the brain to form sulcal and gyral regions (Treble et al., 2013; White et al., 2010; Chi et al., 1977; Zilles et al., 1988). This process starts *in utero* as early as the third trimester of pregnancy (Chi et al., 1977; White et al., 2010, Mangin et al., 2010; Armstrong et al., 1995), peaks in early childhood, and continues to develop more slowly into late adolescence/early adulthood. After gyrification changes comes a decrease in cortical complexity and change in brain connectivity (Treble et al., 2013; White et al., 2010; Magnotta et al., 1999). The development process follows a similar inverted U-shaped pattern to cortical thickness, which peaks in late childhood/early adolescence (White et al., 2010; Raznahan et al., 2011, Magnotta et al., 1999). Gyrification is measured by the gyrification index (GI), which is the ratio of the amount of cortex buried in the sulcal fold to the cortex on the visible surface (Schaer et al., 2012; White et al., 2010) as shown in **Figure 2.4**. When GI is measured for a localized region of interest it is known as local gyrification index (LGI).

The cortical grey matter contains neuronal cells bodies and performs complex higher order neuronal signal processing (White et al., 2010; Kallianpur et al., 2011; Thompson et al., 2005[a]), while the subcortical white matter consists of the axonal branches of these cells and facilitates the transmission and reception of neuronal signals (Kallianpur et al., 2011; Thompson et al., 2005[a]). Fitting a larger number of cell bodies into a smooth, thicker cortex would increase brain size and volume (Zilles et al., 1988; White et al., 2010; Sowell et al., 2002). The folding pattern according to a mechano-tensile theory

increases the surface area of the cortical grey matter (Magnotta et al., 1999; Armstrong et al., 1995; Sowell et al., 2003; 2004) allowing a compact grey matter structure and ensuring efficient organization of neural connectivity (Armstrong et al., 1995; White et al., 2010; Magnotta et al., 1999). Hence, cortical folding (gyrification) may be important for higher order activities and may also have implications for neuropsychological skills and intelligence especially in developing children.

There are many theories of the mechanism by which the gyral and sulcal regions are generated. The most popular proposes that the most connected neurones aggregate together, which leads to the buckling of that region, and formation of gyri, while the most dispersed neuronal cells tend to pull away from each other forming the sulci (Magnotta et al., 1999; White et al., 2010). If this is true, it is reasonable to conclude that gyral and sulcal formation continues to change throughout life, as axonal pruning occurs and new connections are made while old ones are disconnected, leading to variations in cortical folding formation at different ages, between sexes, as well as in different regions of the brain (White et al., 2010; Zille et al., 1988; Magnotta et al., 1999). The timeous development of gyrification in children may be important in acquiring skills needed for the rest of their lives. The effect of early ART initiation on the normal pattern of cortical folding development in perinatal HIV-infected children therefore requires investigation.

Compared to cortical thickness, gyrification is less frequently investigated in diseases affecting brain structure. However, it has shown promise for investigating morphological changes associated with neuronal development, neurodegenerative disorders and disease patterns in the brain (Magnotta et al., 1999; White et al., 2010) and may be sensitive to the effects of HIV and HIV-related events (Lewis-de los Angeles, 2017; Hoare et al., 2018; Nwosu et al., 2018). Gyrification has been investigated together with cortical thickness in disease conditions like spina bifida myelomeningocele (Treble et al., 2013) and has been found to be related to IQ and motor dexterity even in healthy children (Treble et al., 2013; White et al., 2010).

Gyrification has been found to be altered in psychiatric disorders; in schizophrenia flatter sulci and steeper gyri have been observed (White et al., 2003), while in velo-cardio-facial syndrome decreased gyrification has been observed in frontal and parietal regions (Schaer et al., 2006) as well as greater gyral complexity in the occipital regions (Bearden et al., 2009). Cao et al. (2017)[b] showed that there is a relationship between number of episodes in bipolar disorder and alterations in brain gyrification. Increased cortical complexity in Williams syndrome has also been shown (Thompson et al., 2005[b]). Kesler et al. (2006) also showed increased temporal lobe gyrification due to preterm birth. Although the development of gyrification in healthy children and adolescents (Cao et al., 2017[a]; White et al., 2010), as well as variation in gyrification between sexes (Luder et al., 2004; Magnotta et al., 1999) has previously been demonstrated, not much is known about the developmental trajectory of gyrification in pediatric HIV infection. Incorporating gyrification into longitudinal morphometric investigations of

HIV-infected children may provide further understanding of the effects of HIV and early ART on structural neurodevelopment.

To our knowledge, studies are yet to investigate the longitudinal long-term effects of HIV and/or ART on gyrification, especially during the critical period of neurodevelopment in children. A recent cross-sectional study of effects of HIV infection and early ART on brain morphometry in children at age 7 years showed that frontal and parietal gyrification is sensitive to HIV infection, while only minor alterations in cortical thickness and regional brain volumes were observed relative to uninfected controls (Nwosu, 2015). Based on those findings, we aimed to determine how early these alterations in gyrification become apparent, by comparing gyrification between children with HIV and controls at age 5 years. We also aimed to investigate the longitudinal development of gyrification in these children to clarify the neurodevelopmental implications of early ART initiation in perinatal HIV.

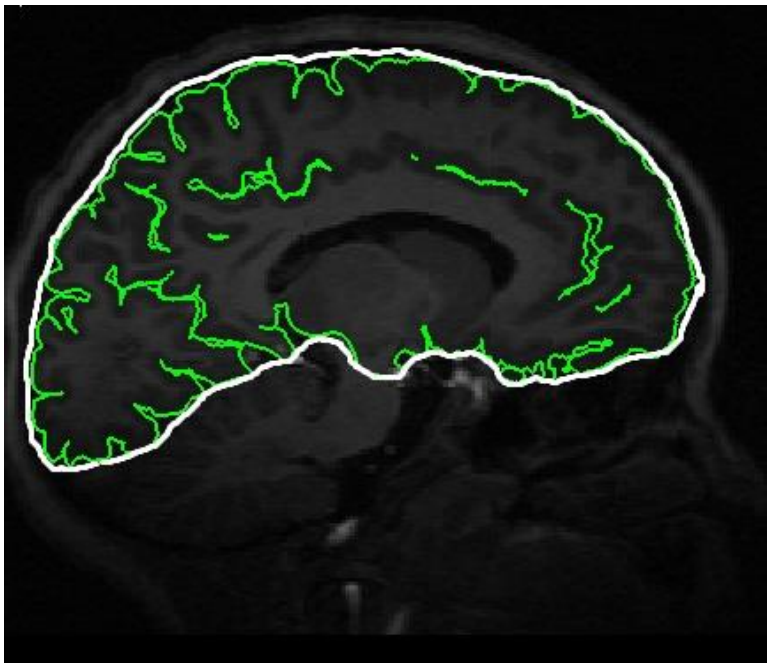

Figure 2.4 Gyrification index (GI): ratio of the folded and convoluted external brain surface (Green line) with the outer surface (White line) excluding the sulci.

2.3.3 Global and regional brain volumes

In adult HIV infection, brain volume reductions are obvious in global grey and white matter, cortical and subcortical grey and white matter (Thompson et al., 2006; Di Scalafani et al., 1997; Becker et al., 2011; Broderick et al., 1993). Subcortical tissues often affected by neuronal atrophy include the corpus callosum, basal ganglia (especially caudate nucleus, putamen, nucleus accumbens, globus pallidum), thalamus, lateral ventricle and hippocampus regions (Di Scalafani et al., 1997; Becker et al., 2011; Epstein et al., 1986). Most studies reviewed by Paul et al. (2002) reported neuronal atrophy and volume reduction of the bilateral caudate nucleus and linked this with neurocognitive impairments, executive dysfunction, and poor memory retention as well as greater disease burden (Raininko et al., 1992; Hall et al., 1996; Jernigan et al., 1993).

In the corpus callosum, HIV infection is associated with regional thinning, myelin damage and increased fluid diffusion, implying poorer white matter integrity (Thompson et al., 2006; Filipi et al., 2001; Ragin et al., 2004; Paul et al., 2002). Corpus callosum thickness has been found to be positively correlated with T-lymphocyte counts, which means that it can be useful in tracking viral disease burden (Thompson et al., 2006). Other studies have also reported increased lateral ventricle volume (Paul et al., 2002; Wachsler-Felder and Golden, 2002; Ances et al., 2012), which is suspected to be because it serves as a channel for the transport of CSF, a major vehicle for viral transmission in the brain (Paul et al., 2002; Kallianpur et al., 2013, Ances et al., 2012).

Neuronal atrophy is similarly associated with pediatric HIV infection. One of its most severe effects in children is global and regional brain volume reduction (Lewis-de los Angeles et al., 2016; 2017; Yadav et al., 2017; Cohen et al., 2016) and enlarged lateral ventricular volume (Assefa et al. 2012; et al., 2001). Neurodevelopmental effects of neuronal atrophy and brain volume reduction include; neurocognitive deficits, memory loss, minor cognitive motor disorder (MCMD), behavioural and emotion-related disorders, and delayed development of mental and intelligence skills (Musielak et al., 2015; Sherr et al., 2014; Paul et al., 2002; Wachsler-Felder and Golden, 2002; Ances et al., 2012). However, there are also reports of greater global and regional gray matter volumes related to HIV infection in children and youth (Sarma et al., 2014; Randall et al., 2017; Blokhuis et al. 2017; Paul et al., 2018). Reasons that have been proposed for these unexpected results include increases in cell size, neural or glial genesis or spine volume (Driemeyer et al., 2005; May et al., 2007). Gray matter hypertrophy may also be due to neuroinflammation induced by HIV viral protein (Kaul et al., 2001; Mattson et al., 2005).

An issue raised in the review by Paul et al., 2002, is the improvement of cognition and white matter abnormalities after ART initiation, without similar structural improvement in the caudate. This highlights the question in children of whether damaging effects of HIV on morphometry are reversible with ART, as well as whether ART can prevent such damage to brain structure when initiated early. In

a recent study comparing HIV-infected children who started early ART and uninfected controls at age 7, most regional brain volumes were not different from those of uninfected controls, except the bilateral putamen and right hippocampus (Nwosu, 2015). This may suggest that early ART initiation in children may protect some of the vulnerable brain tissues from insult caused by HIV infection.

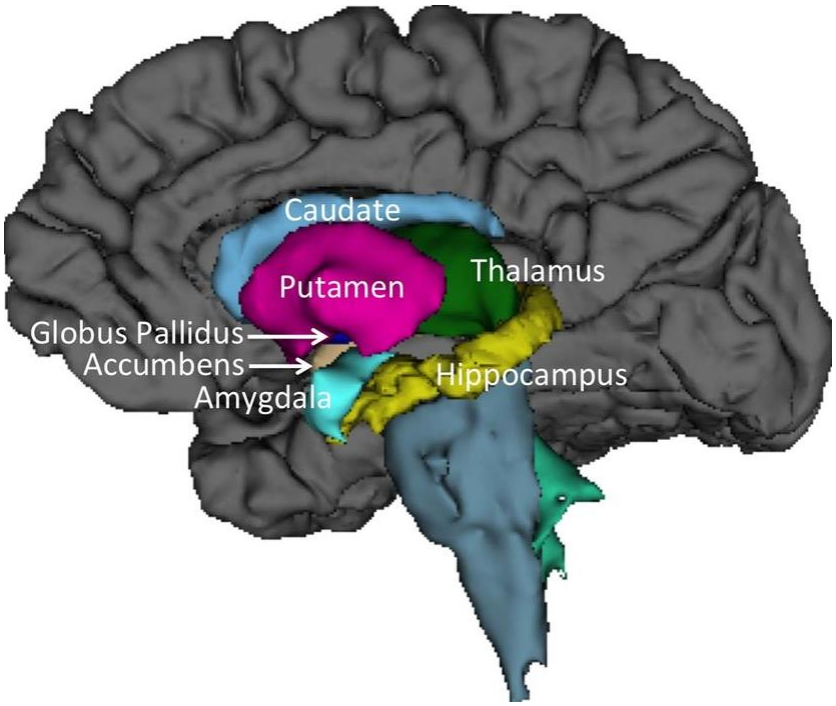

Figure 2.5 Subcortical structures: Some of the key subcortical tissues affected by HIV infection especially in pediatric cohorts. Source: Jung et al., 2014

2.7 Hypotheses

After reviewing existing literature, we hypothesized that:

1. There would be moderate to strong relationship between brain volumes generated from FreeSurfer automated processing and manual segmentation although FreeSurfer may overestimate sub-cortical volumes of interest compared to manual method (Sanchez-Benavides et al., 2010; Wenger et al., 2014).

2. That HIV status-related statistical group comparison would be similar using outputs from both methods, although HIV infection is expected to affect the accuracy of automated segmentation.

3. At age 5 years, because of the beneficial effect of early ART we would observe little or no difference or similar results as in age 7 (Nwosu et al., 2018) of thicker cortex and lower LGIs in HIV-infected children compared to uninfected controls. The difference will be due to residual damage that may persist but is less severe than without early ART.

4. At age 5 years, ART interruption will not affect morphometry development, due to the resilience of children's immune systems, early ART initiation and relatively short duration of ART interruption.

5. At age 5 years, neurodevelopment would be affected by higher viral load, poor immune health before ART and HIV-related encephalopathy leading to regionally lower cortical thickness and gyrification

6. In the longitudinal study, early ART initiation would lead to normal morphometric development, even in regions with HIV-related differences identified in cross-sectional analyses. Furthermore, ART interruption and HIV-related encephalopathy will not impact developmental trajectories.

Chapter 3 – Comparison of manual tracing and automated FreeSurfer segmentation of subcortical brain structures in a cohort of 7-year old HIV-infected children and uninfected controls.

3.1 Introduction

In typical childhood development the brain undergoes rapid changes due to neurodevelopmental processes including cortical pruning, neural rewiring and myelination (Shaw et al., 2008; Sowell et al., 2003; 2004; White et al., 2010). During the critical period from embryo through to adolescence (Rice et al., 2000), pediatric brain is particularly vulnerable to damage from a range of infectious and other diseases (Giedd et al., 2010; Granato et al., 2018; Friedman et al., 2015; Richards et al., 2013) as well as environmental factors (Weiss et al., 2000; Rice et al., 2000; Lyden et al., 2016). Perinatal HIV infection, for instance, is known to lead to structural brain alterations in children, including ventricular enlargement and sulcal widening (van Arnhem et al., 2013), cortical thinning (Yadav et al., 2017; Lewis-de los Angeles et al., 2017), basal ganglia calcification (Govender et al., 2011), white matter lesions/abnormalities and atrophy (van Arnhem et al., 2013; Uban et al., 2015; Ackermann et al., 2016; Sarma et al., 2014), neural atrophy and brain volume alterations (Yadav et al., 2017; Lewis-de los Angeles et al., 2017, Sarma et al., 2014).

To quantify disease-related volumetric alterations of subcortical structures, manual segmentation is considered the most accurate and reliable method, and therefore the "gold standard" (Pardoe et al., 2009; Rodionov et al., 2009; Barnes et al., 2009; Boccardi et al., 2011; Grimm et al., 2015; Wenger et al., 2014). It involves the manual delineation of brain structures on anatomical boundaries based on a pre-defined atlas or protocol. Manual brain segmentation, although more reliable than automated methods, is tedious, time intensive and requires expert knowledge of the neuroanatomy of the structure of interest to ensure accurate segmentation (Schoemaker et al., 2016; Grimm et al., 2015; Fraser et al., 2018). Moreover, in the era of large MRI datasets, manual segmentation is inefficient and can introduce inconsistencies in boundary delineation due to human and fatigue-related biases (Lyden et al., 2016; Akudjedu et al., 2018) and non-uniformity if more than one person is tracing a dataset.

The large MRI datasets used in neuroimaging research require automated algorithms that can perform segmentation faster and delineate brain structures efficiently and objectively. Automated segmentation is consistent, uniform and allows for batch processing of large amounts of data based on algorithmically-defined anatomical boundaries. In addition, less time is required for segmentation in

comparison to manual delineation. There exist several user-friendly and easily accessible automated segmentation tools. FreeSurfer (http://www.freesurfer.net/) is a commonly-used tool that performs segmentation by assigning each voxel a structural label derived from a manually segmented training data set using Markov random field-based probabilistic estimation (Fischl et al., 2002). The FreeSurfer atlas was generated from a training data set of 39 manually segmented adult brains (aged 18-87 years) (Sabuncu et al., 2010; Fischl et al., 2002; 2004; Makris et al., 2004). Nevertheless, FreeSurfer is currently also used for investigating pediatric brain structures (e.g. Barch et al., 2019; Nwosu et al., 2018; Shiohama et al., 2019; Harrach et al., 2019), which may not have the same size and anatomical boundaries as their adult counterparts (Casey et al., 2008; Shaw et al., 2008; Sowell et al., 2003; 2004).

Studies on the reliability and validity of automated segmentation tools have shown outputs to be comparable to manually delineated brain volumes (Morey et al., 2009; Fischl et al., 2002) but focus mostly on adult cohorts (Akudjedu et al., 2018; Dewey et al., 2010; Wenger et al., 2014). Key validation measures for comparison between segmentation methods are spatial overlap between techniques, measures of segmented volume agreement and consistency (e.g. correlation) between techniques, similarity of contralateral structure volumes (Dewey at al 2010) or comparison of associations between a variable of interest and, manually and automatically derived brain volumes (Lyden et al., 2016). The similarity of outputs from automated segmentation and manual delineation depends on the structure being quantified, the technique or protocol used for segmentation and the neuroanatomical characteristics of the study population (Schoemaker et al., 2016; Sanchez-Benavides et al., 2010). Mostly moderate to strong (r=0.45-0.87) relationships have been shown between FreeSurfer outputs and manual techniques in the hippocampus (Cherbuin et al., 2009; Sánchez-Benavides et al., 2010), amygdala (Schoemaker et al., 2016; Grimm et al., 2015), and caudate nucleus (Akudjedu et al., 2018; Dewey et al., 2010). However, there may be greater differences between automated and manual segmentation techniques in the presence of atrophy, as well as an age-differential bias (Sanchez-Benavides et al., 2010; Wenger et al., 2014).

There is relatively little evidence of the reliability and accuracy of automated segmentation tools in children, and the few existing studies have focused mainly on the hippocampus and amygdala (Lyden et al., 2016; Schoemaker et al., 2016; Bender et al., 2018). Because of the smaller size of children's brains, inter-individual variation in brain size and growth, and differences in the rate of development of different brain structures during childhood (Casey et al., 2008; Shaw et al., 2008; Sowell et al., 2003), automated segmentation may compromise accuracy when used for pediatric brain volume quantification. Volume quantification in children is further complicated by neuropathology (Lyden et al., 2016; Giedd et al., 2010) such as HIV that targets specific brain structures leaving others unaffected. Perinatal HIV infection is known to particularly affect the basal ganglia and deep white matter (Mitchell et al., 2001) and structural alterations in the basal ganglia and corpus callosum (Hoare et al., 2018;

Randall et al., 2017; Nwosu et al., 2018; Wade et al., 2019) have been observed in HIV+ children on antiretroviral therapy (ART). However, to our knowledge, only one study has compared automated and manual segmentation of basal ganglia structures in children (Loh et al., 2016) and none have examined the corpus callosum. Validating the reliability of FreeSurfer for quantifying these subcortical volumes in HIV+ children will further its use for investigating brain volume trajectories during typical development, and in the presence of disease conditions, including HIV.

The aim of the study is to validate the accuracy of FreeSurfer's automated cross-sectional processing stream for segmentation and quantifying of subcortical brain structures in a cohort of 7-year-old children living with HIV. This is achieved by comparing volume measures to those obtained via gold standard manual delineation of the same structures. We focus on the corpus callosum and the basal ganglia structures – comprising caudate nucleus, nucleus accumbens, putamen and globus pallidus – regions that are implicated in pediatric HIV but have received little attention in previous validation studies. Further aims are to investigate whether the results of a group comparison of subcortical volumes between HIV+ and HIV- children would give the same results regardless of method used, and to determine whether there is any interaction of segmentation method and HIV status on output volumes.

We hypothesized a moderate to strong correlation between the outputs of manual segmentation and FreeSurfer, but that FreeSurfer would overestimate volumes of the structures of interest relative to manual tracing (Sanchez-Benavides et al., 2010; Wenger et al., 2014). Regardless, we expected that HIV status group differences would be similar using outputs of either method, even if HIV infection affected the accuracy of automated segmentation.

3.2 Methods

3.2.1 Study participants

Participants in the study are 82 South African children – 42 children living with HIV (HIV+) and 40 uninfected controls (HIV-). HIV+ children were recruited from the Cape Town cohort of the children with HIV early antiretroviral therapy (CHER) clinical trial, who are currently undergoing neurodevelopmental and clinical follow-up.

The original CHER trial was conducted at the Family Clinical Research Unit at Tygerberg Children's Hospital, Cape Town. In the trial, children on early time-limited ART were compared to later continuous ART to investigate the outcome of early ART initiation on vertically HIV-infected children. Infants with CD4 percentage ≥ 25% were randomized at age 6 -12 weeks to receive either limited ART– interrupted at 40 or 96 weeks – and restarted treatment when clinical and/or immunological criteria were met, or to commence continuous ART only when they developed HIV symptoms or CD4 percentage dropped below 20% (25% in the first year) as per guidelines at the time (WHO, 2006; Cotton et al., 2013; Violari et al., 2008). All HIV+ children started ART before 76 weeks of age and viral loads were suppressed at the time of scan.

The HIV- controls were recruited from an interlinking vaccine trial (Madhi et al., 2010) and comprised children born to mothers living with HIV (HIV-exposed uninfected, HEU; n=17) and to HIV- mothers (HIV-unexposed; HU; n=23).

3.2.2 Magnetic resonance image (MRI) acquisition

MRI scans of all participants were acquired around about their 7th birthday on a 3T Allegra brain scanner (Siemens, Erlangen, Germany) at the Cape Universities Brain Imaging Centre (CUBIC), according to a previously described scanning protocol (Nwosu et al., 2018) optimized for automated processing of MRI data.

Ethics approval for the study was obtained from the Human Research Ethics Committees of the Universities of Cape Town and Stellenbosch. Parents or guardians of participants gave written informed consent and participants gave their oral assent for the scans.

3.2.3 Manual segmentation.

MRI scans were manually inspected for quality, and low-quality images were excluded. MR images were subsequently manually transformed for anterior commissure-posterior commissure (AC-PC) plane realignment for symmetrical display of all scans with *BrainVoyager* (https://www.brainvoyager.com/) software and converted from DICOM format to Analyze format before manual delineation.

After transformation, images were imported into *MultiTracer* (http://www.bmap.ucla.edu/portfolio/software/MultiTracer/) – a Java-based tool for anatomical segmentation (Wood, 2003) – running on the Windows 10 operating system. Anatomical delineation was performed on a 13-inch Wacom Cintiq Pro display monitor with Wacom stylus pen. All data were segmented at 4X magnification, display brightness of 92, contrast between 13000- and 18000-pixel intensity units (PIU) depending on the structure being traced, with pixel scaling at 1.35. Segmentation was performed with protocols developed by an expert neuroanatomist as described by Randall (2015), Biffen et al. (2018) and Randall et al. (2017).

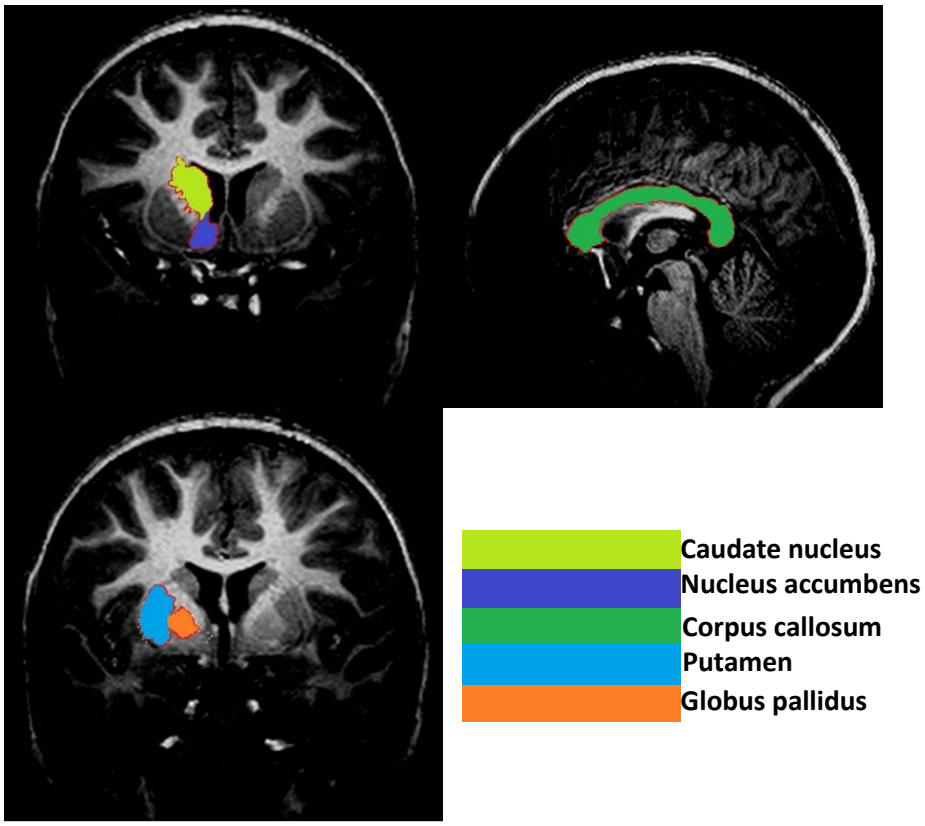

Figure 3.1: Manually segmented subcortical regions of interest where automated and manual brain segmentation techniques were compared in children at 7-years-old.

In the first instance, two trained researchers together traced a selected sample of data to ensure consistency and agreement. Subsequently, both raters traced subsets of the AC-PC aligned data based on the developed protocol while blinded to each other's outputs. Segmented regions of interest are the sagittal area of the corpus callosum, and bilateral basal ganglia regions including caudate nucleus, nucleus accumbens, putamen and globus pallidus (as shown in **Figure 3.1**). The corpus callosum was traced in the sagittal view, caudate nucleus and nucleus accumbens were traced in the coronal view while putamen and globus pallidus were traced in axial and coronal views. Brain volume measures for each subject and each region were extracted from MultiTracer and used for further statistical analyses.

3.2.4 Automated segmentation with FreeSurfer

Automated subcortical segmentation was performed on all MRI scans with FreeSurfer version 6.0 on a Linux Ubuntu version 16.04 LTS machine. Each DICOM image file was converted and reconstructed with the FreeSurfer "recon-all" pipeline. Quality checks were performed on all outputs. Subcortical volume measures for corpus callosum, bilateral caudate nucleus, nucleus accumbens, putamen and globus pallidus for all subjects were extracted with FreeSurfer's asegstats2table command for comparison with manually generated volume measures.

3.2.5 Statistical analyses

All brain volume data generated from manual and automated segmentation were collated and exported to R version 3.4.1 (https://www.r-project.org/) under RStudio version 1.0.143 (2016) for further statistical analyses.

To check the similarity of subcortical tracings by two different tracers, we calculated the Pearson correlation, intra-class correlation (ICC) for consistency and agreement and performed a one sample t-test on the difference between the volumetric outputs from the different tracers.

To investigate differences between the outputs of manual and automated segmentation we computed the percentage volume difference (Δ %) for each structure of interest:

$$\Delta\ \% = ((AV - MV)/MV) * 100$$

where AV – Automated volume
MV – Manual volume

A one sample t-test was performed on the differences. Bland-Altman plots were used to visualize the agreement between methods and the ICC for consistency and agreement were calculated between manual and automated outputs.

Secondly, to investigate the relationship between volume measures from automated and manual techniques, we used scatter plots of manual vs. automated volumes and fitted a least-squares linear regression line for comparison with the line of no difference with slope (s) – = 1 and intercept (i) =0. For each region of interest, we report the goodness-of-fit of the linear regression model (R^2).

To investigate whether selection of a particular segmentation technique would affect the results of a group comparison, we performed analysis of covariance (ANCOVA) comparing brain volumes of regions of interest between HIV+ and HIV- groups and HEU vs. HU groups, and examined the results

from automated and manual techniques. Statistical tests for HIV status group differences in FreeSurfer volume measures were performed accounting for sex and estimated intracranial volume (ETIV). Statistical tests for HIV status group differences in manually segmented data additionally accounted for the two tracers. False discovery rate (FDR) correction was performed to account for multiple testing. We consider an FDR corrected $p<0.05$ statistically significant for all tests.

We further sought to determine whether HIV status influences discrepancies between the two segmentation techniques. The mean difference in regional volumes between the two methods was also computed for HIV+ and HIV- groups separately. The interaction effect of HIV status and segmentation technique on volume measures was investigated with a repeated measure analysis of covariance (ANCOVA). We report the *p*-value of the interaction term.

3.3 Results

After excluding the MRI scan of one HIV+ subject for poor image quality due to motion, we present results for 81 children. **Table 3.1** shows the demographic data for all participants. Groups were similar, except that there were fewer Afrikaans-speaking (mixed ancestry) children in HIV+ and HEU groups.

Table 3.1: Sample demographics.

	HIV+	HIV-		f^b or χ^2	*p*-value
		HEU	HU		
Sample size (*N*)	41	17	23		
Age at scan (years)	7.24 (0.18)	7.22 (0.14)	7.25 (0.15)	0.18	0.84
Number of males (% males)	19 (46)	10 (59)	12 (53)	0.78	0.68
Home language (Afrikaans /Xhosa)	5/36	1/16	7/16	5.29	0.07
Birth weight (g)	3136 (414)	3175 (585)	3079 (395)	0.24	0.79
Estimated total intracranial volume (ETIV) (cm^3)	1427 (111)	1449 (145)	1427 (124)	0.22	0.80
Neuropsychological measures					
KABC[a] II scores accessed at ages 7 years					
Mental processing index (MPI)	73 (8.40)	74 (9.52)	76 (10.82)	0.97	0.38
Non-verbal index (NVI)	74 (11.02)	73 (12.42)	76 (11.64)	0.41	0.66

[a]Kaufman Assessment Battery for Children: second edition composite [b]f-values are for 3-way ANOVA

Table 3.2 shows the comparison and agreement of outputs for 29 subjects manually segmented by both tracers for all the regions of interest. There is strong correspondence between the two tracers' outputs as shown by the Pearson's correlation co-efficient (*r*) and ICCs, with lowest agreement for the globus pallidus. Percentage differences between the two tracers in all regions were in single digits except right globus pallidus with a difference of 12.33%.

Table 3.2: Relationship between raters outputs (N= 29; raters = 2).

Brain regions	Pearson correlation		One-sample t-test				Percentage difference	Intra class correlation (ICC) (Consistency)		Intra class correlation (ICC) (Absolute agreement)	
	R	*p*-value	Mean diff. (mm^3)	SEM[a]	*t*-value	*p*-value	Δ%	co-efficient	*p*-value	co-efficient	*p*-value
L caudate nucleus	0.90	<0.001	76.78	25.82	2.05	0.05	2.12	0.90	<0.001	0.89	<0.001
R caudate nucleus	0.96	<0.001	32.15	12.15	1.83	0.08	0.82	0.98	<0.001	0.98	<0.001
L nucleus accumbens	0.83	<0.001	-29.53	13.50	-2.19	0.04	-6.08	0.82	<0.001	0.80	<0.001
R nucleus accumbens	0.98	<0.001	-6.10	3.33	-1.83	0.08	-1.24	0.99	<0.001	0.98	<0.001
Corpus callosum	0.93	<0.001	-3.50	2.97	-1.07	0.29	1.94	0.93	<0.001	0.93	<0.001
L putamen	0.96	<0.001	-138.42	26.34	-5.07	<0.001	-2.94	0.96	<0.001	0.93	<0.001
R putamen	0.95	<0.001	-151.07	30.30	-4.81	<0.001	-3.21	0.96	<0.001	0.92	<0.001
L globus pallidus	0.67	<0.001	-21.83	29.65	-0.71	0.48	-1.39	0.66	<0.001	0.66	<0.001
R globus pallidus	0.60	<0.001	186.43	31.95	5.63	<0.01	12.33	0.59	<0.001	0.41	0.05

ICC is based on Shrout et al., 1979; Bartko et al., 1966; McGraw et al., 1996 [a] Standard error of the mean

3.3.1 Differences between manual and automated output volumes

Using manually segmented data as the reference, **Table 3.3** and the Bland Altman plots in **Figure 3.2** show that automated segmentation tends to overestimate volumes of all regions except the right caudate nucleus, which showed the smallest discrepancy between segmentation methods. The bilateral nucleus accumbens, corpus callosum and right globus pallidus had the lowest absolute agreement. There was a generally high ICC for consistency, particularly for the putamen.

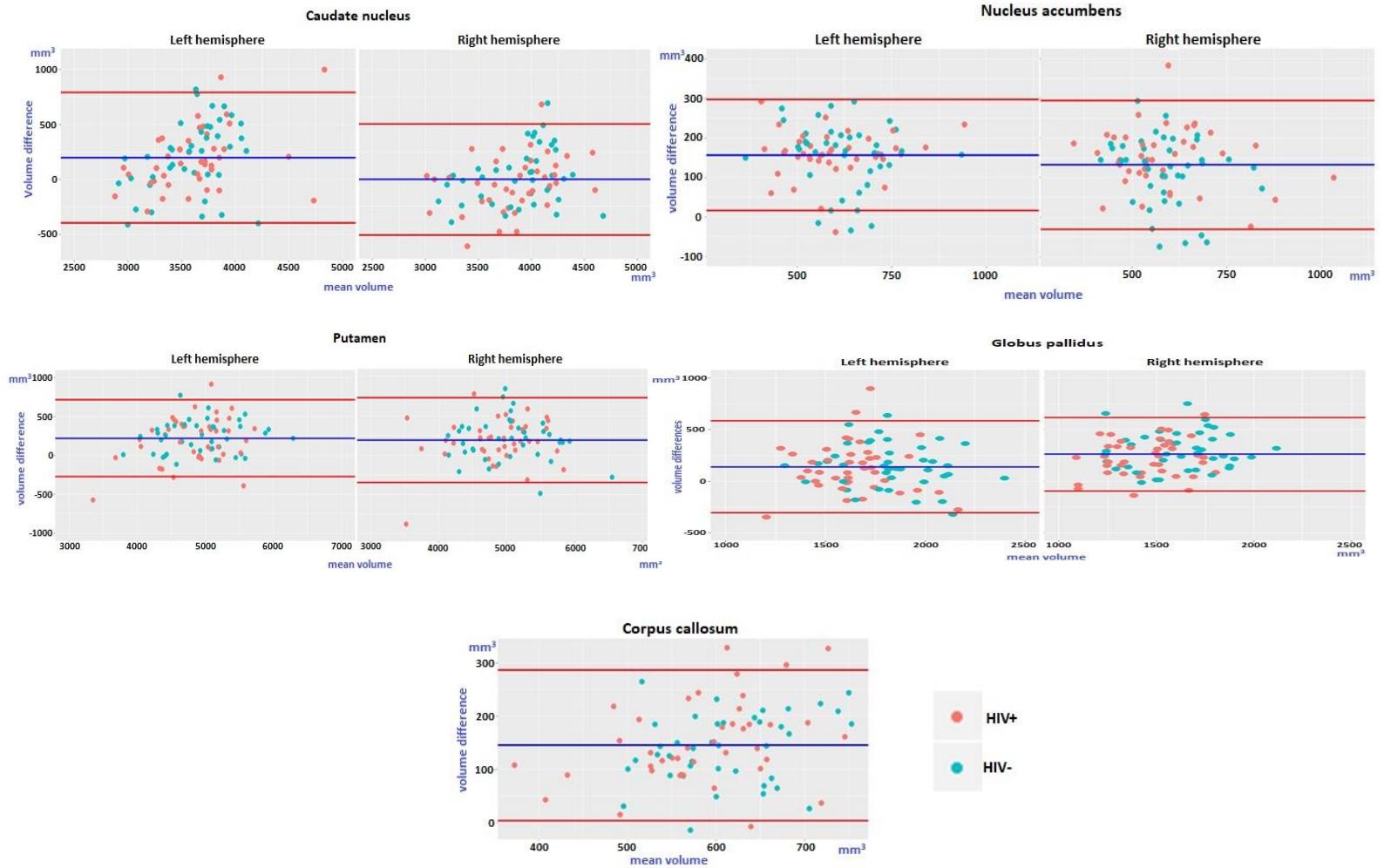

Figure 3.2: Bland-Altman mean-difference plots for automated compared to manual segmentation. The blue line on each plot is the mean volume difference (bias) while the red lines on each plot are the 95% limits of agreement.

Table 3.3: Differences in regional volumes between automated and manual techniques (N=81).

Brain regions	Mean difference (SE) mm^3	Δ %	*t*-value	*p*-value	Intra class correlation (ICC) (Consistency)		Intra class correlation (ICC) (Absolute agreement)	
					co-efficient	*p*-value	co-efficient	*p*-value
L caudate nucleus	196 (34)	5.59	5.83	<0.001	0.72	<0.001	0.64	<0.001
R caudate nucleus	-7 (29)	-0.20	-0.27	<0.001	0.81	<0.001	0.81	<0.001
L Nucleus Accumbens	157 (8)	29.58	19.63	<0.001	0.82	<0.001	0.44	0.11
R Nucleus Accumbens	132 (9)	25.17	14.24	<0.001	0.77	<0.001	0.49	0.08
Corpus callosum	145 (8)	27.54	18.08	<0.001	0.64	<0.001	0.26	0.15
L Putamen	219 (28)	4.59	7.82	<0.001	0.90	<0.001	0.83	<0.001
R Putamen	189 (31)	3.90	6.17	<0.001	0.89	<0.001	0.84	<0.001
L Globus Pallidus	138 (25)	8.26	5.46	<0.001	0.63	<0.001	0.56	<0.001
R Globus pallidus	260 (20)	18.53	12.88	<0.001	0.72	<0.001	0.46	0.07

SE – standard error Δ % - percentage volume difference

3.3.2 Relationship between automated and manual segmentations

Figure 3.3 shows the scatterplot and least-squares regression line (blue) for automated against manual volumes, the line of no difference (red) for all regions of interest. The highest R^2 (best linear fit) was obtained for the putamen (R^2: left= 0.81, right= 0.78). Overestimation in the automated method vs. manual is apparent for most structures, with points falling one side of the slope=1 line of no difference.

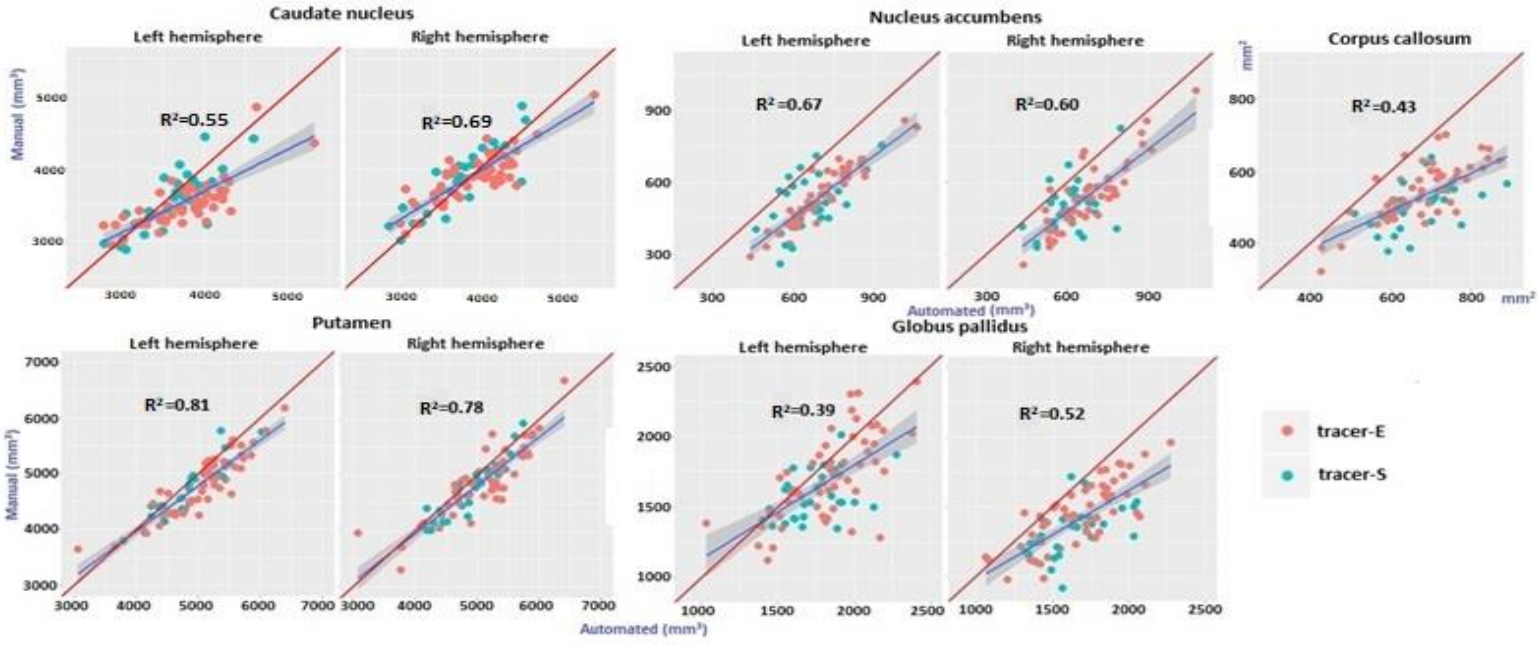

Figure 3.3: Scatter plot of automated and manual segmentation volumes for regions of interest. Least-squares regression line for automated against manual volumes are shown in blue. Red lines have slope=1 and intercept =0. The R^2 value is indicated on each graph.

3.3.3 HIV status and HIV exposure volumetric differences using manual and automated techniques

Analysis of group differences between HIV+ and HIV- children showed similar results using automatically or manually traced volumes (**Table 3.4**). There were no significant differences between HIV+ and HIV- groups in bilateral caudate nucleus, nucleus accumbens and putamen using either segmentation method. Similarly, both techniques showed that HIV- children had larger globus pallidi than HIV+ children, which remained significant even after multiple comparison correction. In manually-segmented data HIV- children showed larger corpora callosa than HIV+ children but this difference did not survive multiple comparison correction and was not detected using the volumes from automated segmentation. In all five brain regions of interest there was no difference between HEU and HU children using either manual or automated segmentation techniques.

Table 3.4: Subcortical volume differences between HIV+ and HIV- groups using automated and manual techniques N=81 (41 HIV+, 17 HEU, 23 HU).

Brain regions	Manual				Automated			
	HIV+ Mean (std.)	HIV- Mean (std.)	*p*-value	FDR Adjusted *p*-value	HIV+ Mean (std.)	HIV- Mean (std.)	*p*-value	FDR Adjusted *p*-value
L caudate nucleus	3531 (373)	3494 (319)	0.64	0.72	3721 (481)	3696 (423)	0.74	0.75
R caudate nucleus	3893 (404)	3865 (362)	0.74	0.74	3855 (501)	3888 (430)	0.67	0.75
L Nucleus Accumbens	515 (122)	544 (120)	0.26	0.45	672 (126)	699 (108)	0.26	0.41
R Nucleus Accumbens	510 (145)	535 (113)	0.34	0.45	658 (135)	650 (95)	0.75	0.75
Corpus callosum	511 (78)	543 (69)	0.04**	0.12	661 (103)	681 (84)	0.27	0.41
L Putamen	4732 (496)	4816 (550)	0.35	0.45	4936 (576)	5051 (576)	0.24	0.41
R Putamen	4784 (546)	4934 (594)	0.12	0.27	4964 (601)	5134 (560)	0.09*	0.27
L Globus Pallidus	1581 (240)	1756 (274)	<0.001**	0.003**	1709 (231)	1902 (246)	<0.001**	<0.001**
R Globus pallidus	1339 (199)	1470 (237)	<0.001**	0.005**	1566 (227)	1764 (248)	<0.001**	<0.001**
	HEU	HU			HEU	HU		
L caudate nucleus	3529 (389)	3469 (262)	0.56	0.93	3799 (435)	3619 (407)	0.12	0.54
R caudate nucleus	3909 (418)	3832 (320)	0.51	0.93	3983 (450)	3817 (410)	0.12	0.54
L Nucleus Accumbens	536 (110)	550 (129)	0.71	0.93	703 (74)	696 (129)	0.81	0.83
R Nucleus Accumbens	551 (122)	523 (107)	0.42	0.93	661 (106)	642 (88)	0.52	0.83
Corpus callosum	546 (62)	540 (79)	0.76	0.93	698 (93)	670 (78)	0.22	0.66
L Putamen	4810 (681)	4821 (448)	0.90	0.93	5034 (715)	5064 (465)	0.83	0.83

R Putamen	4943 (692)	4928 (526)	0.93	0.93	5095 (647)	5163 (499)	0.60	0.83
L Globus Pallidus	1734 (344)	1772 (215)	0.51	0.93	1913 (256)	1895 (244)	0.74	0.83
R Globus pallidus	1435 (304)	1497 (176)	0.22	0.93	1789 (289)	1745 (218)	0.41	0.83

*p<0.1 **p<0.05

3.3.4 Does HIV status influence differences between the two segmentation techniques?

Table 3.5 shows the mean differences between the two techniques (manual - automated) in HIV+ and HIV- children separately for all regions of interest. Repeated measures ANCOVA showed that segmentation technique did not interact significantly with HIV status in any of these regions as shown by p-value of the interaction term in **Table 3.5**.

Table 3.5: Mean difference comparison between HIV+ and HIV-, and interaction effects between HIV status and segmentation technique (N=81).

Brain regions	HIV+ Mean diff. (std.)	HIV- Mean diff. (std.)	p-value for HIV status and segmentation method interaction term in repeated measures ANCOVA
L caudate nucleus	- 191 (281)	- 202 (327)	0.93
R caudate nucleus	38 (259)	- 23 (262)	0.65
L Nucleus Accumbens	-158 (60)	-155 (83)	0.41
R Nucleus Accumbens	-147 (76)	-115 (88)	0.95
Corpus callosum	151 (78)	139 (66)	0.66
L Putamen	-204 (293)	-235 (204)	0.86
R Putamen	-179 (280)	-200 (275)	0.91
L Globus Pallidus	-128 (242)	-147 (213)	0.81
R Globus pallidus	-228 (178)	-293 (182)	0.36

3.4 Discussion

In this study we compared an automated segmentation tool, FreeSurfer, to manual tracing of subcortical structures in a 7-year-old pediatric cohort made up of children living with HIV and uninfected controls. Our study adds to the limited knowledge on the reliability of FreeSurfer for automated brain segmentation in children (Loh et al. 2016, Schoemaker et al., 2016), both in healthy controls and those with HIV.

3.4.1 Consistency and agreement of subcortical volumes between methods

We found moderate to strong Pearson correlations (r=0.63–0.90) between FreeSurfer outputs and manual segmentation across the structures considered, as well good consistency (*ICC*=0.63–0.90). Previous studies have similarly shown that FreeSurfer outputs are comparable with manual segmentation (e.g. Akudjedu et al., 2018; Fraser et al., 2018; Dewey et al., 2010), although most strongly recommend visual inspection and manual editing of FreeSurfer outputs (Dewey et al., 2010; Schoemaker et al., 2016). We found that absolute agreement (*ICC*=0.26 – 0.84) was lower than consistency and was lowest for the nucleus accumbens, corpus callosum and globus pallidus, which unlike other structures, showed a mean volume difference between methods of greater than 5%. The poor agreement between automated and manual segmentation in the nucleus accumbens may be due to different protocols for selection of a separation boundary between it and surrounding structures, since this is defined algorithmically rather than anatomically (Biffen et al., 2018; Randall et al., 2017). This is supported by the high inter-rater reliability for the manually traced nucleus accumbens. The globus pallidus on the other hand showed low agreement and consistency between tracers as well as between methods.

The lower absolute agreement between manual and automated segmentation was largely due to FreeSurfer overestimating the volumes of structures including the putamen, nucleus accumbens and globus pallidus, as well as the left caudate nucleus. Volume overestimation of the hippocampus and amygdalae has frequently been noted (Dewey et al., 2010, Schoemaker et al., 2016; Cherbuin et al., 2009; Nugent et al., 2013; Pipitone et al., 2014), and is attributed to the more liberal structure boundaries in FreeSurfer's segmentation algorithm (Grimm et al., 2015; Wenger et al., 2014). A handful of studies have also reported volume overestimation in the basal ganglia, including the putamen and caudate nucleus (Nugent et al., 2013; Perlaki et al., 2017; Makowski et al., 2018; Dewey et al., 2010), globus pallidus (Nugent et al., 2013, Makowski et al., 2018) and nucleus accumbens in healthy adult cohorts and in various disease conditions including HIV (Dewey et al., 2010).

Akudjedu et al. (2018), however, showed that despite overestimating hippocampus volume, FreeSurfer underestimated caudate nucleus volumes compared to manual segmentation. Similarly, in children FreeSurfer has been found to overestimate volumes of the nucleus accumbens and putamen compared

to manual tracing, but not the caudate nucleus and globus pallidus (Randall 2015, Loh et al. 2016). Interestingly, although we observed overestimation of the left caudate nucleus, we found very little mean difference between right caudate nucleus volumes from automated and manual segmentations. The right caudate nucleus was also larger than the left in this sample of subjects, which might have made it easier to trace accurately by hand, as suggested by the fact that inter-rater reliability was higher for the right caudate. Alternatively, its larger size may be more similar to that of an adult's and FreeSurfer's overestimation of the left caudate volume may be an indication that automated methods are less able to capture developmental asymmetry.

It should be noted that automated software is continually being improved and all the aforementioned comparison studies have used FreeSurfer version 5.3 or older. FreeSurfer version 6.0 is known to differ from older versions (Bigler et al., 2018) and produces outputs that are closer to those from manual segmentation, even in children. In studies that use older FreeSurfer versions, percent differences between manual and automated volumes were ~65% for the globus pallidus (Makowski et al., 2018), -17% (Akudjedu et al., 2018) and 5% (Perlaki et al., 2017) for the caudate, and 10-15% for the putamen (Loh et al., 2016, Perlaki et al., 2017), whereas in the current study using FreeSurfer 6.0 the caudate and putamen were both overestimated by less than 5% relative to manual segmentation.

The accuracy of an automated tool is more severely affected by variable errors, but consistent systematic errors in automated segmentation outputs can be minimized or corrected for afterwards (Dewey et al. 2010). Irrespective of the slight bias for larger structures using FreeSurfer, we found good consistency between methods, suggesting that the ability to capture group differences might be preserved. Dewey et al. (2010) reported that FreeSurfer's consistent overestimation was reflected in a lower sample standard deviation in many subcortical structures than the Individual Brain Atlases using Statistical Parametric Mapping (IBASPM) method, which showed less consistent errors relative to manual tracing. By contrast, we found lower standard deviation in the manually segmented caudate nucleus compared to FreeSurfer segmentation. This was apparent in both HIV+ and HIV- groups, implying that it is not an effect of HIV infection. The lower variation could imply greater consistency in manually traced data but could also possibly reflect FreeSurfer's robustness to pick up subtle inter-individual variations in brain structures that are known to exist in younger children (Casey et al., 2008; Shaw et al., 2008; Sowell et al., 2003; 2004; White et al., 2010). Fatigue and human bias in deciding anatomical boundaries may lead to inaccurate delineation if the protocol designed for segmentation is not flexible enough to capture inter-subject variation, particularly for complex structures such as the caudate nucleus. Robust automated tools can maintain accuracy and consistency in delineation of complex boundaries, particularly in large samples of MRI scans (Akudjedu et al., 2018).

3.4.2 Volumetric differences between HIV status groups

Group analysis using manual and automated outputs were largely in agreement. Both manual and automated segmentation methods showed no volume differences between HIV+ and HIV- children in caudate nucleus, nucleus accumbens and putamen, but smaller bilateral globus pallidi in HIV+ children. Manual segmentation showed that the corpus callosum was smaller in HIV+ children, but this result did not survive multiple comparison correction and was not observed using FreeSurfer. This may either represent a type 1 error or reflect greater accuracy and sensitivity of manual tracing. On images from the Siemens Allegra scanner used in this study, the intensity and contrast of arteries in close proximity to the corpus callosum was similar to that of white matter, so that FreeSurfer tended to misclassify arteries as part of the corpus callosum. A software add-on was subsequently developed to address this. Other recommended tools with improved corpus callosum segmentation include **CCSeg** (https://www.nitrc.org/projects/ccseg/; Szekely et al., 1996), **C8** – a standalone MATLAB toolbox for computation of corpus callosum from a high resolution T1 MRI – (https://www.nitrc.org/projects/c8c8; Herron et al., 2012) and other customized techniques (Ardekani et al., 2012; Adamson et al., 2014). The finding of smaller corpus callosum in HIV is, however, consistent with findings of Yadav et al (2017) as well as with a manual tracing study on our cohort at age 5 (Randall et al. 2017). However, in the current study as well as the latter, the protocol for manual tracing of the corpus callosum is restricted to the 3 most central slices in the sagittal view representing a cross-sectional area, differing substantially from the volume that FreeSurfer describes, partitioned into anterior, mid-anterior, posterior, mid-posterior and central segments. This limits comparison between methods, as can be seen from the low between-method ICC for agreement (0.26). It is therefore difficult to draw conclusions about the marginal reduction in corpus callosum size that was found only in the small section that was traced manually.

Although several studies have compared manual and automated segmentation methods, fewer have looked at the relationship between variables of interest (e.g HIV) and subcortical volumes obtained using different segmentation methods. Dewey et al. (2010) found different correlations with HIV clinical variables depending on the segmentation method used. Similarly, in an adolescent cohort Lyden et al. (2016) found that different segmentation methods resulted in different associations between early family aggression and volumes of the hippocampi and amygdalae. Morey et al. (2009) showed that two different automated methods had significant overlap with manual segmentation but found smaller hippocampal volumes in individuals with depression using FreeSurfer and not FSL. However, in first episode psychosis larger striatum and pallidum were found across different methods (Makowski et al., 2018), which is comparable to our finding of smaller globus pallidus with HIV but no other basal ganglia volume differences using both manual and automated segmentation.

In HIV+ adults, basal ganglia volume reductions have been frequently observed (Ances et al., 2102; Aylward et al., 1993; Becker et al., 2011; Wright et al., 2016), although more recent studies find smaller effects as ART has become more effective (O'connor et al., 2018). In contrast to our findings, Randall et al. (2017) using manual tracing in a subset of this cohort at age 5, reported marginally *larger* volumes of left globus pallidus, as well as larger nucleus accumbens and putamen in HIV+ children. Studies using FreeSurfer have also found larger nucleus accumbens (Yadav et al., 2017) and a trend for larger putamen (Blokhuis et al. 2017) in HIV+ children, attributed to inflammation and chronic stress. Interestingly, recent work has shown larger volumes of the caudate and accumbens in HIV+ children under 12 years, with no volume differences among older children (Paul et al., 2018), suggesting that HIV-related enlargement of subcortical structures may not persist at older ages.

The fact that some studies have failed to detect basal ganglia volume changes in HIV+ children on ART, suggests that effects of HIV on the basal ganglia are subtle (Wade et al. 2019). Shape analysis has revealed deformations consistent with localized volume loss of the thalamus, caudate, pallidum, and putamen related to peak HIV viral load (Lewis-de Los Angeles et al., 2016). Pertinent to our globus pallidus finding, Wade et al. (2019) found no basal ganglia volume differences, but a subregion of the globus pallidus that was significantly thinner in HIV+ children (Wade et al. 2019). In addition, lower CD4 count was associated with larger globus pallidus volume. Baseline CD4 count was also positively associated with volume change at follow-up, implying that children with low CD4 counts initially had larger globus pallidus volumes, but these decreased more rapidly within a year than those of children with higher CD4 counts, whose volumes remained stable or increased slightly. A similar pattern of change within the HIV+ children in our cohort might explain our observations of increased globus pallidus volume in HIV+ children at 5 years but decreased volume relative to controls 2 years later.

Immune health depletion and HIV severity affects the basal ganglia probably because of its proximity to the ventricles (Ances et al., 2012; Avison et al., 2004) and may reflect local breakdown of the blood-brain barrier (Avison et al., 2004). Even in children on continuous ART, severe past disease may result in changes in thickness, surface area, volume, and metabolism (Wade et al., 2019; Randall et al., 2017; Blokhuis et al., 2017), which may explain the globus pallidus volume reductions we observe. The basal ganglia are involved in motor control as well as motor learning, executive functions and behaviour (Lanciego et al., 2012; Hall, 2015), suggesting that HIV-related structural alterations in this region may have consequences for these functional domains.

Although in this study we did not find any group differences in putamen volume, we previously reported smaller putamen in HIV+ than HIV- children using FreeSurfer in the same cohort described here (Nwosu et al., 2018). However, the previous study included 24 HIV+ and 10 HIV- children whose scans were not manually traced and therefore did not form part of the current study. The current study also

incorporated data from an additional 5 HIV+ and 8 HIV- children. Although we see a trend for lower right putamen volume in HIV+ children, the reduced sample size and increased variability may have affected our power to detect small volume differences. The globus pallidus, in which we detect an HIV-related volume difference, was not examined in our previous study. It is noteworthy that this difference was detected using both manual and automated segmentation, despite the globus pallidus being the structure with the lowest consistency and agreement between methods, as well as having the lowest inter-rater reliability in manual tracing.

3.4.3 Interaction between segmentation method and HIV status.

Since greater discrepancies between automated and manual segmentation methods can be expected in cases of brain atrophy (Sanchez-Benavides et al., 2010; Wenger et al., 2014), one of the aims of the study was to determine whether HIV-related neuropathology would affect the accuracy of either segmentation method. Repeated measure ANCOVA did not detect a significant interaction between HIV infection and segmentation method, suggesting that either method could be selected for analysis of HIV-related volume alterations.

3.4.4 Limitations

Because no intracranial volume data was obtained for manual segmentation, we used estimated intracranial volume (ETIV) generated from FreeSurfer to control for brain size variation in statistical analyses for manually segmented data. AC-PC alignment was done before manual segmentation but is not part of the protocol for FreeSurfer segmentation as it is not part of the protocol of the automated segmentation. However, we aimed to compare each technique as it is normally performed. Manual segmentation by two tracers may introduce human-related bias. However, tests showed good inter-rater reliability and the effect of tracer was accounted for in all statistical analyses.

3.5 Conclusion

FreeSurfer overestimates volumes of most subcortical structures compared to manual segmentation except for the right caudate nucleus where the difference between methods is small. However, there is moderate to strong consistency between methods; highest in the putamen and lowest in the globus pallidus. This consistency allows very similar results to be obtained from group difference analysis between HIV+ children and HIV- controls, despite systematic volume overestimation by FreeSurfer. FreeSurfer basal ganglia volumes are comparable with those from manual segmentation, even in children, and may be used equivalently for neuroimaging research provided that quality control protocols in the form of visual inspection and manual corrections are implemented. Because of its demands, manual segmentation should be reserved for high precision quantification of brain structural volumes in small samples (Akudjedu et al., 2018).

Chapter 4 – Cortical structural changes related to early antiretroviral therapy (ART) interruption and disease history in perinatally HIV-infected children at age 5 years.

4.1 Introduction

Untreated perinatal HIV infection has severe consequences that include depletion of immunity and permanent neurodevelopmental and cognitive deficits (Weber et al., 2017; Sánchez-Ramón et al., 2003; 2002). High viral load burden in perinatally HIV-infected (pHIV+) children is associated with neurological consequences including HIV encephalopathy (HIVE) (Sánchez-Ramón et al., 2003; 2002). In addition, pHIV+ infants are at greater risk for co-infections including cytomegalovirus (CMV) (Adachi et al., 2018; Kfutwah et al., 2017; Slyker et al., 2009), which itself is a major cause of hearing loss and cognitive impairment (Adachi et al., 2018; Barbi et al., 2006; Manicklal et al., 2013).

International guidelines including the pediatric HIV guideline of the World Health Organisation (WHO 2008; ART Guideline, 2008; PENTA, 2009) have recommended early antiretroviral therapy (ART) initiation as the standard for treatment of pediatric HIV infection. Early ART aims to achieve viral load suppression within the shortest possible time to prevent mortality and severe clinical events in infancy (Ndongo et al., 2018; Crowell et al., 2015; Phongsamart et al., 2014; Violari 2008). Starting ART within the first year of life minimises neurological insult (Weber et al., 2017; Crowell et al., 2015; Puthanakit et al., 2013; 2012). The early treatment strategy has increased survival amongst HIV+ infants and provided protection from at least the short-term clinical and neuropsychological consequences of HIV (Laughton et al., 2013; Cotton et al., 2013; Brahmbhatt et al., 2014).

Several factors predispose to ART interruption. These include poor adherence, stock-outs, ART intolerance due to lack of pediatric ART formulation and pill size. (Dubrocq and Rakhmanina, 2018; Ananworanich et al., 2016; Wamalwa et al., 2016; Ebonyi et al., 2015; Biadgilign et al., 2009). Recently, HIV cure research has employed an intensive monitored antiretroviral pause as the ultimate test for an HIV cure (Ananworanich et al., 2016; Li et al., 2015). However, ART interruption may lead to viral rebound, resistance or neurodevelopmental consequences, especially with a longer period of interruption (Montserrat et al. 2017; Wamalwa et al., 2016; Ananworanich et al., 2016).

ART interruption affects children and adults differently (Lewis et al., 2017; Calin et al., 2016; Ananworanich et al., 2016). In adults and adolescents, since ART plays dual roles of both treatment and prevention of further HIV replication (Calin et al., 2016; Tubiana et al 2002; Ananworanich et al., 2016), interruption may have severe adverse effects (Wamalwa et al., 2016; Ananworanich et al., 2006;

Danel et al., 2006). Long term ART interruption may lead to rapid viral rebound that may not be reversed within at least the first two years of ART resumption, with possible neurological consequences (Calin et al., 2016; Montserrat et al., 2017) and immune health remaining lower than on continuous treatment (Ananworanich et al., 2006; Danel et al., 2006; Lewis et al., 2017). On the other hand, since early treatment prevents many of the adverse effects associated with pediatric HIV (Lewis et al., 2017; Wamalwa et al., 2016; Ananworanich et al., 2016; Bunupuradah et al., 2013[a]), interruption may have little effect on children in the short term (Lewis et al., 2017). Infants' immune systems are also more plastic and dynamic than those of older children and adults (Lewis et al., 2017; Wamalwa et al., 2016) and children restarting ART after a planned interruption are likely to have CD4 recovery similar to children on continuous treatment (Bunupuradah et al., 2013[a]; Lewis et al., 2017). Interruption may, however, affect development, and pHIV+ children may be particularly at risk if ART is interrupted during critical developmental cycles.

In the Children with HIV Early antiRetroviral therapy (CHER) trial, early ART prevented a decline in CD4 count, but did not lead to complete recovery to the CD4 counts seen in uninfected children (Lewis et al. 2017). ART interruption led to a decline in CD4 T-cells, which on resumption of treatment returned to the original levels before interruption. This study concluded that immune health before ART initiation is an important indicator of overall CD4 level and immune health during subsequent development. Early ART initiation helps to stabilize immune health, to the extent that any disturbance due to ART interruption will recover once treatment is resumed. Whether this short-term recovery and dynamism in children will translate to normal neurodevelopment is not known. While timing of first ART initiation and duration on ART before interruption are considered relevant as determining factors for neurodevelopmental insult (Ananworanich et al., 2016; Puthanakit et al., 2013; Bunupuradah et al., 2013[b]), the effect of ART interruption on neurodevelopment in children has not been studied.

Our main aims in this study were, first to investigate the effect of early limited ART followed by ART interruption, on brain morphometry at age 5 years in a subset of children from the CHER study resident in Cape Town. Further, we proposed to determine whether elements of HIV disease history, including HIV viral load and immune health (CD4 percent, CD4/CD8 ratio and CD8 count) at study enrolment and CDC staging, affect neurodevelopment at age 5 years – a critical period in brain development. We aimed to identify which of these factors influence brain morphometry – cortical thickness (CT) and cortical folding, measured via local gyrification indices (LGIs) – in early treated pHIV+ children.

We hypothesized that early ART would prevent structural damage and that there would be little or no morphometric difference between HIV+ and HIV- children. We also predicted no difference between ART interrupted children and children on continuous treatment, due to the resilience of children's immune systems, early ART initiation and relatively short duration of ART interruption. We hypothesized that neurodevelopment would be more strongly influenced by higher viral load and poorer

immune health before starting treatment, as well as occurrence of HIV-related adverse events, and that these factors would be associated with regionally higher cortical thickness and gyrification.

4.2 Methods

4.2.1 Study participants

Study participants were 83 South African children (53 HIV+, 30 uninfected controls (HIV-); age 5.44 ± 0.37 years; 38 boys) from a follow-up study of the CHER trial conducted at the Family Clinical Research Unit at Tygerberg Children's Hospital, Cape Town. In this trial, HIV+ infants with CD4 percentage ≥ 25% were randomized at age 6 -12 weeks to receive immediate limited duration ART followed by planned interruption, restarting when clinical and/or immunological criteria were met, or to start continuous ART only when they developed clinical symptoms or CD4 percentage dropped below 20% (25% in the first year) as per treatment guidelines at the time (WHO, 2006). All HIV+ children started ART before 76 weeks of age and received comprehensive immunological and clinical follow-up. The first line ART regimen consisted of Zidovudine (ZDV) + Lamivudine (3TC) + Lopinavir-ritonavir (LPV/r, Kaletra®) (CHER, 2010; Violari *et al*. 2008; Cotton *et al*. 2013). The HIV-control group was recruited from an interlinked vaccine trial (Madhi et al., 2010) and comprised both children born to HIV+ mothers (HIV exposed uninfected, HEU; n=17) and to HIV- mothers (HIV-unexposed, HU; n=13). The Griffiths Mental Development scales were performed at 5 years of age to assess neurodevelopment.

4.2.2 Image acquisition and analysis

The children completed magnetic resonance imaging at age 5 years using a procedure described previously (Nwosu et al., 2018). Scans were performed without sedation according to protocols approved by the Faculty of Health Sciences Human Research Ethics Committees of both the Universities of Cape Town and Stellenbosch. Parents/guardians provided written informed consent and the children gave oral assent. Viral loads were supressed (<400 copies/mL) at time of scanning in 93.5% of children.

MR images were manually checked and those with poor quality were excluded. The remaining images were processed using the automated stream in FreeSurfer version 6.0 (https://surfer.nmr.mgh.harvard.edu/fswiki/ReleaseNotes), which generates cross sectional morphometric data for all subjects. FreeSurfer outputs were manually checked for errors. Outputs were manually edited and reconstructed if there were minimal errors in cortical segmentation but were excluded completely for major errors. Reconstructed data were sampled to the FreeSurfer average subject template for vertex-wise analysis. The smoothing kernel for cortical thickness analyses was 10mm FWHM; no smoothing was used for LGI.

4.2.3 Vertex-wise analysis of cortical thickness and LGI

Group comparisons of CT and LGIs over the whole brain were performed using FreeSurfer's mri_glmfit function. We examined differences due to HIV status, ART interruption (ART interrupted or continuous), the presence and severity of HIV-related disease (CDC-severe, i.e. CDC class C and severe B, or CDC-mild), and viral load (VL) at enrolment (high: >750,000 copies/mL or low: 400-750,000 copies/mL). In each case, groups were compared to HIV- controls.

Vertex-wise regression analyses of CT and LGI were performed using immune health variables (CD4%, CD4/CD8 ratio, CD8 count) at initial clinical trial study enrolment to investigate whether immune health before ART initiation relates to brain morphometry at age 5 years.

Since HIV+ and HIV- groups differed on age at scan, all analyses were performed adjusting for the age at scan variable. Moreover, since sex-related differences in cortical and sub-cortical structures have been reported in brain development (Wierenga et al., 2017; Fisher et al. 2016), we adjusted for sex. All vertex-wise results were thresholded at an initial uncorrected threshold of $p<0.05$, after which cluster-wise correction for multiple comparisons was performed using precomputed Monte Carlo simulation for a two-tailed test. We report clusters surviving a cluster-wise corrected threshold of $p<0.05$, with no adjustment for the two hemispheres.

Mean LGI and CT for significant clusters generated from the vertex-wise regression analysis were extracted from FreeSurfer and exported to the statistical analysis programming language R (https://www.r-project.org/) for plotting, visualization and computing Pearson's correlation coefficient (r).

4.3 Results

4.3.1 Sample characteristics

We excluded data for 7 HIV+ children due to inaccurate automated cortical segmentation; one HIV- child was excluded due to incomplete MRI acquisition. There were no failures in LGI computation. Biographical data for all participants included in this analysis are presented in **Table 4.1**, and clinical data for HIV+ children in **Table 4.2**. The HIV+ group was significantly younger and comprised only 4% Afrikaans speaking children compared to 38% for the HIV- group. Among the HIV+ children, 21 children (46%) had ART interrupted and restarted. Age at nadir CD4% was lower in the ART uninterrupted children. Viral loads of all except 8 HIV+ children were suppressed (<400 copies/mL) before 2 years of age.

Table 4.1: Biographical data for all participants (N=75).

	HIV+	HIV-	t or χ2	*p*-value
Sample size (*N*)	46	29		
Age at scan (years)	5.3 ± 0.2	5.6 ± 0.4	-4.00	<0.001
Number of males (%)	20 (44%)	16 (55%)	0.56	0.45
Home language (Afrikaans/Xhosa)	2/44	11/18	11.75	<0.001
Birth weight (g)	3066 ± 416	3005 ± 586	0.56	0.58
Estimated total intracranial volume (ETIV) (cm^3)	1373 ± 98	1361 ± 111	0.50	0.62
GMDS[a] assessed at age 5 years				
Performance (EQ) scores	73.9 ± 9.8	76.5 ± 18.5	-0.83	0.41
Practical reasoning (FQ) scores	76.8 ± 8.3	76.2 ± 10.2	0.27	0.78
Sub-scales aggregate (GQ) scores	83.3 ± 6.1	83.1 ± 8.1	0.11	0.91

[a] Griffiths Mental Development Scales – Extended Revised: 2-8 years. All values are mean ± standard deviation except where indicated otherwise. In the design of the CHER trial children who started ART before 12 weeks were interrupted at either 40 or 96 weeks.

Table 4.2: Clinical data for HIV+ children (N=46).

	ART-Interrupted	Continuous ART
Sample size (N)	21	25
Clinical data at ART enrollment(6-8 weeks)		
CD4 count (cells/mm^3)	1934 ± 1080	1777 ± 824
CD4% (cells/mm^3)	35 ± 9	33 ± 10
CD4/CD8 ratio	1.4 ± 0.7	1.3 ± 0.8
CD8 count (cells/mm^3)	1464 ± 645	1706 ± 988
Viral load at enrolment		
High (>750,000 copies/mL)	9 (42.86%)	16 (64%)
Low (400-750,000 copies/mL)	12 (57.14%)	9 (36%)
Suppressed (<400 copies/mL)	0 (0%)	0 (0%)
Clinical data at scan (5 years)		
CD4 count (cells/mm^3)	1072 ± 360	1317 ± 675
CD4% (cells/mm^3)	35 ± 6	37 ± 8
CD4/CD8 ratio	1.2 (0.4) [0.5 – 30.2] [a]	1.2 (0.8) [0.5 – 4.2] [a]
CD8 count (cell/mm^3)	920 ± 398	1069 ± 553

Viral load at scan (Age 5 years)		
High (>750,000 copies/mL)	0 (0%)	0 (0%)
Low (400-750,000 copies/mL)	1 (5 %)	2 (8%)
Suppressed (<400 copies/mL)	20 (95%)	23 (92%)
Other		
Age at ART initiation (weeks)*	8.3 (2.6) [6.6 – 12.0] [a]	20.9 (25.9) [6.3 – 75.7] [a]
ART interruption age (40weeks / 96 weeks)	15 / 6	-
Age of first viral load suppression (weeks)	34.1 (16.8) [30.6 – 213.3] [a]	47.6 (50.4) [29.1 – 169.7] [a]
Duration of ART interruption (weeks)	44.1 (53.9) [5.7 - 299.4] [a]	0
Cumulative duration on ART (weeks)	211± 54	252 ± 24
Nadir CD4% (cells/mm^3)	20 ± 6	20 ± 6
Age at nadir CD4% (weeks)	99 (69) [2 - 278] [a]	30 (30) [5 - 259] [a]
CDC classification		
A	4 (19%)	0 (0%)
B	4 (19%)	4 (16%)
Severe B	0 (0%)	8 (32%)
C	13 (62%)	11(44%)
Unknown	0 (0%)	2 (8%)
HIV encephalopathy diagnosis	4 (19%)	3 (12%)

*All **ART-Interrupted** were initiated before age 12 weeks, **12 Continuous ART** were initiated before 12 weeks, **13 Continuous ART** were initiated after 12 weeks. Values are mean ± standard deviation, except where indicated otherwise.
[a] median (IQR) [range].

Table 4.3 summarises regions showing cortical thickness and gyrification differences compared to uninfected control children for the group comparisons performed.

4.3.2 Effects of HIV status on cortical thickness and gyrification

HIV+ children had significantly thicker cortex than HIV- controls in bilateral frontal and left superior temporal/insular regions (**Figure 4.1a**), and lower gyrification in an overlapping left superior frontal region, as well as bilateral medial orbitofrontal regions extending into rostral anterior cingulate cortex (**Figure 4.1b**).

Table 4.3: Regions showing cortical thickness and gyrification differences compared to uninfected control children (HIV-)

Comparison	CORTICAL THICKNESS			GYRIFICATION		
	Region	**Size (mm^2)**	**MNI peak Coordinates**	**Region**	**Size (mm^2)**	**MNI peak Coordinates**
Infection						
HIV+ vs HIV-	↑ L superior frontal gyrus	3748	(-9, 42, 25)	↓ L superior frontal gyrus	1512	(-7, 19, 58)
	↑ R caudal middle frontal	880	(46, 24, 32)	↓ L medial orbitofrontal extending into rostral anterior cingulate	1138	(-16, 25, -22)
	↑ L superior temporal / insula	1445	(-56, 3, -11)	↓ R medial orbitofrontal extending into rostral anterior cingulate	1664	(15, 35, 21)
Treatment Interruption						
ART interrupted vs HIV-	↑ L rostral middle / superior frontal	974	(-30, 30, 28)	↓ L precuneus	1789	(-9, -74, 45)
				↓ R rostral and caudal anterior cingulate	722	(16, 44, 9)
	↑ R insula	763	(35, -20, 1)	↑ R lateral occipital	1334	(25, -87, -9)
Continuous ART vs HIV-	No differences			↓ R superior frontal gyrus, posteriorly	518	(8, 3, 58)
				↓ R superior parietal lobule	588	(15, -39, 72)
				↑ L fusiform	936	(-41, -53, -12)
				↑ R rostral middle frontal / pars triangularis / pars orbitalis	832	(50, 34, -7)
				↑ R lateral occipital	469	(36, -77, -12)
Early Disease Severity						
CDC-mild vs HIV-	↑ R superior frontal gyrus, anteriorly	1028	(8, 44, 28)	↑ L fronto-temporal-insular region	2498	(-35, -17, 19)
				↑ L inferior temporal	1353	(-56, -45, -19)
				↑ R fusiform	5735	(29, -68, -7)
				↑ R lingual	469	(23, -51, 2)
CDC-severe vs HIV-	↑ L fusiform	774	(-31, -61, -8)	↓ R superior parietal lobule	757	(17, -46, 66)
	↑ R insula	918	(34, -21, 16)	↑ R fusiform	623	(41, -70, -15)
Viral load at Enrolment						
HVL vs HIV-	↑ R caudal anterior cingulate and adjoining superior frontal gyrus	831	(12, 6, 45)	↑ R fusiform	1546	(30, -73, -12)
				↑ R postcentral	653	(48, -23, 48)
LVL vs HIV-	↑ L inferior frontal / insula / anterior superior temporal	836	(-33, -22, 3)	No differences		

↑ greater; ↓ lower; L left; R right; HVL high viral load at baseline; LVL low viral load at baseline

CT: HIV+ vs HIV-

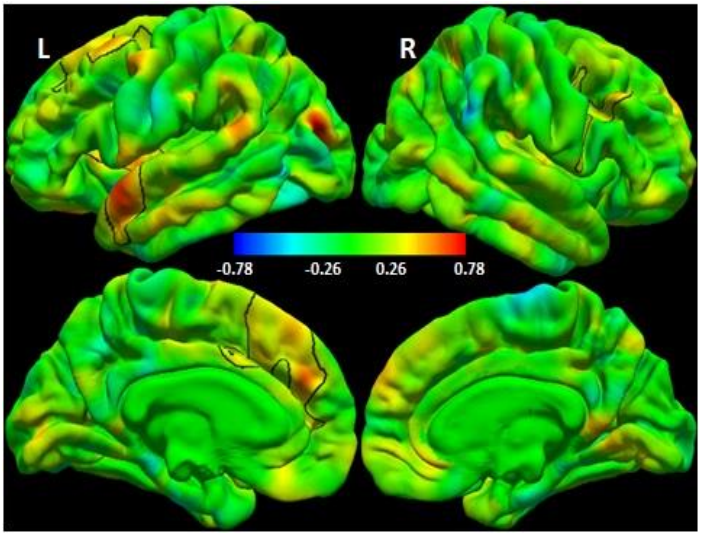

a

LGI: HIV+ vs HIV-

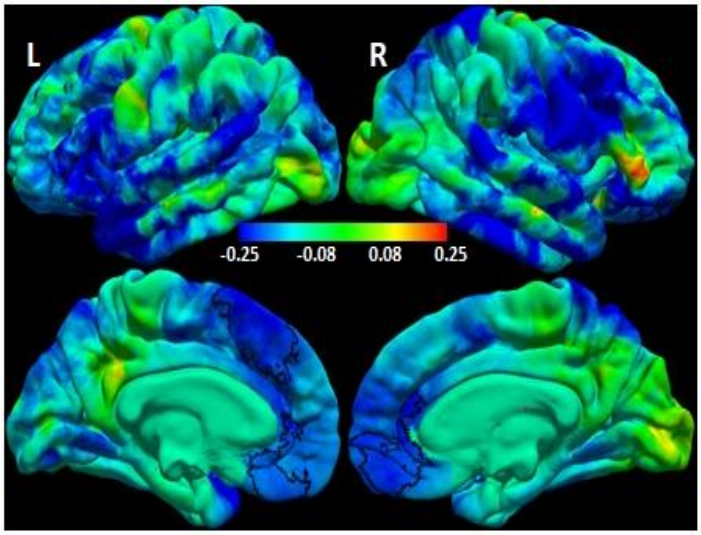

b

Figure 4.1 Colour maps showing parameter estimates for HIV status from vertex-wise unstandardized regression of (a) cortical thickness (CT) and (b) local gyrification indices (LGIs), controlling for sex, age and ethnicity. Positive regression coefficients (red/yellow) indicate HIV+ > controls (HIV-) and negative coefficients (cyan/blue) indicate HIV+ < controls. The colour bar scale applies to both lateral (top) and medial (bottom) views. N=75 (46 HIV+, 29 HIV-). Results reported at a threshold of $p<0.05$, with a cluster size corrected threshold of $p<0.05$.

a) Frontal (left: superior frontal/cingulate/precentral/caudal middle frontal and right: caudal middle frontal) and left superior temporal / insula regions outlined in black indicate where HIV+ children have thicker cortex compared to HIV- controls.

b) The black outlines show the left superior frontal and bilateral medial orbitofrontal / rostral anterior cingulate regions where HIV+ children have smaller local gyrification indices compared to HIV- controls.

4.3.3 Effects of ART interruption on cortical thickness and gyrification

HIV+ children whose treatment had been interrupted had thicker cortex than HIV- controls in left superior/rostral middle frontal and right insular regions (**Figure 4.2a**), while HIV+ children on continuous treatment showed no significant difference in cortical thickness from HIV- controls.

ART-interrupted children showed lower gyrification than controls in left precuneus and right rostral and caudal anterior cingulate regions, but higher gyrification in a right lateral occipital region (**Figure 4.2b).** Children on continuous treatment showed lower gyrification posteriorly in the right superior frontal gyrus and superior parietal lobule than HIV- controls, but higher gyrification in left fusiform, and right rostral middle frontal/pars triangularis/pars orbitalis and lateral occipital regions (**Figure 4.2c**).

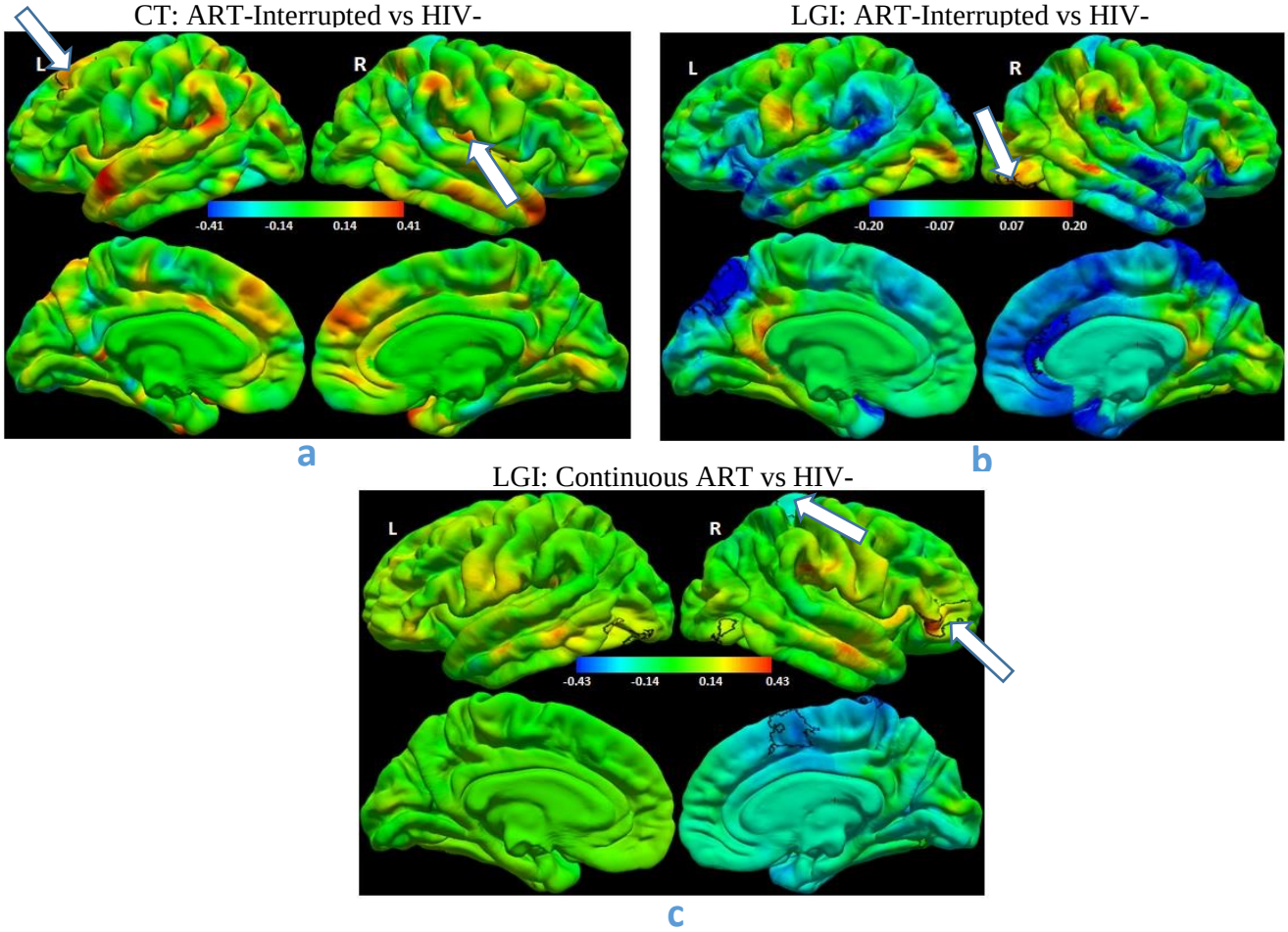

Figure 4.2: Colour maps showing parameter estimates for group (ART-Interrupted or Continuous ART vs. HIV- controls) from vertex-wise unstandardized regression of (a) cortical thickness (CT) and (b, c) local gyrification indices (LGIs), controlling for sex, age and ethnicity. Positive regression coefficients (red/yellow) indicate ART-Interrupted/Continuous ART > controls, and negative coefficients (cyan/blue) indicate ART-Interrupted/ Continuous ART < controls. The colour bar scale applies to both lateral (top) and medial (bottom) views. N=75 (21 ART-Interrupted, 25 Continuous ART, 29 HIV- controls). Results reported at a threshold of $p<0.05$, with a cluster size corrected threshold of $p<0.05$.

a) The left superior / rostral middle frontal region and right insula outlined in black show where ART-Interrupted children have thicker cortex compared to HIV- control children.

b) The left precuneus and right rostral and caudal anterior cingulate regions outlined in black show where ART-Interrupted children have lower gyrification compared to HIV- control children, while higher gyrification is observed in a right lateral occipital region (indicated with a white arrow).

c) The posterior right superior frontal and superior parietal lobule (indicated with a white arrow) regions outlined in black show where Continuous ART children have lower gyrification compared to HIV- control children, while higher gyrification is observed in the left fusiform, right rostral middle frontal / pars triangularis / pars orbitalis (indicated with a white arrow) and lateral occipital regions.

4.3.4 Effects of early disease severity on cortical thickness and gyrification

When compared to HIV- control children, CDC-mild children showed thicker cortex only anteriorly in the right superior frontal gyrus (**Figure 4.3a**), but higher gyrification in a large left fronto-temporal-insular region, as well as left inferior temporal, right fusiform and right lingual regions as shown in **Figure 4.3b**.

In contrast, CDC-severe children showed thicker cortex than HIV- control children in the left fusiform and right insula (**Figure 4.3c**). While there were no gyrification differences in the left hemisphere, CDC-severe children showed lower gyrification in the right superior parietal lobule and higher gyrification in the right fusiform region as shown in **Figure 4.3d**

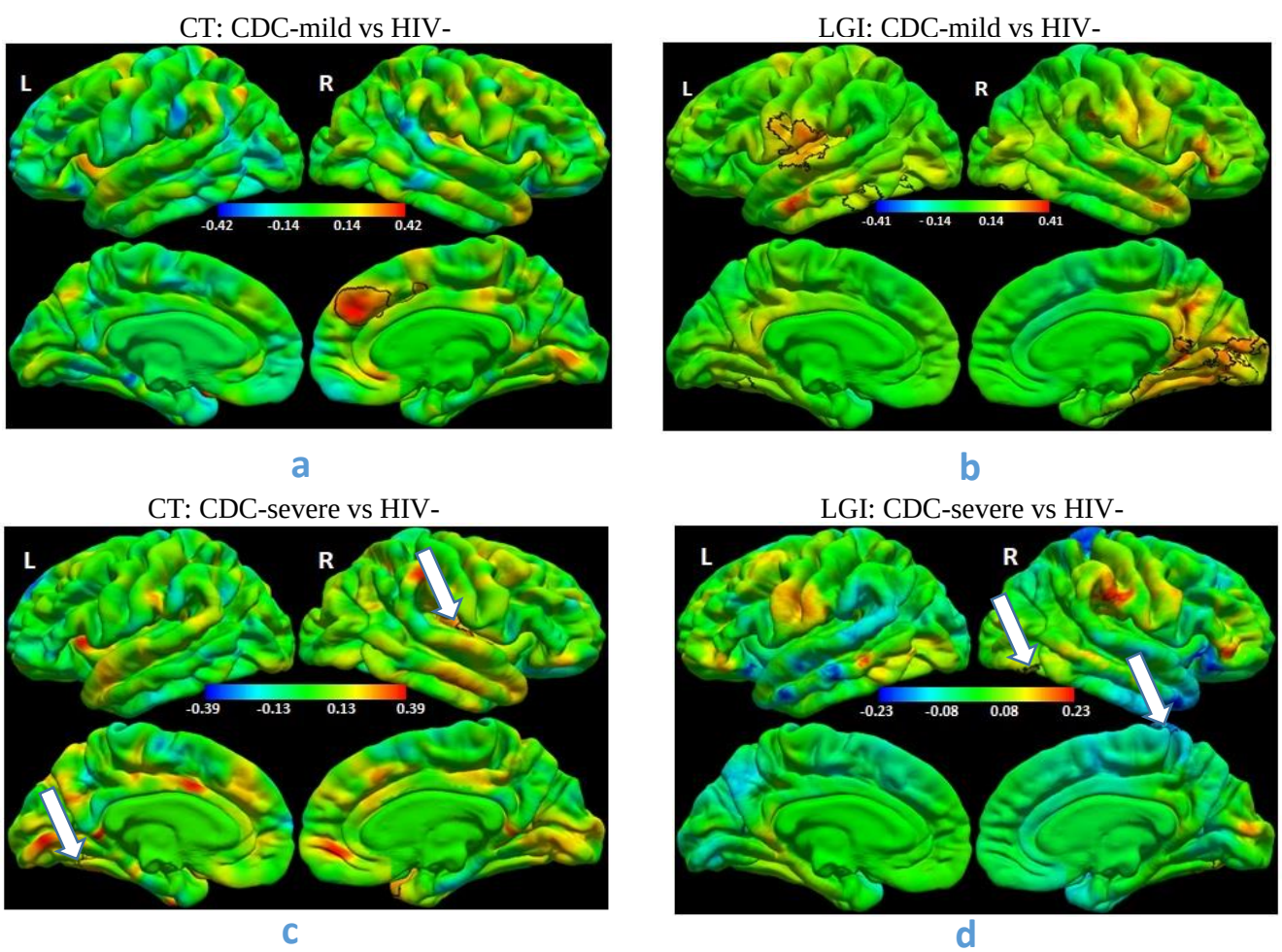

Figure 4.3: Colour maps of parameter estimates for group (CDC-mild or CDC-severe vs. HIV- controls) from vertex-wise unstandardized regressions of (a, c) cortical thickness (CT) and (b, d) local gyrification indices (LGIs), controlling for sex, age at scan and ethnicity. Positive regression coefficients (red/yellow) indicate CDC-mild/CDC-severe > controls, and negative coefficients (cyan/blue) indicate CDC-mild/CDC-severe < controls. The colour bar scale applies to both lateral (top) and medial (bottom) views. N=73 (12 CDC-mild, 32 CDC-severe, 29 HIV- controls). Results reported at a threshold of $p<0.05$, with a cluster size corrected threshold of $p<0.05$.

a) The right medial frontal region outlined in black shows where CDC-mild children have thicker cortex compared to HIV- control children.

b) The left fronto-temporal-insular and inferior temporal, and right fusiform and lingual regions outlined in black show where CDC-mild children have higher gyrification compared to HIV- control children.

c) The left fusiform and right insula regions outlined in black show where CDC-severe children have thicker cortex compared to HIV- control children.

d) The right superior parietal lobule and fusiform regions outlined in black show where CDC-severe children have lower and higher gyrification, respectively, compared to HIV- control children.

4.3.5 Effects of early immune health on cortical thickness and gyrification

In comparison to HIV- control children, children with high baseline (>750, 000 copies/mL) viral load (HVL) (n= 25) showed thicker cortex only in a right caudal anterior cingulate region extending into the adjoining superior frontal gyrus (**Figure 4.4a**), and higher gyrification in right fusiform and postcentral regions (**Figure 4.4b**).

Children with low (400 – 750,000 copies/mL) viral load (LVL) (n=21) at baseline showed thicker cortex than HIV- control children in a left fronto-temporo-insular region (**Figure 4.4c**) but did not differ in gyrification from HIV- control children.

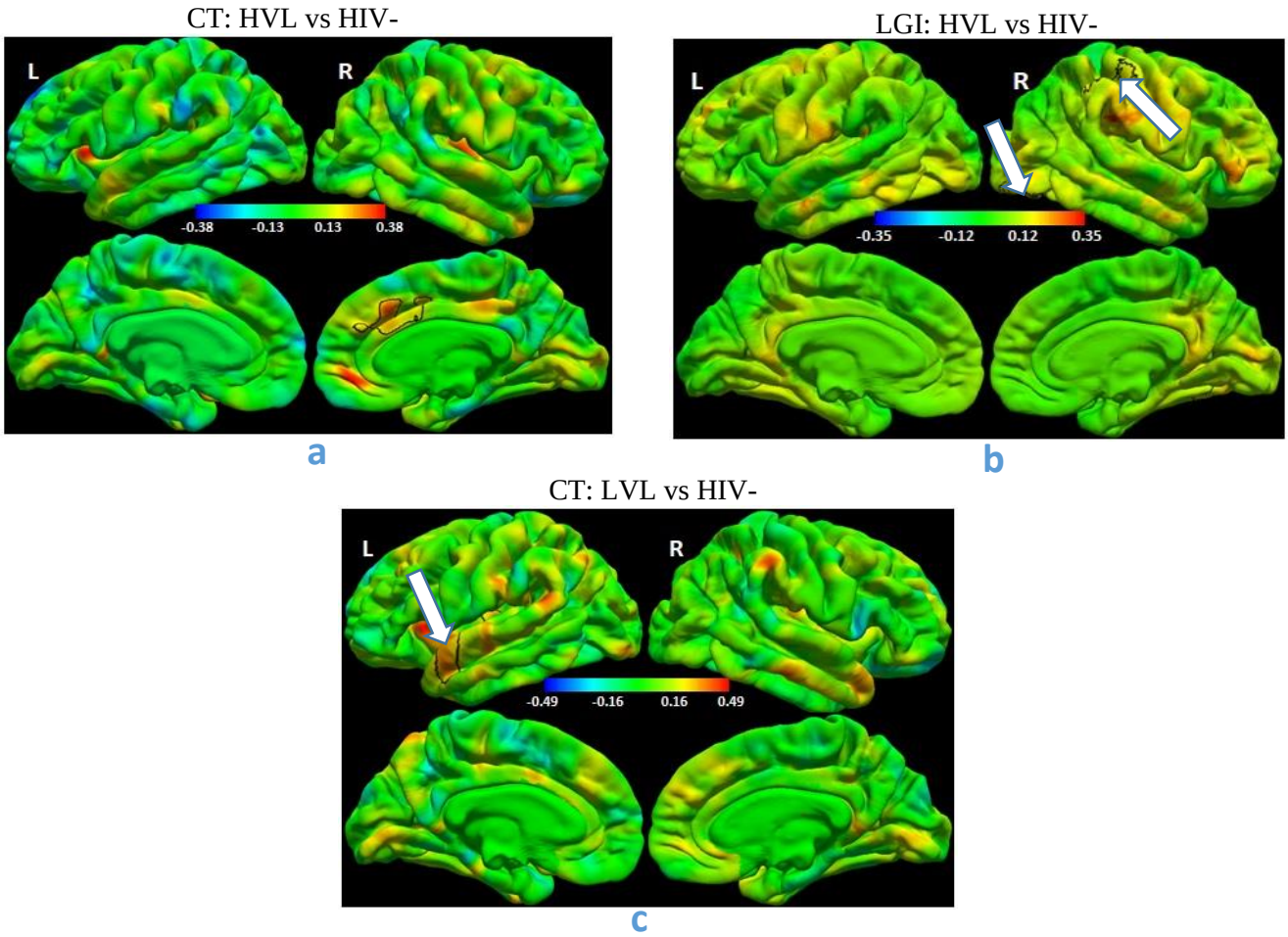

Figure 4.4: Colour maps of parameter estimates for group (HVL or LVL vs. HIV- controls) from vertex-wise unstandardized regressions of (a, c) cortical thickness (CT) and (b) local gyrification indices (LGIs), controlling for sex, age at scan and ethnicity. Positive regression coefficients (red/yellow) indicate HVL/LVL > controls, and negative coefficients (cyan/blue) indicate HVL/LVL < controls. The colour bar scale applies to both lateral (top) and medial (bottom) views. N=75 (25 HVL, 21 LVL, 29 HIV- controls). Results reported at a threshold of $p<0.05$, with a cluster size corrected threshold of $p<0.05$.

a) The right caudal anterior cingulate/superior frontal region outlined in black shows where HVL children have thicker cortex compared to HIV- control children.

b) The right fusiform and postcentral regions outlined in black show where HVL children have higher gyrification compared to HIV- control children.

c) The left insula region extending into the inferior frontal gyrus and anterior portion of the superior temporal gyrus where LVL children have thicker cortex compared to HIV- control children.

Among HIV+ children we found no regions where cortical thickness was associated with clinical measures at enrolment into the CHER trial (at age 6-12 weeks). In contrast, lower CD4% at enrolment was associated with greater cortical gyrification at age 5 in the regions listed in **Table 4.4** and shown in **Figure 4.5a**. Similar results were observed for CD4/CD8 ratio, while higher CD8 count was associated with greater cortical gyrification in left superior (MNI co-ordinates at peak: -43.6 -10.6 -15.7, cluster size: 5852.74 mm^2, r=0.47) and right middle (MNI co-ordinates at peak: 64.0 -43.8 -5.7 cluster size: 927.45 mm^2, r=0.48) temporal regions. **Figure 4.5 b-d** show mean LGI in the large left fronto-parieto-temporal cluster, as well as the left superior parietal and rostral middle frontal clusters, as a function of CD4%.

Table 4.4: Regions where lower CD4% at baseline was associated with higher local gyrification indices at age 5 years. N = 46 (Male=20, Female=26).

Location	**MNI co-ordinates at peak (x, y, z)**	**Size (mm^2)**	**Cor. Coeff. (*r*)**
Left hemisphere			
Fronto-parieto-temporal	(-45.5 -2.7 13.5)	6456.31	-0.49
Inferior parietal	(-43.5 -64.3 10.3)	573.88	-0.28
Superior parietal	(-28.1 -56.7 59.0)	567.61	-0.43
Rostral Middle frontal	(-37.9 46.1 12.0)	556.36	-0.44
Postcentral	(-43.2 -21.6 36.4)	530.23	-0.34
Right hemisphere			
Medial orbitofrontal	(6.0 39.7 -23.2)	1713.80	-0.34
Inferior temporal	(56.0 -25.2 -18.8)	1292.16	-0.39
Caudal middle frontal	(36.4 16.8 49.5)	754.25	-0.36
Lateral occipital	(28.4 -96.1 -0.9)	573.25	-0.35

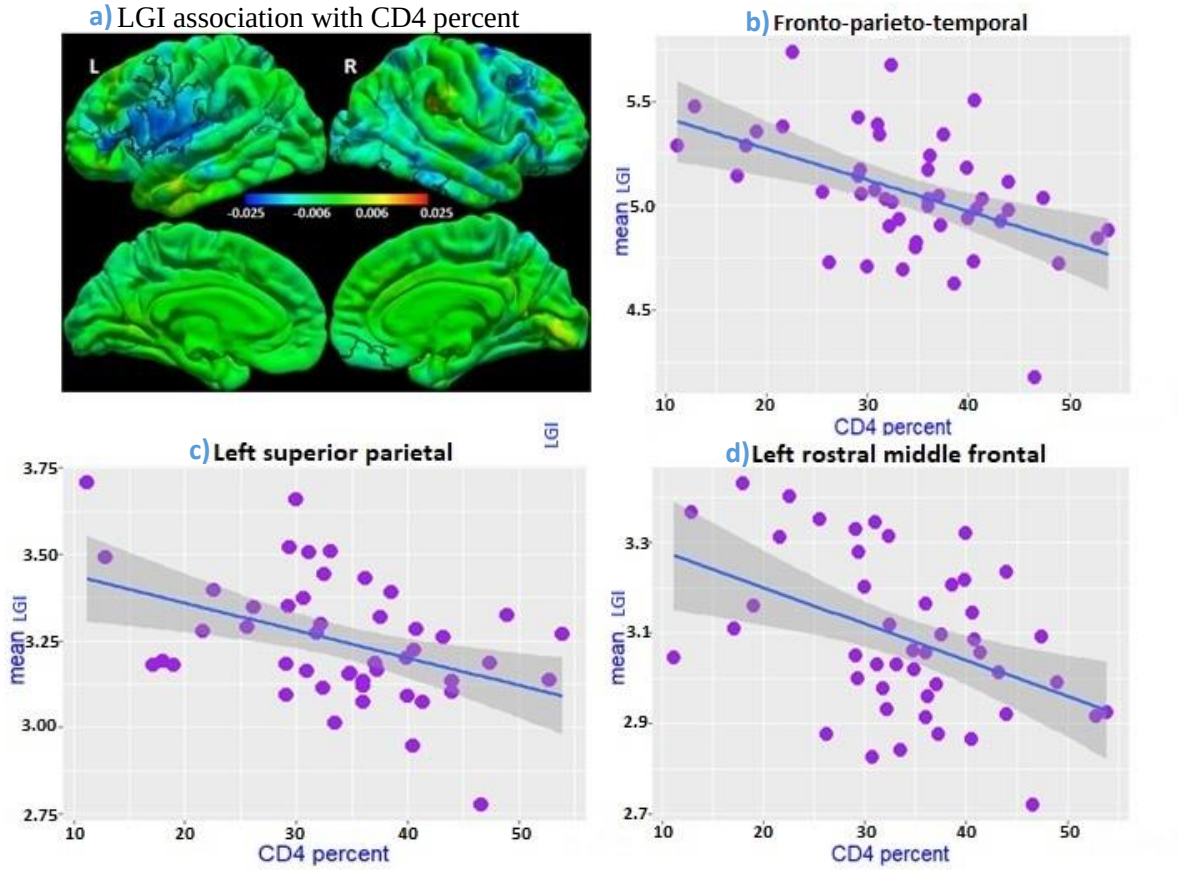

Figure 4.5: (a) Colour map of unstandardized regression coefficients for LGI at age 5 years on CD4 percentage at enrolment. Clusters outlined in black show the regions indicated in Table 4 where lower CD4 percentage was associated with greater LGI, after controlling for sex and age at scan.

(b - d) Plots of mean LGI at age 5 years as functions of CD4 percent at enrolment in the left fronto-parieto-temporal, superior parietal and rostral middle frontal regions.

4.4 Discussion

This study is the first to investigate the effect of early ART interruption and HIV disease history on neuromorphometric development in young virally suppressed HIV+ children on treatment. HIV+ children had thicker cortex than HIV- controls in frontal regions of both hemispheres and a left superior temporo-insular region. Since children in whom treatment had been interrupted had thicker cortex in similar left frontal and right temporo-insular regions, while those on continuous ART showed no CT differences to HIV- controls, thicker cortex in these regions may be attributable, in part, to treatment interruption. Children who previously experienced severe CDC disease demonstrated thicker cortex in a similar right insular region as interrupted children, and in left fusiform, while the CDC-mild group had thicker cortex in the right superior frontal gyrus. Children with high viral load at enrolment had thicker cortex in right caudal anterior cingulate, and those with low viral load in a left fronto-temporal region.

HIV+ children had lower gyrification than HIV- controls bilaterally in rostral anterior cingulate and medial orbitofrontal regions, as well as a left superior frontal region similar to that where HIV+ children had thicker cortex. Of these, the lower gyrification in the right anterior cingulate was also evident in the subset of children in whom treatment had been interrupted, but not in those on continuous ART. Interrupted children additionally demonstrated lower gyrification compared to controls in the left precuneus – a region not seen in the HIV+ group as a whole nor continuously treated children – and higher gyrification in a right lateral occipital region. In continuously treated children, we found higher gyrification in a similar right lateral occipital region, as well as left fusiform and right middle frontal regions, and lower gyrification posteriorly in the right superior frontal gyrus and right superior parietal lobule. Notably, the lower and higher gyrification seen in the continuously treated children were also evident in the ART-interrupted group, although mostly not significant. With regards to disease history, the CDC-mild group showed greater gyrification in left fronto-temporal-insular, left inferior temporal and right lingual regions, while both the CDC-mild and -severe groups had greater gyrification in right fusiform. None of these regions showed HIV- or interruption-related gyrification differences, but right fusiform also had greater gyrification in children with high viral load at enrolment. The CDC-severe group additionally had lower gyrification in the right superior parietal lobule – the same region where lower gyrification was seen in the continuous ART group.

4.4.1 Effects of HIV

Similar to our findings here of lower medial frontal LGI and thicker right lateral frontal, left medial frontal and left temporo-insular cortex at age 5 years in HIV+ children relative to HIV- controls, we previously reported lower bilateral medial parietal and right temporal gyrification in children from the same cohort at age 7 (Nwosu et al., 2018). At age 7 years, thicker cortex was only observed in a left inferior lateral occipital region.

Although to date a very small number of studies have examined gyrification in HIV, Hoare et al. (2018) recently also reported lower gyrification in the right lateral occipital gyrus and left inferior temporal gyrus in HIV+ adolescents compared to uninfected controls. Lewis-de los Angeles (2017) similarly observed lower gyrification in perinatally HIV-infected youths in bilateral lateral and medial frontal regions and medial temporal lobe. Lower regional cortical folding due to perinatal HIV infection is therefore a consistent finding across studies, both in early childhood and into adolescence. The reason for the variation in regions showing these differences in different age groups is not clear and may be related to spatial variation in the rate of development of gyrification during childhood, as well as varying disease course during and preceding this period.

The period of greatest increase in gyrification is thought to be after 24 weeks gestation (White et al., 2010), continuing postnatally till age 2 years (Li et al., 2014) where it peaks (Raznahan et al., 2011). Findings on gyrification during childhood and adolescence have been varied. An early study found increasing cortical complexity from 6-16 years in bilateral inferior and left superior frontal cortices (Blanton et al., 2001), while others have reported decreasing mean global gyrification after 3-4 years of age (Raznahan et al., 2011; Cao et al., 2017), or regional decreases from pre-adolescence through young adulthood, including in later maturing frontal and temporal regions (Su et al., 2013; Klein et al., 2014; Aleman-Gomez et al., 2013). Recently, a study in children aged 1-6 years found age-related gyrification increases in some regions over this period and decreases in others (Remer et al., 2017), suggesting that gyrification is still increasing in some regions during early childhood, while it has already peaked and is decreasing in others.

The regionally lower gyrification in HIV+ children than controls seen here could therefore result from a failure or delay of gyral formation in early life, or an acceleration of the hypothesized normal reduction in LGI that has been observed to occur during childhood maturation from about 4 years, and into adulthood (Raznahan et al., 2011; Cao et al., 2017). Accelerated aging is known to occur in HIV+ adults and adolescents (Horvath et al., 2018) and a similar phenomenon in HIV+ children might increase the rate at which gyrification changes during maturation.

If gyrification failure or delay is the main cause of observed differences, one would expect deficits to persist or resolve at an older age, while differences resulting from accelerated aging would presumably appear or get progressively worse with age. Neither process alone can, however, explain our findings of lower gyrification at age 5 years in distinctly different regions than reported previously in the same children at age 7 years (Nwosu et al., 2018) – widespread lower medial frontal gyrification at 5 compared to more localised medial parietal and temporal regions at 7. Instead our findings suggest that both processes play a role, albeit in different regions. In rostral anterior cingulate, for example, where LGI has been shown to increase significantly from ages 1 to 6 years (roughly 61% on the right and 22% on the left; Remer et al., 2017), LGI reductions appear to be due to HIV-related developmental delay

that resolves by age 7 years. In contrast, in middle and superior temporal cortices where LGI decreases from 1 to 6 years in normal developing children range from 4.9% to 9.4% (Remer et al., 2017), HIV-related lower LGI seen at age 7 years are likely attributable to accelerated aging. Notably, we did see non-significant lower gyrification in temporal regions at age 5 years, consistent with this interpretation. In left superior frontal and bilaterally in medial orbitofrontal and paracentral cortices, LGI appears to plateau over the period from 1 to 6 years, changing by ±3% or less (Remer et al., 2017), making it more difficult to unambiguously attribute differences observed in these regions to either process, although the fact that lower LGI seen at 5 are not evident at 7 years, and vice versa, suggest developmental delay in the former and accelerated aging in the latter.

It is interesting that the medial frontal regions where HIV+ children showed lower gyrification than controls at age 5 correspond closely with the regions where, at age 7, children who initiated ART before 12 weeks had lower gyrification than controls, and those who initiated ART after 12 weeks had greater gyrification (Nwosu et al., 2018). This discrepancy may explain why this region did not show HIV-related differences at that age and supports that LGI differences in this region are due to alterations in early life gyral formation which would be most impacted by differences in treatment timing. It is not clear, however, why earlier treatment (before 12 weeks), which is considered beneficial, would result in lower gyrification than later ART, unless this is an effect of interruption in early treated children. Notably, interruption coincided with a period when rostral anterior cingulate gyrification increases rapidly, especially on the right (Remer et al., 2017). An interruption-related effect is supported by our finding at age 5 years of lower LGI in right anterior cingulate only in the subset of children in whom ART had been interrupted and not in those on continuous ART. However, at age 7 years, lower medial frontal gyrification was evident in both continuous and interrupted early treated children, suggesting an effect of treatment timing rather than interruption. We found similar results in the same region at age 5 years for interrupted early treated children as at age 7 years but did not have enough power at age 5 to perform separate comparisons for children on continuous ART who had initiated ART before and after 12 weeks to rule out a treatment timing effect.

HIV-related higher cortical thickness at age 5 years involved more regions, covered greater surface area and were observed in both hemispheres, compared to age 7 years where only a small left inferior lateral occipital region demonstrated thicker cortex (Nwosu et al., 2018). Similar to gyrification, neither developmental delay nor HIV-related accelerated aging can satisfactorily account for the disparate and anatomically distinct regions where cortical thickness differences were seen at these two ages, suggesting that both processes play a role.

Maturation of cortical gray matter density in primary sensorimotor cortices, and frontal and occipital poles is followed by progressive parietal to prefrontal development, with superior temporal association areas maturing last (Gogtay et al., 2004). By age 2 years, CT is 97% of adult values (Lyall et al., 2015),

where after logarithmic or linear thinning ranging from 10% to 20% occurs until age 6 years in most brain regions, except for posterior regions where CT follows a quadratic trajectory with initial thinning followed by thickening of 50-80% (Remer et al., 2017).

Thicker cortex at age 5 in left superior frontal, left superior temporo-insular and right caudal middle frontal cortices, regions that show linear thinning ranging from 4.6% to 17.4% from 1 to 6 years of age in normal development (Remer et al., 2017), point to HIV-related developmental delay. Since no differences were found in these regions at 7 years, sustained viral load suppression and maintained immune health appear to normalise CT development. In contrast, thicker cortex seen in HIV+ children at age 7 years (but not age 5) in the left lateral occipital region, a region where CT normally increases by 52% from age 1-6 years (Remer et al., 2017), may be a consequence of accelerated aging.

In contrast to our findings, recent studies have shown region-specific lower as well as higher cortical thickness due to perinatal HIV infection. In a pediatric cohort on ART, Yadav et al. (2017) reported thinner cortex in the bilateral postcentral and right superior temporal regions, and thicker cortex in the left rostral middle frontal and right rostral anterior cingulate regions. Lewis-de los Angeles (2017) similarly reported thinner cortex in the bilateral frontal and temporal lobes and left cingulate gyrus, but thicker cortex in the occipital lobe, in a cohort of HIV+ adolescents all but one of whom were on ART. Yu et al. (2019) reported thicker left occipital cortex (middle and inferior gyri) and right olfactory sulcus, but thinning in middle temporal gyrus, temporal pole and orbitofrontal regions in HIV+ adolescents on ART compared to HIV-exposed uninfected adolescents.

It is interesting that we found only one region, namely left superior frontal cortex, that demonstrated both thicker cortex and lower gyrification in HIV+ children. For the remainder, HIV-related cortical thickness differences were observed on lateral surfaces and gyrification differences medially. This finding is similar to that of Klein et al. (2014) who found age-related cortical thinning and LGI decreases from 12 to 24 years in largely distinct regions, and no associations of LGI with CT in the 8 regions showing the largest age-dependent LGI decreases.

4.4.2 Effect of ART interruption

Contrary to our hypothesis that a short duration interruption would have little or no effect on children's brain morphometry at this age, we observed regionally thicker cortex and regions with lower and higher gyrification than HIV- controls. In contrast, the continuous ART group showed no differences in cortical thickness to HIV- controls and gyrification alterations in different regions to those seen in the interrupted group, except that greater gyrification was again seen in a similar right lateral occipital region. Notwithstanding these findings, Ananworanich et al. (2016) reported no effect of interruption on neurocognitive measures 2 years after ART resumption in children whose ART was interrupted for 48 weeks or till CD4% dropped to 20% (PENTA, 2010). A short duration ART interruption also did not affect immune health in children after resumption of treatment (Lewis et al., 2017; Wamalwa et al.,

2016). Since cortical thickness in both regions decreases logarithmically from 1-6 years (Remer et al., 2017), disruptions to the normal age-related decrease during interruption could account for the thicker cortex seen at age 5 years. However, the fact that the thicker cortex observed in ART interruption children was restricted to small left frontal and right insula regions suggests that short term interruption may not have severe consequences on children's cortical thickness when ART is initiated early.

Gyral folding appears to be affected to a greater extent by early childhood events and we have previously reported its long-term sensitivity to timing of ART initiation (Nwosu et al., 2018). This sensitivity may play a role in the differing effects on gyrification seen here in interrupted and continuously treated children. Notably, children in the interruption group all started ART before 12 weeks, while all those who started ART after 12 weeks were on continuous treatment. In addition to right anterior cingulate discussed earlier where gyrification was lower in both 5-year-old interruption children and earlier ART children at age 7 years, the right pars triangularis region where continuously treated children showed greater LGI at age 5 years, is adjacent to a region where later ART initiation was associated with increasing LGI at age 7 years. These overlapping yet different results make it difficult to distinguish between treatment- and interruption-related effects.

In normal development, LGI in the right lateral occipital region decreases logarithmically by about 5% from 1 to 6 years (Remer et al., 2017). Greater LGI in this region at age 5 years in both interrupted and continuously treated children, in whom viral load trajectories would have differed across the first few years of life, suggests therefore that changes seen at this age may be due to effects of HIV on early life gyral formation, before treatment differences would have played a role. However, greater LGI in a region characterised by age-related decreases, together with the absence of differences in this region at age 7 years (Nwosu et al., 2018), points to developmental delay. This region was probably not seen in the HIV+ group as a whole due to the fact that the regions showing differences in the two subgroups were in slightly different, albeit adjacent, locations.

From ages 1 to 6 years, gyrification changes in the left precuneus in normal development follow a quadratic trajectory – slightly decreasing first, followed by a slight increase of about 2.7% (Remer et al, 2017). Since the interruption period in the children studied here coincides with the trajectory minimum, it is possible that higher viral loads during and following interruption disrupt the normal age-related LGI increase that should be occurring in this region at this time, resulting in lower LGIs at age 5 years.

While changes in right pars triangularis, superior frontal and superior parietal cortices in normally developing children from ages 1 to 6 years are small, making interpretation of LGI differences observed in these regions in continuously treated children difficult, LGI in left fusiform has been shown to decrease logarithmically by 8.5% over this period (Remer et al., 2017). Greater LGI in this region at age 5 years in only the continuously treated group, 52% of whom started ART after 12 weeks, therefore

points to an effect of HIV on the normal age-related decrease that should have occurred in the first year of life.

4.4.3 Effect of early HIV disease history on brain development

Although immune health status at enrolment into the CHER trial (6-12 weeks of age) showed no association with cortical thickness at age 5 years, alterations in the trajectory of early gyrification may not have been reversed by 5 years of age. High viral load, low CD4%, CD4/CD8 ratio and high CD8 count at enrolment were all associated with regionally higher gyrification on the lateral surface of the cortex in HIV+ children.

We previously reported an effect of infant immune health in children from the same cohort on brain metabolism at age 5 years (Mbugua et al., 2016) and brain connectivity at age 7 (Toich et al., 2018). The current findings provide further support for the long-term consequences of early immune compromise on brain development.

Since cortical folding increases within the first 2 years of life (Li et al., 2014), where after it begins to decrease as part of cortical maturation, it is difficult to understand how immune compromise at age 6-12 weeks could lead to greater rather than less gyrification at age 5 years. One possibility is that poor immune health in infancy may result in an inflammation-related acceleration of the maturation process during the early life period when gyrification is still increasing (Li et al., 2014), leading to greater cortical folding in childhood. Alternatively, perinatal HIV infection and neuroinflammation in infancy may change the developmental trajectory of microglia, which play a role in synaptic pruning and regulation of synaptic plasticity and function (Schafer et al., 2012; Hong et al., 2016). This change in turn may alter later-life immune function leading to disruptions in normal age-related gyrification decreases and greater gyrification. Poor immune health earlier in infancy may therefore have a different net effect on gyrification at 5 years compared to poor immune health due to interruption that occurred much later in cortical development.

Our results also showed that CD8 count at enrolment – associated with higher frequency of activation and proliferation with increased viral burden (Sainz et al., 2013; Nasi et al., 2018) – showed a positive relationship with gyrification at age 5 years. This further supports the theory that immunoactivation and regional cortical inflammation leads to greater gyrification. In addition, higher regional gyrification (right fusiform and postcentral) observed in children with high viral load (HVL) at enrolment in comparison to HIV- control children, while low viral load children (LVL) do not differ in gyrification from HIV- controls, suggests immunoactivation and cortical inflammation due to viral burden. Abnormally high cortical gyrification (hypergyria) has previously been reported in neurodevelopmental disorders including schizophrenia (Narr et al., 2004; Sasabayashi et al., 2017; Palaniyappan et al., 2012), autism (Jou et al., 2010; Wallace et al., 2013) and Williams syndrome (Gaser et al., 2006).

4.4.4 Effects of CDC staging on cortical development

To our knowledge no study has investigated the effect of later CDC staging of HIV+ children on cortical development. Surprisingly, the CDC-mild group showed greater gyrification than HIV- controls both in more and more extensive regions than the CDC-severe group. The right fusiform was the only region observed in both groups, and in children with high baseline viral load, but the implicated region was roughly 9 times larger in the CDC-mild than the CDC-severe group. Although both groups demonstrated regionally thicker cortex, affected regions were also distinctly different. Notably the right superior frontal gyrus region seen in the CDC-mild group is similar, but on the opposite side, to the region where cortex was thicker in the HIV+ group as a whole compared to HIV- controls.

It is of interest that the right superior parietal lobule and fusiform regions showing gyrification alterations in the CDC-severe group, were also implicated (although for the fusiform on the left) in children receiving continuous ART. This may be due to treatment not being interrupted in children with severe CDC diseases resulting in significant overlap in these groups. 19 children were common to both groups.

4.5 Conclusion

Our study was focused on investigating the effects of ART interruption, early HIV-related events and immune health in infancy on the brain morphometry of children at the neurodevelopmentally critical age of 5 years. Cortical folding (gyrification) is sensitive to early life events and accordingly we find it affected by interruption, early HIV-related disease, immune health status and early viral burden. In contrast, cortical thickness development at age 5 years is less affected by early life events and infant immune health. Immune health resilience in children can translate to long term preservation of neurodevelopment especially for those on early and continuous treatment. The neuropsychological implication of morphometric alterations in cortical folding requires further investigation.

Chapter 5 – Longitudinal trajectories of cortical thickness and gyrification in HIV-infected children on early antiretroviral therapy (ART) and uninfected controls from 5 to 9 years.

5.1 Introduction

As of mid-2017, there were an estimated 1.8 - 2.1 million vertically HIV-infected (HIV+) children under 15 years of age living in sub-Saharan Africa (SSA) (USDHHS, 2017; WHO, 2018; UNAIDS, 2018). Although the number of new vertical infections is declining due to the government's implementation of prevention of mother to child transmission (PMTCT) strategy, in South Africa there are still about 320,000 children living with HIV (CLWH) (UNAIDS, 2017). Early antiretroviral therapy (ART) initiation upon testing HIV seropositive is the current standard of care for perinatally HIV+ children (Violari et al., 2008; Lindsey et al., 2007; WHO, 2008). However, the consequences of long-term ART on the developing brain are not well understood. As such, there is a need for longitudinal brain development studies of well-described HIV+ cohorts on ART.

A key study that led to the international adoption of early ART was the children with HIV early antiretroviral therapy (CHER) trial, which was conducted between 2005 and 2011 in Johannesburg and Cape Town, South Africa. The study aimed to investigate clinical outcomes of early time-limited ART in asymptomatic perinatally HIV-infected infants compared to deferred, continuous ART. Clinical, neuropsychological and neuroimaging follow-up of the Cape Town CHER participants was performed to investigate effects of perinatal infection, early ART initiation and interruption on the central nervous system (CNS), which is a key viral reservoir, even in the combination ART (cART) era (Van Rie et al., 2007).

In this cohort, both neuropsychological testing (Laughton et al., 2018; 2013; 2012) and cross-sectional neuroimaging investigations suggest small but persistent effects of HIV/early ART on the developing brain in subcortical regions, our group has found HIV-related volume increases and decreases at different ages (Randall et al., 2017; Nwosu et al., 2018). At 5-, 7- and 9-years HIV-related differences in metabolite levels in the basal ganglia were observed (Mbugua et al., 2016; Robertson et al., 2018). In terms of white matter development, at 5-and 7-years HIV-associated abnormalities in localized white matter integrity have been reported (Ackermann et al., 2016; Jankiewicz et al., 2017). Even though no HIV–related microstructural differences were found in the corpus callosum, at age 5 we found reduced corpus callosum volumes in HIV+ children (Randall et al., 2017).

Looking at cortical gray matter, at 5 years we find HIV associated thicker cortex (CT) increases in bilateral frontal and left temporal regions, as well as lower local gyrification indices (LGI) in bilateral

medial orbitofrontal regions extending into the rostral anterior cingulate and left superior frontal regions (Chapter 4). At 7 years we find similar HIV-associated thicker cortex in a small left lateral occipital region and lower LGI in bilateral paracentral and right temporal regions (Nwosu et al., 2018).

While HIV-related alterations have been observed cross-sectionally at each age, many of the alterations are not observed across multiple time points. Longitudinal analysis may clarify the longer-term consequences of cross-sectional findings. Longitudinal data is informative because it allows the modeling of developmental changes as either physiologically normal or pathological in relation to various disease conditions (Shaw et al., 2008), thereby enhancing understanding of developmental patterns in the presence of these conditions. Longitudinal neuroimaging studies are increasingly desirable in neuroimaging research due to their high sensitivity and potential to account for inter-subject variability (Reuter et al., 2012).

Brain morphometric measures such as CT – the distance between the inner white/gray matter boundary and the outer gray/pial interface in the cerebral cortex (Moeskops et al., 2015; Mills et al., 2014; Fischl et al., 2000) and LGI – a measure of cortical folding, which increases the number of neurons and cortical surface area within a limited skull space (Cao et., 2017; Li et al., 2014; Mills et al., 2014) can provide valuable information on cortical anatomical development. Important micro-anatomical changes, including synaptic pruning, neuronal specialization, rewiring of fibre tracts and structural folding and compacting occur during development from late childhood into adolescence, and determine the subsequent optimal function of the brain in adult life (Mill et al., 2014; Lebel &Beaulieu, 2011; Aubert-Broche et al., 2013; Tamnes et al., 2013). Longitudinal investigation of these microstructural parameters in CLWH is key to understanding whether the developmental trajectory of cortical anatomy during a critical period of brain development (Mills et al., 2014; Lebel &Beaulieu, 2011; Aubert-Broche et al., 2013; Tamnes et al., 2013) differs from that of uninfected controls.

The aim of this study was therefore to describe the longitudinal trajectory of morphological development of the cerebral cortex between the ages of 5 and 9 years in the Cape Town arm of the CHER cohort, who started ART before 2 years of age. We hypothesized that early ART initiation would lead to normal morphometric development, even in regions with HIV-related differences identified in cross-sectional analyses. In addition, we posited that periods of ART interruption would not impact developmental trajectories. Lastly, we explored the possible effect of HIV-related encephalopathy (HIVE) diagnosis on these measures.

5.2 Methods

5.2.1 Study participants

Study participants were 141 children (75 HIV+ and 66 uninfected controls (HIV-); 72 male and 69 female). HIV+ children were from the Cape Town cohort of the CHER clinical trial conducted at the Family Clinical Research Unit at Tygerberg Children's Hospital, Cape Town. On the CHER trial, infants with CD4 percentage ≥ 25% were randomized at age 6 -12 weeks to receive either limited ART– interrupted at 40 or 96 weeks – and restarted when clinical and/or immunological criteria were met, or to start ART only when they developed HIV symptoms or CD4 percentage dropped below 20% (25% in the first year) as per guidelines at the time (WHO, 2006). All HIV+ children started ART before 76 weeks of age and received comprehensive immunological and clinical follow-up thereafter, including assessment for HIV-related encephalopathy. First line ART regimen consisted of Zidovudine (ZDV) + Lamivudine (3TC) + Lopinavir-Ritonavir (LPV/r, Kaletra®) (CHER, 2010; Violari *et al*. 2008; Cotton *et al*. 2013) and all HIV+ children were on first line ART regimen until the end point of the clinical trial (CHER, 2010). The CHER cohort were matched with HIV- controls recruited from an interlinking vaccine trial (Madhi et al., 2010) comprising children born to HIV+ mothers (HIV exposed uninfected, HEU; n=31) and to HIV- mothers (HIV-unexposed; HU; n=35).

5.2.2 Image acquisition and analysis

Study participants underwent brain MRI scanning on a Siemens 3T Allegra scanner at 5, 7 and 9 years of age, using a protocol and procedure described previously (Nwosu et al., 2018). Scans were performed without sedation according to protocols approved by the Faculty of Health Sciences Human Research Ethics Committees of the Universities of Cape Town and Stellenbosch. Parents/guardians of study participants provided written informed consent and the children gave oral assent at ages 5 and 7, and written assent at 9 years.

MRI images were reviewed by a senior radiologist. Scans that met visual quality control criteria were processed using the automated 3 stage longitudinal processing stream in FreeSurfer version 6.0 (https://surfer.nmr.mgh.harvard.edu/fswiki/LongitudinalProcessing). The longitudinal processing stream first performs cross-sectional segmentation and cortical reconstruction for all subjects at all time points. The next stage of the pipeline samples the cross-sectional data of each subject to a base template. From the base template, longitudinal data are generated at all time points (Reuter et al., 2010, 2011, 2012). Outputs from the longitudinal stream were manually checked for errors. Reconstructed data were sampled to the FreeSurfer average subject template for vertex-wise analysis. A 10mm full-width, half-maximum (FWHM) of the spatial gaussian filter smoothing kernel was used for CT analyses. No smoothing was used for LGI.

5.2.3 Longitudinal vertex-wise analyses of cortical thickness and LGI

Morphometric data were analysed using FreeSurfer's spatiotemporal linear mixed effect model (LME) toolbox in MATLAB R2017a (https://www.mathworks.com/; Bernal-Rusiel et al., 2013). LME models can handle longitudinal data such as ours that contains observations for each subject at a varying number of time points. To establish regional CT and LGI trajectories in typically developing children, we first created an LME model with HIV- children only. To investigate the influence of HIV and early treatment on morphometric development in this age range, we performed an analysis on all participants using an LME model that included an age by HIV interaction term to identify possible HIV-related differences in developmental trajectories.

Further, the rates of change in CT and LGI of HIV+ children who had interrupted ART (Interrupted ART) and HIV+ children who had continuous ART (Continuous ART) were compared to HIV- controls. To assess the possible effect of encephalopathy on the trajectory of cortical development in HIV+ children, we also compared children with a HIVE diagnosis to HIV- controls.

All analyses were done using a vertex-wise LME model, with group as categorical fixed effect and random participant-specific intercepts. Rate of CT and LGI change with age in HIV- control children were modelled as follows:

$$Y_{ij} = \beta_1 + \beta_2 * t_{ij} + b_{1i} + e_{ij}$$

where

Y_{ij} = cortical thickness or gyrification of subject i at time point *j*

β_1 = intercept

t_{ij} = time variable – age in years of subject *i* at scan time point *j*

b_{1i} = participant-specific intercept

e_{ij} = error

To allow for different slopes in HIV+ (or HIVE or interrupted ART or continuous ART) and HIV- children, the following model was used:

$$Y_{ij} = \beta_1 + \beta_2 * t_{ij} + \beta_3 * HIV_i + \beta_4 * HIV_i * t_{ij} + \beta_5 * sex_i + b_{1i} + e_{ij}$$

where

sex_i = 1 if subject *i* was female and 0 if male

HIV_i = variable for HIV status (or HIVE status or Interrupted ART or Continuous ART)

The null hypothesis of no difference in rate of change in CT/LGI with age between HIV+ and HIV- groups was tested. Correction for multiple comparisons was performed using a false discovery rate (FDR) corrected threshold of $p < 0.05$ for a two-tailed test. We report regression coefficients (β) – indicating the rate of change of morphological parameters across the whole brain.

In addition, we present plots of the trajectories of LGI and CT for HIV+ and HIV- children in regions where group differences were reported in previous cross-sectional studies at ages 5- (*N*=75) and 7- (*N*=102) years (chapter 4, Nwosu et al., 2018).

5.3 Results

We present results for 141 participants whose MRI scan data at ages 5, 7 and 9 years were processed for longitudinal analyses. Fifty-six children received a single scan, 63 children were scanned twice, and 22 children had 3 scans, for a total of 248 time points. Viral loads of 93.5% of children in this study were suppressed (<400 copies/mL) at the first scan around age 5 years. There were no failures in automated LGI computation, nor errors in cortical segmentation. **Table 5.1** shows biographical data of all HIV+ and HIV- children at age 5, 7 and 9 years. **Table 5.2** presents clinical data for the HIV+ children.

HIV+ and HIV- children were age-matched at the time of scan, except at age 5 when HIV+ children were 0.21 years younger than HIV- children. Scores on the Griffiths' Mental Development Scales (GMDS) – Extended Revision for South Africa at age 5 and on the Kaufman Assessment Battery for Children (KABC) at ages 7 and 9, were not different between HIV+ and HIV- children. The number of children diagnosed with HIVE was similar in the continuous and interrupted ART groups.

Table 5.1: Biographical data for all participants (N=141; 75 HIV+, 66 HIV-).

Age: 5 years (N=82)				
	HIV+	HIV-	t or $\chi 2$	p-value
Sample size (N)	52	30		
Age at scan (years)	5.39 ± 0.31	5.60 ± 0.43	-2.64	0.01
Number of males (% males)	21 (40%)	16 (53%)	1.37	0.24
Birth weight (g)	3125 ± 386	2973 ± 603	1.47	0.14
Estimated total intracranial volume (ETIV) (cm^3)	1375 ± 96	1363 ± 110	0.53	0.60
Neuropsychological measures				
GMDS[a]				
Performance scores	74 ± 10	76 ± 18	-0.55	0.58
Practical reasoning scores	77 ± 8	76 ± 11	0.60	0.55
Sub-scales aggregate scores	83 ± 6	83 ± 8	0.23	0.82
Age: 7 years (N=125)				
Sample size (N)	71	54		
Age at scan (years)	7.20 ± 0.13	7.24 ± 0.13	-1.40	0.16
Number of males (% males)	36 (51%)	30 (56%)	0.13	0.72
Birth weight (g)	3081 ± 454	3081 ± 481	-0.01	0.99
Estimated total intracranial volume (ETIV) (cm^3)	1419 ± 101	1444 ± 137	-1.17	0.24
Neuropsychological measures				
KABC[b] composite scores				
Mental processing index	72 ± 8	75 ± 10	-1.90	0.06
Non-verbal index	74 ± 11	76 ± 12	-0.96	0.34
Age: 9 years (N=41)				
Sample size (N)	12	29		
Age at scan (years)	9.13 ± 0.27	9.03 ± 0.56	0.58	0.57
Number of males (% males)	7 (58%)	16 (55%)	<0.001	1
Birth weight (g)	3126 ± 479	3171 ± 466	-0.28	0.78
Estimated total intracranial volume (ETIV) (cm^3)	1422 ± 683	1437 ± 135	-0.38	0.71
Neuropsychological measures				
KABC[b] composite scores				
Mental processing index	73 ± 10	79 ± 12	-1.49	0.14
Non-verbal index	78 ± 10	80 ± 14	-0.46	0.65

[a]Griffiths' Mental Development Scales – extended revised: 2-8 years

[b]Kaufman Assessment Battery for Children second edition All values are mean ± standard deviation except where indicated otherwise

Table 5.2: Clinical data for all HIV+ children (N=75).

	Interrupted ART	Continuous ART
Sample size (N)	39	36
Clinical data at baseline (6-8 weeks)		
CD4 count (cells/mm^3)	1826.95 ± 955.41	1738.9 2± 833.22
CD4% (cells/mm^3)	33.18 ± 10.15	32.52 ± 10.12
CD4/CD8 ratio	1.39 ± 0.88 [0.23 – 4.39][a]	1.22 ± 0.73 [0.23 – 3.39][a]
CD8 count (cells/mm^3)	1659.92 ± 1217.64	1686.28 ± 871.28
Viral load at enrolment		
High (>750,000 copies/mL)	21 (53.8%)	23 (63.9%)
Low (400-750,000 copies/mL)	18 (46.2%)	13 (36.1%)
Suppressed (<400 copies/mL)	0 (0%)	0 (0%)
Other		
Age at ART initiation (weeks)	8.70 ± 1.62 [6.57 - 12][a]	21.49 ± 17.13 [6.00 – 75.71][a]
Age at ART interruption (weeks)	65.11 ± 28.48	-
Age of first viral load suppression (weeks)	62.92 ± 60.36 [30.57 – 213.29][a]	68.92 ± 54.59 [29.14 – 285.57][a]
Duration of ART interruption (weeks)	57.43 ± 68.39 [5.70 – 299.43][a]	0.00 ± 0.00 [0.00-0.00][a]
Nadir CD4% (cells/mm^3)	19.15 ± 5.57	20.29 ± 6.28
Age at nadir CD4% (weeks)	91.18 ± 58.09	50.01 ± 58.72
CDC classification		
A	8 (20%)	1 (3%)
B	9 (23%)	7 (19%)
Severe B	2 (5%)	7 (19%)
C	20 (51%)	19 (53%)
Unknown	0 (0%)	2 (6%)
HIV encephalopathy diagnosis	7 (18%)	5 (14%)

[a] mean ± standard deviation [range]

5.3.1 Rate of change in CT and LGI in HIV- control children.

Thickness

In HIV- children, there was widespread cortical thinning over the period from age 5 to age 9. This decrease in thickness was significant at an FDR-corrected threshold *p*-value of 0.05 over much of the lateral surface of the cortex and in medial superior parietal/lateral occipital/supramarginal regions as well as in medial frontal regions. The decrease was greatest in the medial bilateral frontal and corpus callosum regions (0.13 mm/year) followed by bilateral pre and post central and temporal regions (0.11 mm/year) as shown in F**igure 5.1a**.

Local gyrification indices

There was increased gyral folding during childhood in large bilateral lateral frontal, temporal regions and right medial inferior parieto-occipital regions. The greatest changes (0.047 units/year) were observed in bilateral rostral middle frontal and right superior temporal regions as well in parts of bilateral post central gyrus and parieto-occipital sulcus areas as shown in **Figure 5.1b**.

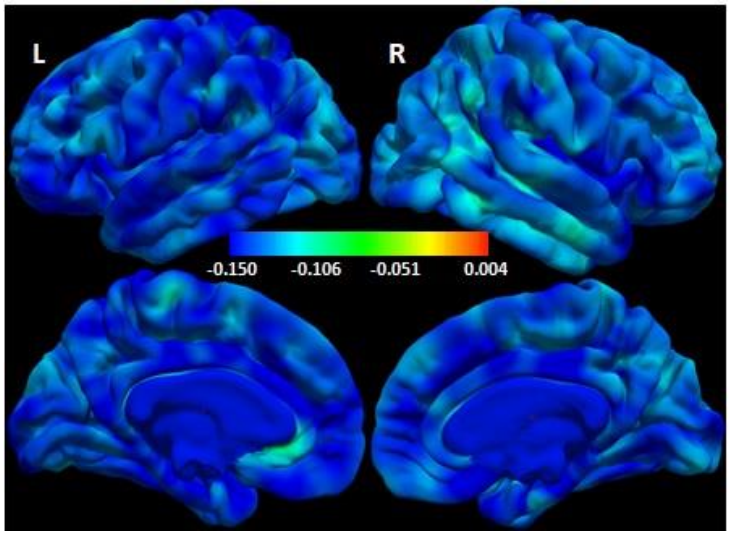

a

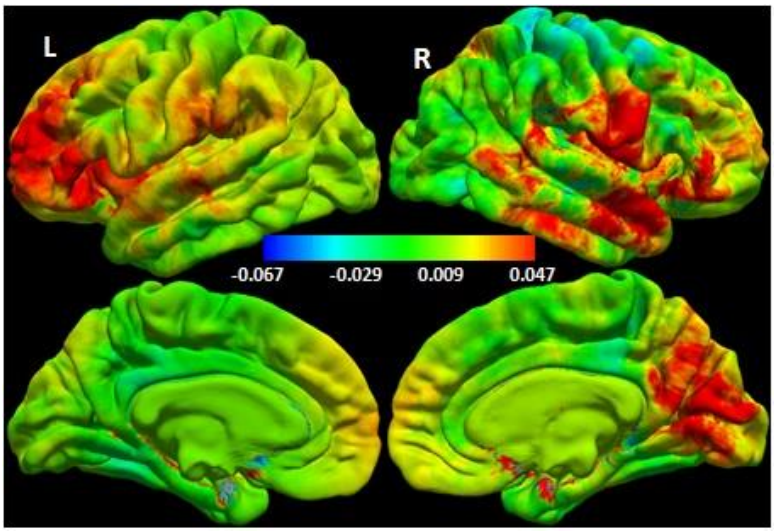

b

Figure 5.1: Colour map of unstandardized regression coefficients for a) cortical thickness and b) local gyrification indices (LGIs) showing rate of change through time points of age 5, 7 and 9 years in HIV-uninfected (HIV-) children controlling for sex. Positive regression coefficients (red/yellow) indicate increases with age, and negative coefficients (cyan/blue) indicate decreases with age. The colour bar scale in each figure applies to both lateral (top) and medial (bottom) views. (N = 66)

5.3.2 Rate of change in CT and LGI with age in HIV- compared to HIV+ children.

The vertex-wise rate of change in CT and LGI of HIV+ children from age 5 to 9 years was not different from that of HIV- children in any region of the brain. There was also no difference in rate of change of CT and LGI between either the Interrupted ART or Continuous ART groups and the HIV- control group.

Figure 5.2 shows plots of cortical thickness/LGI against age in regions where there were significant differences between HIV+ and HIV- children in previous cross-sectional analyses at ages 5- and 7-years (chapter 4, Nwosu et al., 2018). For longitudinal analyses, regions of cross-sectional differences showed significant differences in cortical thickness trajectories with time but no differences in LGI trajectories.

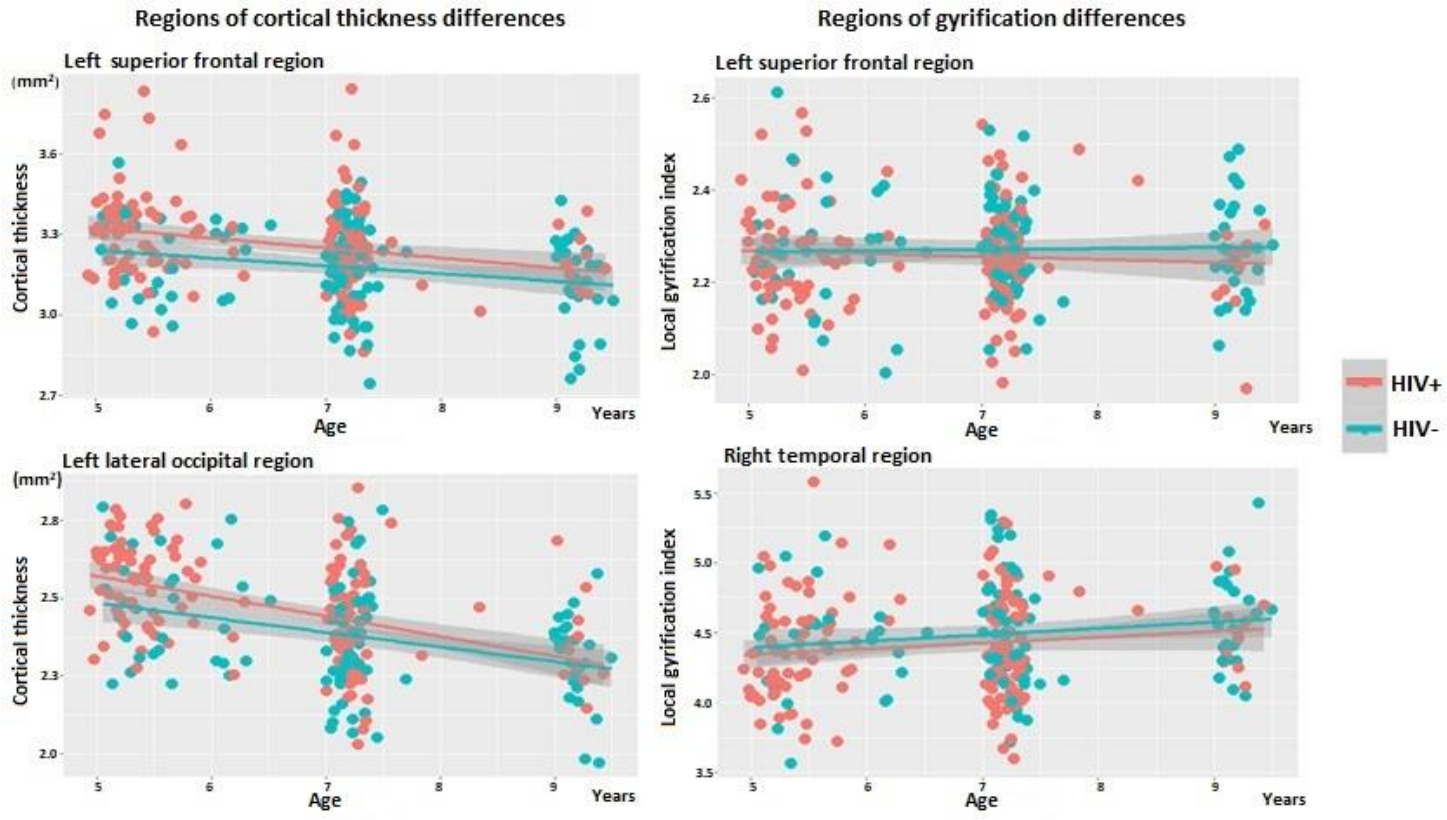

a

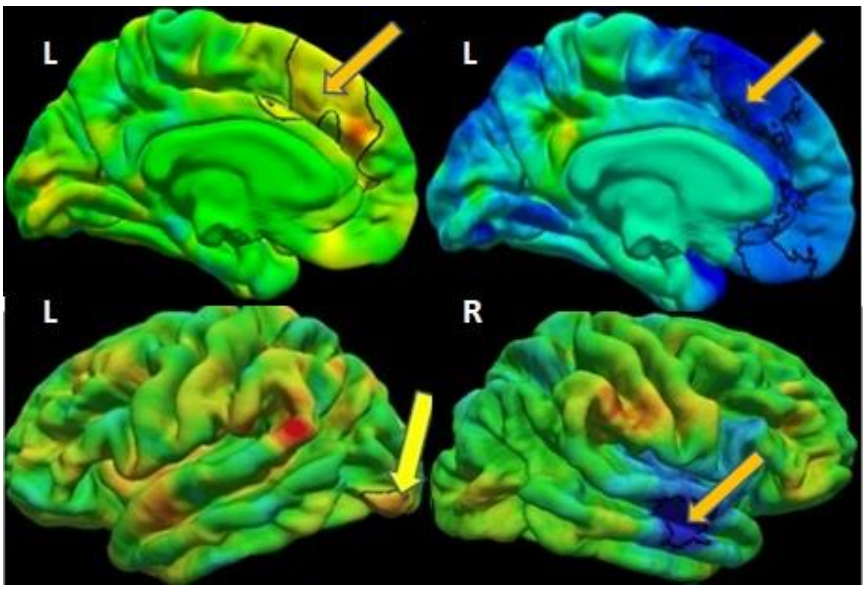

b

Figure 5.2: a) Plots of change with age (5 – 9 years) in cortical thickness and gyrification in regions where HIV+ differed from HIV- children in cross-sectional comparisons at ages 5 and 7 years respectively. b) Clusters outlined in black and shown with yellow arrow are regions where HIV+ differed from HIV- children in cross-sectional comparisons.

5.3.3 HIVE compared to HIV- controls

Although there was no significant difference in rate of change in CT between HIVE and HIV- children, HIVE children showed nearly constant gyrification with time in bilateral rostral middle frontal regions while HIV- controls showed a gyrification increase over this period as shown in F**igure 5.3b**. The observed difference in rate of change in gyrification between HIV- children and HIVE children was significant in the left hemisphere (MNI co-ordinates at peak: -38.6 45.9 1.5, cluster size: 1702.56 mm^2) outlined in blue (**Figure 5.3a)**.

Difference in change with time between children with HIV-related encephalopathy (HIVE) and uninfected controls (HIV-)

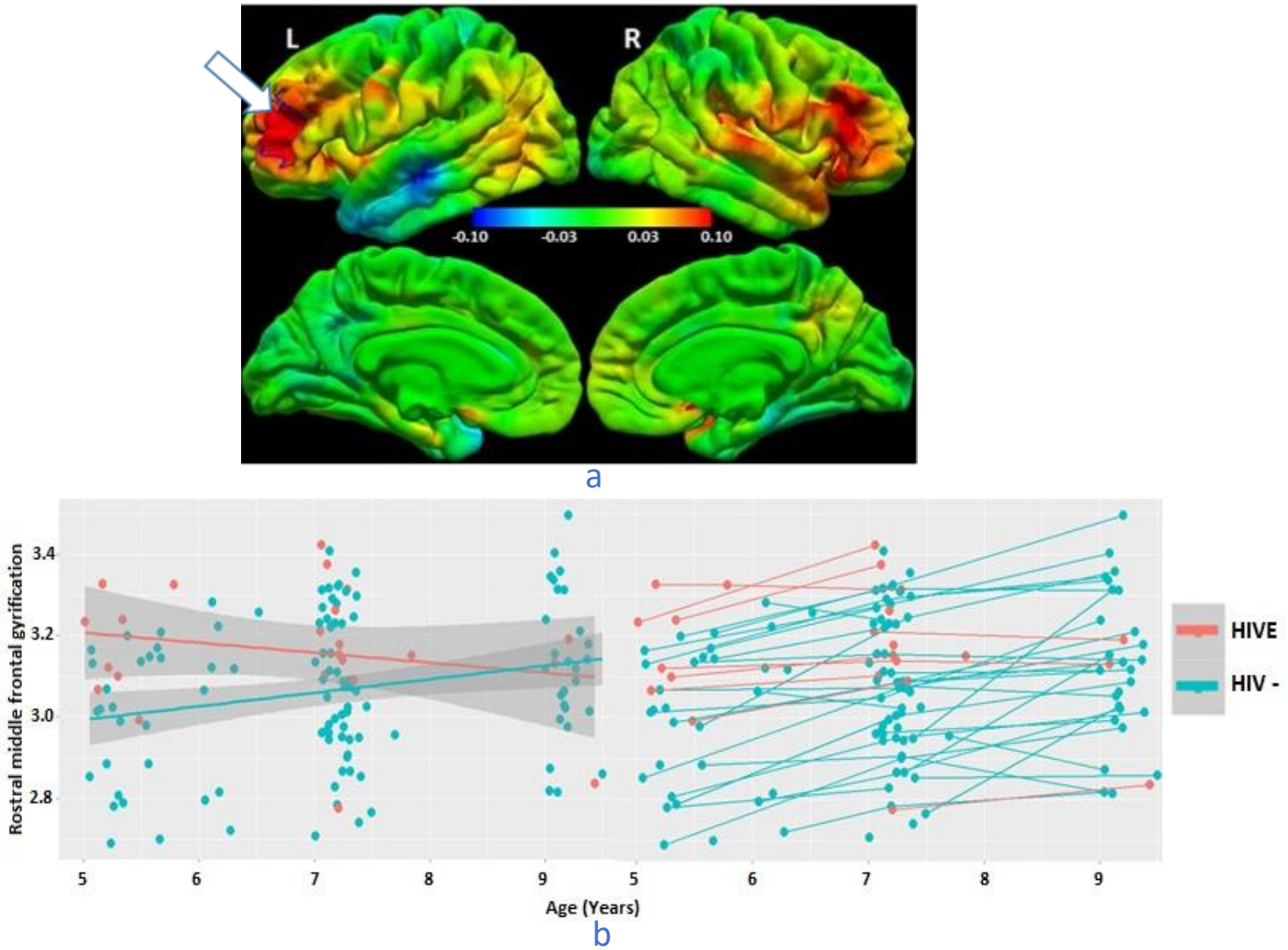

Figure 5.3: Colour map of unstandardized regression coefficients for local gyrification indices (LGIs) showing differences in rate of change through time points of age 5, 7 and 9 years between HIV-uninfected children (HIV-) and children diagnosed with HIV-related encephalopathy (HIVE) controlling for sex. Positive regression coefficients (red/yellow) indicate HIV- children > HIVE children, and negative coefficients (cyan/blue) indicate HIV- children < HIVE children. The colour bar scale applies to both lateral (top) and medial (bottom) views. (HIV- = 66, HIVE = 12).

a) Bilateral rostral middle frontal regions where rate of change in gyrification differed between HIVE and HIV-. Left hemisphere regions outlined in blue are where the difference is significant at a threshold of $p<0.05$, with a cluster size corrected threshold of $p<0.05$

b) Plot showing the difference in rate of change (between age 5 and 9 years) in gyrification between HIVE and HIV- (left) and spaghetti plot of individual trajectories for rate of change with time (right) in the rostral middle frontal region.

5.4 Discussion

To the best of our knowledge, this study is the first neuroimaging investigation of longitudinal cortical development in CLWH in a resource-limited setting who received ART before age 2 years. Similar to previous studies, typically-developing control children showed a widespread decrease in cortical thickness from age 5 to 9 years. There was less change in gyrification during this period, although notably gyrification was observed to increase in frontal and temporal regions. The developmental trajectory of cortical thickness and gyrification in CLWH was similar to that of matched typically developing HIV- children during this important period of brain development.

5.4.1 Morphometric development in typically-developing HIV- children from age 5-9 years

The cortical thinning with age observed in both HIV+ and HIV- children is similar to findings from previous studies (Raznahan et al., 2011; Shaw et al., 2008; Sowell et al., 2004; Durcharme et al., 2016). Cortical thinning from childhood into early adolescence is associated with physiological processes related to neurodevelopment and regional specialization of the developing brain. These include myelinogenesis (Sowell et al 2004; 2003; Shaw et al., 2008), synaptic pruning, and dendritic arborisation (Sowell at al. 2004; 2003; White et al, 2010; Mills et al., 2014) which lead to a reduction in the size and number of neurons and their synaptic processes (Mills et al., 2014; Sowell et al., 2004; 2003) and contribute the cortical thinning. It has been suggested that the process of myelination in the lower cortical layer closest to the cortical white/grey matter interface may be the main process that influences cortical thinning with brain growth (Shaw et al., 2008; Sowell et al., 2004; Gogtay et al., 2004). These neurodevelopmental processes work together to reinforce and strengthen fibres and connections that are in consistent use for transmitting brain impulses, while redundant fibres are "pruned" or removed (Santos and Noggle, 2011).

We also observed increased gyrification with age in bilateral frontal regions. Although, the developmental trajectory of cortical folding is not yet fully understood, the frontal cortex controls the complex executive skills of planning, working memory and cognitive flexibility that develops in late childhood (Shaw et al., 2008; Huizinga et al., 2006; Diamond 2002), corresponding to the period studied here. Maturation of cortical morphology follows a back-to-front – occipital-to-prefrontal – (Gogtay et al., 2004) developmental sequence, with prefrontal cortex maturing last in the continuous process of development from childhood into adolescence. The regional variation in rate of change and development in brain morphometry may be related to the complexity associated with the cytoarchitecture, information processing and co-ordination functionalities of different cortical regions (Shaw et al., 2008). In terms of functional complexity, primary sensory areas change and develop faster

than the more complex polymodal, higher-order association areas (Shaw et al., 2008; Gogtay et al., 2004).

A key theory of cortical folding formation links gyral and sulcal formation in the brain to neural connectivity (Van Essen, 1997). It postulates that regions with greater neural connectivity are associated with greater tension, ensuring that such brain regions are in close proximity during brain growth, forming gyri, while regions with lower connectivity follow a similar pattern to form sulci (White et al., 2010; Van Essen, 1997). Functional connections are associated with acquiring new skills and abilities during neurodevelopment, leading to changes in surface morphology of the cortex. Hence it may be worthwhile for future longitudinal studies to investigate gyrification development in relation to neural connections using DTI measures. The increases in cortical folding we observed in this study may be functionally related to the acquiring of critical developmental skills in late childhood into adolescence (Chung et al., 2017; Kersbergen et al., 2016). The rostral middle frontal region observed to increase in gyrification till age 9 years is similar to findings of Cao et al. (2017), who reported that although regional gyrification decreases from medial to lateral regions starting as early as age 4, frontal gyral complexity continues to increase, possibly into the teenage years (Blanton et al., 2001; Cao et al., 2017).

5.4.2 Effect of perinatal HIV infection and early ART initiation on morphometry development

The main focus of this study was the long-term effect of perinatal HIV infection and early ART initiation. By examining neuroimaging morphometry changes across multiple time points, we hoped to further understand neurodevelopmental implications of pediatric HIV and early ART treatment.

Previous cross-sectional neuroimaging studies have investigated brain developmental indices between CLWH and healthy controls and found that HIV infection was associated with regionally specific thickening and thinning of the cortex (Lewis-de los Angeles, 2017; Yu et al., 2019; Yadav et al., 2017) as well as regionally specific lower gyrification (Lewis-de los Angeles, 2017; Hoare et al., 2018) , and neuropsychological investigations recently started to examine the long-term developmental outcomes (Laughton et al., 2018).

Our previous cross-sectional study in this cohort at age 7 years showed little difference in cortical thickness and gyrification between CLWH and healthy controls, except for a small left lateral occipital region where CLWH children showed thicker cortex, and a bilateral paracentral region where HIV-children showed higher gyrification. Cross-sectional investigation of this cohort at age 5 years showed more widespread differences due to HIV infection, specifically thicker cortex in the frontal, temporal and insula regions and reduced gyrification in the frontal lobe, extending into the rostral anterior cingulate (Chapter 4). Although poorer visual perception scores at age 5 years were observed in CLWH

from the CHER cohort compared to uninfected controls (Laughton et al., 2018), there was no relationship between cortical thickness and visual perception at age 5 years (Ibrahim et al., 2019). There were no other deficits in neuropsychological performance in CLWH, pointing to the resolution of earlier observed differences (Laughton et al., 2018). In view of the near-normal performance on cognitive assessments, the unaltered trajectory of cortical development relative to controls may better reflect the effects of HIV on cognitive function than cross-sectionally observed alterations in LGI and CT.

Given the lack of HIV-related differences in cortical development from 5 – 9 years, early ART initiation combined with ongoing treatment may prevent persistent HIV associated damage to the cortex in young children. We suggest that previously reported HIV-related abnormalities at 5 and 7 years represent transient localized maturation differences that may be a side effect of long-term HIV infection and ongoing treatment.

5.4.3 Effect of ART interruption on morphometry development

Since perinatally HIV+ children start a lifetime of ART at birth, there is much interest in the possibility of safe treatment interruption(s). Due to the design of the CHER trial, one of the goals of this follow up study was to assess the long-term implication of either planned interruption or continuous ART in perinatally infected, early ART initiated children. Cross-sectional comparison at age 5 years showed that ART interrupted children had thicker cortex than HIV- controls in the left rostral and superior frontal, and right insula regions, and lower gyrification in the left precuneus and right rostral and caudal anterior cingulate regions, but higher gyrification in the right lateral occipital regions (Chapter 4). However, longitudinal analysis showed that planned ART interruption had no significant effect on brain morphometry developmental trajectories at least up to age 9 years.

According to previous studies, immune compromise related to a planned short ART interruption has a similar recovery pattern as continuous ART (Lewis et al., 2017; Bunupuradah et al., 2013). Research has shown infants' immune systems to be dynamic and malleable, allowing them to recover from short ART interruption (Lewis et al., 2017; Wamalwa et al., 2016). Several studies demonstrate that the most important factors in perinatal HIV treatment is ART initiation timing, and duration on treatment before interruption (Cotton et al., 2013; Bunupuradah et al., 2013; Ananworanich et al., 2016). Early ART initiation is beneficial for improved immune system and viral suppression as well as improved neurodevelopmental outcome (Violari et al., 2008; Laughton et al., 2012; Cotton et al., 2013). These results suggest that when ART is initiated before critical developmental processes are affected by viral replication, a short interruption may not affect long-term immune health. In contrast, a longer interruption may lead to viral rebound, resistance and neuropsychological consequences (Wamalwa et al., 2016; Ananworanich et al., 2016; Monteserrat et al., 2017). The range of interruption durations for the children in the cohort under study is quite large (6 – 300 weeks). Our study has shown that such

longer ART interruption may lead to age specific alteration in brain morphometry development which may not persist at later ages (Chapter 4).

In the current study, absence of ART interruption-related effect is consistent with general outcomes from the CHER trial (Cotton et al. (2013) as well as 5-year longitudinal neuropsychological outcomes. Results from the CHER studies and other similar studies have shown that timing of ART initiation but not treatment interruption influences neurodevelopment (Lewis et al., 2017; Ananworanich et al., 2016). The present study adds long-term neuroimaging measures to previous results. In conclusion, our findings suggest cortical development is not affected by treatment interruption in childhood in the presence of early ART initiation.

5.4.4 Effect of HIVE on morphometry development

There has been a continuous decline in HIVE incidence with the introduction of ART (Donald et al., 2014; Chriboga et al., 2005). We found that 16% of our early-treated HIV+ cohort had HIV-related encephalopathy diagnoses, compared with an incidence of 20-60% in previous studies of perinatally infected but ART-naïve pediatric cohorts (Foster et al., 2006; Lobato et al., 1995; Donald et al., 2014). There was no difference in developmental trajectory of cortical thickness or gyrification between the HIVE group and the HIV- controls except in the left rostral middle frontal region where HIVE showed decreasing gyrification relative to HIV- controls. The small number of HIVE subjects calls into question the reliability of the findings, however, the low number of HIVE children in our sample and the limited number of localized regions found to show altered developmental trajectories, together reinforce the benefits of early ART in reducing the occurrence and severity of neurologic conditions such as HIVE.

The left rostral middle frontal region identified in this study is in close proximity to the primary motor cortex of the frontal lobe and may be connected to pyramidal tract-related neuromotor deficits reported previously in HIVE on ART (Mitchell, 2006; Assefa, 2012). The corticobulbar set of the pyramidal tracts originates from the primary cerebral motor cortex of the frontal lobe (Hall, 2015). Changes in cortical folding are largely influenced by neural connectivity related factors (Van Essen, 1997) including synaptic pruning and dendritic arborisation (Mills et al., 2014; Gogtay et al., 2004; White et al, 2010). Regions with greater neural connectivity are associated with greater tension which ensures that such brain regions are in close proximity during brain growth, forming gyri. The gyrification decreases with age in HIVE children may be a sign of delayed neural connectivity in primary motor cortex. However, there was no difference in neuromotor assessment between HIVE and HIV- control children at any of the ages within this study.

The frontal lobe of the brain is expected to develop last, since brain development moves from posterior (occipital lobe) to anterior (frontal lobe) (Gogtay et al., 2004). Maturation of gyri varies across the

cortex and is expected to exhibit little or no change in late childhood (Mills et al., 2014; Mutlu et al., 2013; White et al., 2010). The reduced regional age-related changes in HIVE children who initiated early ART may point to developmental delay.

5.4.5 Limitations and future work

The small sample size at age 9 years, with fewer HIV+ children compared to HIV- controls, was due to the decommissioning of the 3T Siemens *Allegra* brain scanner used for this study. More participants were scanned at age 9 years on a 3T Siemen *Skyra* whole-body scanner, but these scans were not included to avoid introducing inter-scanner variation. The small number of children diagnosed with HIVE precludes strong conclusions about group differences. Although FreeSurfer's longitudinal pipeline was not originally designed for pediatric cortical segmentation, manual quality checks were performed on the cortical model to ensure accurate extraction and segmentation of cortical surface.

Future investigations could look at the developmental trajectories of brain morphometry in conjunction with data from other MRI modalities, for example DTI and functional MRI, to understand how other brain developmental indices are linked to these changes. The relationship between cortical developmental trajectories and longitudinal neuropsychological outcomes should also be examined.

5.5 Conclusion

We present results from a follow-up neuroimaging study of a subset of children from the CHER trial during an important stage in neurodevelopment (5-9 years). We report similar developmental trajectories of cortical thickness and gyrification in perinatally HIV-infected children who initiated ART early and uninfected controls. Across all children, generalized cortical thinning was observed from age 5 to 9 years, where the rate of thinning varied by region. Age-related changes in gyrification were only observed in the bilateral frontal regions. Planned ART interruption did not affect development of cortical morphology. HIV-related encephalopathy was associated with decreasing gyrification with age in bilateral rostral middle frontal regions, compared to an increase with age in uninfected controls. Our results suggest that early ART initiation preserves normal development of cortical morphology between the ages of 5 and 9 years in perinatal HIV infection.

Chapter 6 – Discussion and conclusion

6.1 Discussion

This study aimed to investigate structural changes in brain morphology – specifically subcortical volumes and cortical thickness and folding (gyrification) – in children living with HIV infection who were initiated to early ART as per pediatric HIV treatment guidelines. We also aimed to explore the effects of early disease-related variables on cortical morphology, including immune health at enrolment onto the CHER trial, viral load at enrolment, CDC classification and HIV-related encephalopathy, as well as the effects of early (before six weeks) ART initiation and short clinically-designed ART interruption, as specified by the design of the clinical trial.

Using automated segmentation software such as FreeSurfer is the most practical way to investigate brain morphology, particularly in longitudinal studies. Although FreeSurfer has been used successfully in several hundreds of studies of adults, it was not originally designed for use in children. Several studies have investigated its suitability for use in children by comparing FreeSurfer segmentation to manual tracing of subcortical structures (e.g Lyden et al., 2016; Schoemaker et al., 2016; Bender et al., 2018), finding moderate consistency. However, the reliability of the latest version (v6.0.0) for segmentation in children has not previously been established. Although it would be ideal to validate both the cortical surface extraction and the subcortical segmentation with respect to manual segmentation, manual tracing of the cortex would be excessively time-consuming. To avoid this, Dewey et al. (2010) recommend a semi-automated process when using FreeSurfer for brain morphometry analyses, which involves visual inspection and manual editing of inaccurate automated parcellation of cortical structures. This is practically achievable and ensures the validity and accuracy of the final output especially for measures like cortical thickness.

We therefore proposed to use semi-automated processes for the cortical morphology components of the study, but first to assess the accuracy of FreeSurfer for processing structural brain data in children by validating the subcortical segmentation from FreeSurfer 6.0 against manual tracing. To do this we selected subcortical regions previously reported to be affected by HIV: the basal ganglia (Wade et al., 2019; Yadav et al., 2017; Lewis-de los Angeles et al., 2016), specifically caudate nucleus, nucleus accumbens, putamen and globus pallidus and white matter structures represented by the corpus callosum (Hoare et al., 2015; Ackermann et al., 2016; Uban et al., 2015).

Consistent with previous studies (Schoemaker et al., 2016; Cherbuin et al., 2009; Nugent et al., 2013; Pipitone et al., 2014), comparison of outputs from manual and FreeSurfer segmentations showed that FreeSurfer tended to overestimate volumes, although by less than 10% in the caudate nuclei, putamen and left globus pallidus. Nucleus accumbens volumes by contrast were overestimated by 25 - 30%. However, strong consistency between methods, and the fact that differences between the segmentation

methods were not influenced by HIV status allowed very similar results to be obtained from an analysis of group differences between HIV+ children and HIV- controls. This suggests that FreeSurfer v6.0 can be used as an alternative to manual tracing in neuroimaging research, provided that quality control protocols in the form of visual inspection and manual corrections are implemented.

Although there are few studies on perinatal HIV infection in early ART era, the existing literature on the effects of perinatal HIV on cortical and subcortical structure reveals diverse findings. This is perhaps due to the heterogeneity of the disease history, as well as sample populations with a wide age range, where the mean age of the study population represents respectively late childhood (Yadav et al., 2017, Hoare et al., 2018, Paul et al., 2018, Wade et al., 2019), or early (Cohen et al., 2016, Blokhuis et al., 2017, Yu et al., 2019) or later (Sarma et al., 2014, Lewis-de los Angeles 2017, Li et al., 2014) adolescence. Considering the rapid trajectory of brain development during childhood and adolescence, it is clear that it is not easy to draw conclusions from cross-sectional findings in these studies.

Neuroimaging on the CHER cohort by our group provides evidence of brain structural changes related to perinatal HIV at earlier ages than these other studies, namely age 5 (e.g. Randall et al., 2017) and 7 years (e.g. Nwosu et al., 2018). The data presented in this thesis therefore depicts aspects of brain development that fill in gaps in knowledge about the effects of HIV and ART in early childhood. The period from 5-9 years is within the critical period in brain development of children (Mills et al., 2014; Lebel &Beaulieu, 2011; Aubert-Broche et al., 2013; Tamnes et al., 2013). Key brain developmental events occur around this time including cortical pruning, alterations in neural connection leading to changes in cortical folding (gyrification) in the brain and myelinogenesis (Sowell et al 2004; 2003; Shaw et al., 2008; Mill et al., 2014; Lebel &Beaulieu, 2011; Aubert-Broche et al., 2013; Tamnes et al., 2013).

At age 5 the combined results of chapter 4 and previous work by Randall et al. (2017), suggest a picture of enlarged basal ganglia in HIV+ children, possibly due to inflammation and chronic stress, as well as thicker cortex in bilateral frontal and left superior temporal/insular regions and lower gyrification in a left superior frontal region and bilateral medial orbitofrontal regions extending into rostral anterior cingulate cortex. Although we expected to find regionally lower gyrification due to HIV infection based on previous studies on pediatric and adolescent samples that reported similar reductions at older ages (Nwosu et al., 2018; Hoare et al., 2018; Lewis-de los Angeles, 2017), the regions were different from those observed in previous studies.

Thicker cortex at age 5 years due to HIV infection and early ART appears to be more widespread than the small left lateral occipital region seen at age 7 years in the CHER cohort, but involves similar frontal regions to those observed by Yadav et al (2017) at age 10-11 years. This suggests a delay in the normal

age-related cortical thinning that occurs during childhood. Widespread and regionally variable nonlinear thinning occurs from ages 7 to 29 years (Tamnes et al. 2017). Age-related cortical thinning has been linked to both synaptic pruning (Rakic et al., 1994; Huttenlocher and Dabholkar, 1997) and white matter maturation (Aleman-Gomes et al, 2013; Paus, 2005). The latter proposes a mechanism whereby the cortex thins out to cover the increasing surface area resulting from white matter thickness increases in the adjacent gyri. Less is known about developmental changes in gyrification, which was attributed to changes in mechanical tension along axons connecting highly interconnected regions (Van Essen, 1997), as well as differential growth rates between inner and outer cortical layers (Richman, 1975).

At 5 years, ART interruption was associated with lower gyrification in left precuneus and right superior frontal regions and a gyrification increase in right lateral occipital regions compared to HIV- controls. Thicker cortex was also observed in left rostral middle frontal and right insula regions in children on interrupted ART. Even though the immune health of children tends to return to pre-interruption state when ARV treatment is recommenced (Lewis et al., 2017; Wamalwa et al., 2016; Bunupuradah et al., 2013[a]), ART interruption appears to affect cortical development. The timing of immune health depletion in pediatric HIV may therefore affect cortical morphology at a later age. Poorer immune health at study enrolment was associated with increased gyrification but not with cortical thickness, suggesting that early immune health depletion (before ART initiation) may affect primarily gyral formation and development, while later depletion (due to ART interruption) affects both cortical folding and thickness. CD4/CD8 ratio showed negative relationships with gyrification in more extensive brain regions than CD4 percentage or CD8 count, providing further evidence that CD4/CD8 ratio may be a more reliable long-term predictor of development in HIV+ children (Mbugua et al., 2016; Sainz et al., 2013; Trickey et al., 2017). The similarity of observed effects of ART interruption to effects of HIV infection relative to controls may imply that in early-treated, perinatal HIV infection, cortical development is affected most by ART interruption and the consequent increased viral load and/or drop in CD4 count.

In older children, varying observations have been made on cortical thickness alterations due to HIV, finding either little (Nwosu et al., 2018) or no (Hoare et al., 2018) difference from controls, or regionally-specific thicker and thinner cortex than controls (Yadav et al., 2017; Yu et al., 2019). Other studies have observed lower cortical volumes in perinatally HIV-infected adolescents (Li et al., 2018, Lewis-de los Angeles 2017). In addition to age at neuroimaging, another difference between the current study and previous studies of brain structure in perinatal HIV infection is the age of ART initiation. Whereas all the children in our cohort had started ART by 18 months of age, in other studies the mean age of ART initiation was ~1-2 years (Blokhuis et al., 2017, Cohen et al., 2016), ~3.5 years (Hoare et al., 2018; Lewis-de los Angeles 2017), ~4.5 years (Sarma et al., 2014), ~6.5 years (Paul et al., 2018, Wade et al., 2019), 8 years (Li et al., 2014), or not specified (Yadav et al., 2017; Yu et al., 2019). Taken

together with the differing ages of the children, this means that time on ART as well as age at initiation was quite variable between studies, which may go some way towards explaining the divergent findings.

From our investigation of subcortical volumes (chapter 3), we observe that the globus pallidus is smaller in HIV+ children at age 7, but not the nucleus accumbens, caudate nucleus or putamen, although smaller right putamen and left hippocampus were observed in a slightly different subsample (Nwosu et al 2018). However, in HIV+ children from a subset of this cohort at age 5, Randall et al (2018) reported marginally larger volumes of left globus pallidus, as well as larger nucleus accumbens and putamen. In our cohort, the absence of enlarged subcortical structures at age 7 occurs simultaneously with a reduced area of thicker cortex (Nwosu et al, 2018) than that observed at age 5, suggesting that gray matter hypertrophy is attenuated with increasing age or longer time on ART. Other studies have found larger nucleus accumbens (Yadav et al., 2017, Paul et al., 2018), caudate (Paul et al., 2018) and a trend for larger putamen (Blokhuis et al. 2017) in HIV+ children. Since this tends to be seen only in younger children (Paul et al., 2018), this provides further support for the hypothesis that this is an effect of age or more recent ART initiation. Alternatively, it may relate to the CD4 count maintained with ART (Wade et al. 2019). Other studies, also in slightly older children have failed to find basal ganglia volume differences (Hoare et al, Blokhuis et al) or found only subtle differences in shape (Lewis-de Los Angeles et al., 2016, Wade et al. 2019), although one other study in adolescents who started ART at a mean age of 8 years, found significantly lower gray matter volume in right pallidum, as well cerebellum, (Li et al., 2014). Although outside of the scope of this thesis, longitudinal analysis of subcortical volume changes, along with HIV and ART characteristics as carried out for cortical analysis in chapter 4, may help to clarify the reasons for the disparate findings between studies.

Longitudinal analyses of HIV-related changes to brain structural development in childhood are currently rare (Van den Hof et al., 2019), however, two studies have performed longitudinal analysis of aspects of structural development affected by perinatal HIV. Wade et al. (2019) found no effects of HIV on subcortical shape or volume within a 1-year follow-up (from mean age of 11 years). Shape abnormalities among HIV+ children at first scan became less pronounced within the follow-up period, but the trajectory of the left pallidum volume was positively associated with baseline CD4 count. Yu et al (2019) also performed a 1-year follow-up investigation on cortical gray matter volume and thickness (from a mean age of 13 years), finding cortical thinning in both HIV+ and HIV- groups over this period but with different spatial patterns, which they attribute to delayed maturation.

In the early childhood period from 5 – 9 years, we similarly find the developmental trajectory in HIV-controls shows decreasing cortical thickness with age, at a varying rate, over the whole brain. Gyrification was stable in most of the cortical regions except an increase in the bilateral frontal and temporal regions and a minor pattern of decrease in the right parietal region in contrast with [a]Cao et al. (2017) that found decrease trajectory in gyrification that follows a logarithmic function of age from

childhood into adulthood. These cortical developmental trajectories were similar in HIV+ children, even in the subgroup on interrupted ART. Notably, none of the regions previously observed to be different in HIV+ children compared to HIV- controls at ages 5 and 7 years differed in the longitudinal investigation. Cortical thickness development was also similar between HIV- and children with HIV-related encephalopathy (HIVE), although in bilateral rostral middle frontal regions, HIVE children showed decreasing gyrification with age, while gyrification in HIV- children increased with age. However, the small number of HIVE children in the longitudinal analysis precludes strong conclusions.

In relation to the cross-sectional study, the longitudinal study implies that early ART initiation in perinatal HIV infection may protect these children from morphological changes in the longer term. Although there were differences in structural brain morphology between HIV+ children who had ART interrupted and controls early in childhood, at age 5 years, these differences appear to resolve during childhood development between 5 and 9 years. This may be attributed to early ART initiation and continued treatment. HIV-related encephalopathy may affect structural development of brain morphology, although much less severely than without early ART initiation. Earlier studies showed that HIVE was linked to neuromotor deficits (Mitchell, 2006; Assefa, 2012). As per theories of neural connectivity (Van Essen, 1997), neuromotor deficits observed in children with HIVE may be related to the different pattern of frontal cortical folding – the only region reported to differ in the long term in our study. However, in our cohort no neuromotor deficits were observed in children with encephalopathy. At age 9 years control children on average performed better than HIVE children in sequential processing/short-term memory scale and learning ability/long-term storage and retrieval scale of the Kaufman Assessment Battery for Children (KABC). In future work, assessment of cortical development and neuropsychological performance of these children will continue at later age.

6.2 Conclusion

This study first sought to validate FreeSurfer as an equivalent tool for pediatric HIV morphometry investigation by comparing the volumes of sub-cortical structures affected by HIV, namely basal ganglia and corpus callosum, to manual segmentation which is held as the gold standard. Although FreeSurfer overestimated most of the regions of interest, outputs are statistically consistent and group comparison results are similar between methods. This shows that FreeSurfer may be used as an alternative to manual segmentation in children with HIV, especially in an era of large MRI datasets where manual segmentation is laborious.

We further showed that perinatal HIV infection, clinically designed ART interruption, and early events due to HIV infection may lead to regional differences in cortical thickness and gyrification at age 5 years in comparison to HIV- controls, even with early ART initiation. Further longitudinal investigation on the long-term effects of some of the key variables showed unaltered trajectories of cortical development over the period from 5 to 9 years, suggesting that the observed cortical effects at age 5

and age 7 years are transient observations that resolve with time, possibly due to early and continued ART. The only variable that affected the trajectory of gyral development in any brain region was a diagnosis of HIV-related encephalopathy, which resulted in a decrease in frontal cortical folding over this period, in contrast to the increase in gyrification observed in HIV- controls.

Further longitudinal analysis of neuroimaging and neuropsychological assessment is important for this cohort as they develop into adolescence.

7.0 References

Ackermann, C., Andronikou, S., Laughton, B., Kidd, M., Dobbels, E., Innes, S., van Toorn, R., Cotton, M. (2014). White matter signal abnormalities in children with suspected HIV-related neurologic disease on early combination antiretroviral therapy. *The Pediatric infectious disease journal*, *33*(8), e207-12.

Ackermann, C., Andronikou, S., Saleh, M. G., Laughton, B., Alhamud, A. A., van der Kouwe, A., Kidd, M., Cotton, M.F., Meintjes, E.M. (2016). Early antiretroviral therapy in HIV-infected children is associated with diffuse white matter structural abnormality and corpus callosum sparing. American Journal of Neuroradiology.

Adachi K, Xu J, Ank B, Watts D.H, Camarca M, Mofenson L.M, Pilotto J.H, Joao E, Gray G, Theron G, Santos B. (2018). Congenital CMV and HIV Perinatal Transmission. The Pediatric infectious disease journal

Adamson, C., Beare, R., Walterfang, M., & Seal, M. (2014). Software pipeline for midsagittal corpus callosum thickness profile processing. *Neuroinformatics*, *12*(4), 595-614.

Akudjedu, T. N., Nabulsi, L., Makelyte, M., Scanlon, C., Hehir, S., Casey, H., Ambati, S., Kenney, J., O'Donoghue, S., McDermott, E., Kilmartin, L. (2018). A comparative study of segmentation techniques for the quantification of brain subcortical volume. *Brain imaging and behavior*, 1-18.

Alemán-Gómez, Y., Janssen, J., Schnack, H., Balaban, E., Pina-Camacho, L., Alfaro-Almagro, F., Castro-Fornieles, J., Otero, S., Baeza, I., Moreno, D., Bargalló, N. (2013). The human cerebral cortex flattens during adolescence. Journal of Neuroscience, 33(38), 15004-15010.

Amunts, K., Lepage, C., Borgeat, L., Mohlberg, H., Dickscheid, T., Rousseau, M. É., Bludau, S., Bazin, P.L., Lewis, L.B., Oros-Peusquens, A.M., Shah, N. J., Lippert, T., Zilles, K., Evans, A.C. (2013). BigBrain: an ultrahigh-resolution 3D human brain model. *Science*, *340*(6139), 1472-1475.

Ananworanich, J., Gayet-Ageron, A., Le Braz, M., Prasithsirikul, W., Chetchotisakd, P., Kiertiburanakul, S., Munsakul, W., Raksakulkarn, P., Tansuphasawasdikul, S., Sirivichayakul, S., Cavassini, M. (2006). CD4-guided scheduled treatment interruptions compared with continuous therapy for patients infected with HIV-1: results of the Staccato randomised trial. *The Lancet*, *368*(9534), 459-465.

Ananworanich J, Melvin D, Amador JT, Childs T, Medin G, Boscolo V, Compagnucci A, Kanjanavanit S, Monetro S, Gibb DM, PENTA 11 Study Group. (2016). Neurocognition and quality of life after reinitiating antiretroviral therapy in children randomized to planned treatment interruption. AIDS, 30(7), 1075-1081

Ances, B. M., Ortega, M., Vaida, F., Heaps, J., & Paul, R. (2012). Independent effects of HIV, aging, and HAART on brain volumetric measures. *Journal of acquired immune deficiency syndromes (1999)*, *59*(5), 469.

Ardekani, B. A., Toshikazu, I., Bachman, A., & Szeszko, P. R. (2012). Multi-atlas corpus callosum segmentation with adaptive atlas selection. In *Proceedings of the ISMRM*.

Armstrong, E., Schleicher, A., Omran, H., Curtis, M., & Zilles, K. (1995). The ontogeny of human gyrification. *Cerebral Cortex*, *5*(1), 56-63.

Assefa, G. (2012). Clinical and neuroimaging profile of HIV-1 encephalopathy in infancy and childhood in a sub-Saharan African country. *Ethiopian medical journal*, *50*(4), 337-347.

Aubert-Broche, B., Fonov, V. S., García-Lorenzo, D., Mouiha, A., Guizard, N., Coupé, P., Eskildsen, S.F., Collins, D. L. (2013). A new method for structural volume analysis of longitudinal brain MRI data and its application in studying the growth trajectories of anatomical brain structures in childhood. Neuroimage, 82, 393-402.

AVERT (2018). HIV and AIDS in South Africa. Retrieved from https://www.avert.org/professionals/hiv-around-world/sub-saharan-africa/south-africa. Accessed 14 September 2018

Avison, M. J., Nath, A., & Berger, J. R. (2002). Understanding pathogenesis and treatment of HIV dementia: A role for magnetic resonance? *Trends in Neurosciences*, *25*(9), 468-473.

Avison, M. J., Nath, A., Greene-Avison, R., Schmitt, F. A., Greenberg, R. N., & Berger, J. R. (2004). Neuroimaging correlates of HIV-associated BBB compromise. *Journal of neuroimmunology*, *157*(1-2), 140-146.

Aylward, E. H., Henderer, J. D., McArthur, J. C., Brettschneider, P. D., Harris, G. J., Barta, P. E., & Pearlson, G. D. (1993). Reduced basal ganglia volume in HIV-1-associated dementia: Results from quantitative neuroimaging. *Neurology*, *43*(10), 2099-2099.

Baker, L. M., Cooley, S. A., Cabeen, R. P., Laidlaw, D. H., Joska, J. A., Hoare, J., Stein, D.J., Heaps-Woodruff, J.M., Salminen, L.E., Paul, R. H. (2017). Topological organization of whole-brain white matter in HIV infection. *Brain connectivity*, *7*(2), 115-122.

Banks, W. A. (1999). Physiology and pathology of the blood-brain barrier: Implications for microbial pathogenesis, drug delivery and neurodegenerative disorders. *Journal of Neurovirology*, *5*(6), 538-555.

Barbi M, Binda S, Caroppo S, Primache V. (2006). Neonatal screening for congenital cytomegalovirus infection and hearing loss. Journal of clinical virology, 35(2), 206-209.

Barch, D. M., Tillman, R., Kelly, D., Whalen, D., Gilbert, K., & Luby, J. L. (2019). Hippocampal volume and depression among young children. *Psychiatry research. Neuroimaging*, *288*, 21.

Barnes, J., Ourselin, S., Fox, N. C. (2009). Clinical application of measurement of hippocampal atrophy in degenerative dementias. *Hippocampus*, *19*(6), 510-516.

Barron, P., Pillay, Y., Doherty, T., Sherman, G., Jackson, D., Bhardwaj, S., Robinson, P., Goga, A. (2013), 'Eliminating mother-to-child HIV transmission in South Africa', *Bulletin of the World Health Organization*, Vol. *91*, *no.* 1, pp. 70-74.

Bartko, J. J. (1966). The intraclass correlation coefficient as a measure of reliability. *Psychological reports*, *19*(1), 3-11.

Bartlett J.C., Lane H.C. (2012). Panel on Antiretroviral Guidelines for Adults and Adolescents. Guidelines for the use of antiretroviral agents in HIV-1-infected adults and adolescents. Department of Health and Human Services, Office of AIDS Research, pp 1–166. http://www.aidsinfo.nih.gov/contentfiles/lvguidelines/adultandadolescentgl.pdf. Accessed 03 March 2016

Bearden, C. E., van Erp, T. G., Dutton, R. A., Lee, A. D., Simon, T. J., Cannon, T. D., Samuel, B.S., McDonald-McGinn, D., Zackai, E.H., & Thompson, P. M. (2009). Alterations in midline cortical thickness and gyrification patterns mapped in children with 22q11. 2 deletions. *Cerebral cortex*, *19*(1), 115-126.

Becker, J. T., Sanders, J., Madsen, S. K., Ragin, A., Kingsley, L., Maruca, V., Cohen, B., Goodkin, K., Martin, E., Miller, E.N., Sacktor, N. (2011). Subcortical brain atrophy persists even in HAART-regulated HIV disease. *Brain imaging and behavior*, *5*(2), 77-85.

Bender, A. R., Keresztes, A., Bodammer, N. C., Shing, Y. L., Werkle-Bergner, M., Daugherty, A. M., Yu, Q., Kühn, S., Lindenberger, U., Raz, N. (2018). Optimization and validation of automated hippocampal subfield segmentation across the lifespan. *Human brain mapping*, *39*(2), 916-931.

Bernal-Rusiel, J. L., Greve, D. N., Reuter, M., Fischl, B., Sabuncu, M. R., & Alzheimer's Disease Neuroimaging Initiative. (2013). Statistical analysis of longitudinal neuroimage data with linear mixed effects models. *Neuroimage*, *66*, 249-260.

Biadgilign, S., Deribew, A., Amberbir, A., & Deribe, K. (2009). Barriers and facilitators to antiretroviral medication adherence among HIV-infected paediatric patients in Ethiopia: A qualitative study. *SAHARA: Journal of Social Aspects of HIV/AIDS Research Alliance*, *6*(4), 148-154.

Biffen, S. C., Warton, C. M., Lindinger, N. M., Randall, S. R., Lewis, C. E., Molteno, C. D., Jacobson, J.L., Jacobson, S.W., Meintjes, E. M. (2018). Reductions in Corpus Callosum Volume Partially Mediate Effects of Prenatal Alcohol Exposure on IQ. *Frontiers in neuroanatomy*, *11*, 132.

Bigler, E. D., Skiles, M., Wade, B. S., Abildskov, T. J., Tustison, N. J., Scheibel, R. S., Newsome, M.R., Mayer, A.R., Stone, J.R., Taylor, B.A., Tate, D. F. (2018). FreeSurfer 5.3 versus 6.0: are volumes comparable? A Chronic Effects of Neurotrauma Consortium study. *Brain imaging and behavior*, 1-10.

Blanton, R. E., Levitt, J. G., Thompson, P. M., Narr, K. L., Capetillo-Cunliffe, L., Nobel, A., Singerman, J.D., McCracken, J.T., Toga, A. W. (2001). Mapping cortical asymmetry and complexity patterns in normal children. *Psychiatry Research: Neuroimaging*, *107*(1), 29-43.

Blokhuis, C., Mutsaerts, H. J., Cohen, S., Scherpbier, H. J., Caan, M. W., Majoie, C. B., Kuijpers, T.W., Reiss, P., Wit, F.W., Pajkrt, D. (2017). Higher subcortical and white matter cerebral blood flow in perinatally HIV-infected children. Medicine, 96(7).

Boccardi, M., Ganzola, R., Bocchetta, M., Pievani, M., Redolfi, A., Bartzokis, G., Camicioli, R., Csernansky, J.G., De Leon, M.J., Detoledo-Morrell, L., Killiany, R. J. (2011). Survey of protocols for the manual segmentation of the hippocampus: preparatory steps towards a joint EADC-ADNI harmonized protocol. *Journal of Alzheimer's disease*, *26*(s3), 61-75.

Bonner, M. F., & Price, A. R. (2013). Where is the anterior temporal lobe and what does it do? *Journal of Neuroscience*, *33*(10), 4213-4215.

Brahmbhatt H, Boivin M, Ssempijja V, Kigozi G, Kagaayi J, Serwadda D, Gray RH (2014) Neurodevelopmental benefits of Anti-Retroviral Therapy in Ugandan children 0–6 Years of age with HIV. J Acquir Immune Def Syndr (1999) 67(3):316–322. https://doi.org/10.1097/QAI.0000000000000295

Broderick, D. F., Wippold II, F. J., Clifford, D. B., Kido, D., & Wilson, B. S. (1993). White matter lesions and cerebral atrophy on MR images in patients with and without AIDS dementia complex. *American Journal of Roentgenology*, *161*(1), 177-181.

Bruck, I., Tahan, T. T., Cruz, C. R. D., Martins, L. T. F., Antoniuk, S. A., Rodrigues, M., Souza, S.M.D., Bruyn, L. R. D. (2001). Developmental milestones of vertically HIV infected and seroreverters children: follow up of 83 children. *Arquivos de neuro-psiquiatria*, *59*(3B), 691-695.

[a]Bunupuradah, T., Duong, T., Compagnucci, A., McMaster, P., Bernardi, S., Kanjanavanit, S., Rampon, O., Faye, A., Saïdi, Y., Riault, Y, De Rossi, A. (2013). Outcomes after reinitiating antiretroviral therapy in children randomized to planned treatment interruptions. AIDS, 27(4), 579-589.

[b]Bunupuradah, T., Kosalaraksa, P., Vibol, U., Hansudewechakul, R., Sophonphan, J., Kanjanavanit, S., Ngampiyaskul, C., Wongsawat, J., Luesomboon, W., Vonthanak, S., Ananworanich, J. (2013). Impact of antiretroviral therapy on quality of life in HIV-infected Southeast Asian children in the PREDICT study. *AIDS patient care and STDs*, *27*(11), 596-603.

Calin, R., Hamimi, C., Lambert-Niclot, S., Carcelain, G., Bellet, J., Assoumou, L. Tubiana, R., Calvez, V., Dudoit, Y., Costagliola, D., Autran, B. (2016). Treatment interruption in chronically HIV-infected patients with an ultralow HIV reservoir. *Aids*, *30*(5), 761-769.

[a]Cao, B., Mwangi, B., Passos, I. C., Wu, M. J., Keser, Z., Zunta-Soares, G. B., Xu, D., Hasan, K.M., Soares, J. C. (2017). Lifespan gyrification trajectories of human brain in healthy individuals and patients with major psychiatric disorders. Scientific reports, 7(1), 511.

[b]Cao, B., Passos, I. C., Wu, M. J., Zunta-Soares, G. B., Mwangi, B., & Soares, J. C. (2017). Brain gyrification and neuroprogression in bipolar disorder. *Acta Psychiatrica Scandinavica*, *135*(6), 612-613.

Cardenas, V. A., Meyerhoff, D. J., Studholme, C., Kornak, J., Rothlind, J., Lampiris, H., Neuhaus, J., Grant, R.M., Chao, L.L., Truran, D., Weiner, M. W. (2009). Evidence for ongoing brain injury in human immunodeficiency virus–positive patients treated with antiretroviral therapy. Journal of neurovirology.

Casey, B. J., Jones, R. M., Hare, T. A. (2008). The adolescent brain. Annals of the New York Academy of Sciences, 1124(1), 111-126.

Centers for Disease Control and Prevention (1993) Revised Classification System for HIV Infection and Expanded Surveillance Case Definition for AIDS Among Adolescents and Adults. Available from: http://www.cdc.gov/mmwr/preview/mmwrhtml/00018871.htm. Accessed 03 March 2016

Chan, D. C., Fass, D., Berger, J. M., & Kim, P. S. (1997). Core structure of gp41 from the HIV envelope glycoprotein. *Cell*, *89*(2), 263-273.

Chang, L., Yakupov, R., Nakama, H., Stokes, B., & Ernst, T. (2008). Antiretroviral treatment is associated with increased attentional load-dependent brain activation in HIV patients. *Journal of Neuroimmune Pharmacology*, *3*(2), 95-104.

Cherbuin, N., Anstey, K. J., Réglade-Meslin, C., Sachdev, P. S. (2009). In vivo hippocampal measurement and memory: a comparison of manual tracing and automated segmentation in a large community-based sample. *PloS one*, *4*(4), e5265.

Chi, J. G., Dooling, E. C., & Gilles, F. H. (1977). Gyral development of the human brain. Annals of neurology, 1(1), 86-93.

Children with HIV Early Antiretroviral Therapy (CHER) Trial. (2010). A phase III randomised, open label trial to evaluate strategies for providing Antiretroviral Therapy to infants shortly after primary infection in a resource poor setting. The National Institute of Allergy and infection Diseases, Division of AIDS (DAIDS). pp. 22-23

Chriboga C.A, Fleishman.S, Champion.S, Gaye-Robinson.L, Abrams.E.J (2005). Incidence and

prevalence of HIV encephalopathy in children with HIV infection receiving highly active anti-retroviral therapy (HAART). The Journal of Pediatrics pp. 401-407

Chung, Y. S., Hyatt, C. J., & Stevens, M. C. (2017). Adolescent maturation of the relationship between cortical gyrification and cognitive ability. *NeuroImage*, *158*, 319-331.

Clark, U. S., Cohen, R. A., Sweet, L. H., Gongvatana, A., Devlin, K. N., Hana, G. N., Westbrook, M.L., Mulligan, R.C., Jerskey, B.A., White, T.L., Navia, B., Tashima, K.T., (2012). Effects of HIV and early life stress on amygdala morphometry and neurocognitive function. Journal of the International Neuropsychological Society, 18(04), 657-668.

Clarkson, M. J., Cardoso, M. J., Ridgway, G. R., Modat, M., Leung, K. K., Rohrer, J. D., Fox, N.C., Ourselin, S. (2011). A comparison of voxel and surface based cortical thickness estimation methods. Neuroimage, 57(3), 856-865.

Clerx, L., Gronenschild, H. B. M., Echavarri, C., Aalten, P., & IL Jacobs, H. (2015). Can FreeSurfer Compete with Manual Volumetric Measurements in Alzheimer's Disease? *Current Alzheimer Research*, *12*(4), 358-367.

Cohen, S., Caan, M. W., Mutsaerts, H. J., Scherpbier, H. J., Kuijpers, T. W., Reiss, P., Majoie, C.B. Pajkrt, D. (2016). Cerebral injury in perinatally HIV-infected children compared to matched healthy controls. *Neurology*, *86*(1), 19-27.

Cotton MF, Violari A, Otwombe K, Panchia R, Dobbels E, Rabie H, van Rensburg AJ (2013) Early time-limited antiretroviral therapy versus deferred therapy in South African infants infected with HIV: results from the children with HIV early antiretroviral (CHER) randomised trial. Lancet 382(9904):1555–1563. https://doi.org/10.1016/S0140-6736(13)61409-9

Cross, S. A., Cook, D. R., Chi, A. W., Vance, P. J., Kolson, L. L., Wong, B. J., Jordan-Sciutto, K.L., Kolson, D. L. (2011). Dimethyl fumarate, an immune modulator and inducer of the antioxidant response, suppresses HIV replication and macrophage-mediated neurotoxicity: a novel candidate for HIV neuroprotection. *The Journal of Immunology*, *187*(10), 5015-5025

Crowell C.S., Yanling H.U.O., Tassiopoulos K., Malee K.M., Yogev R, Hazra R, Rutstein RM, Nichols S.L., Smith R.A., Williams P.L., Oleske J, Muller W.J., PACTG 219C and PHACS study teams (2015) Early viral suppression improves neurocognitive outcomes in HIV-infected children. AIDS (London, England) 29(3):295–304. https://doi.org/10.1097/QAD.0000000000000528

Danel, C., Moh, R., Minga, A., Anzian, A., Ba-Gomis, O., Kanga, C., Nzunetu, G., Gabillard, D., Rouet, F., Sorho, S, Chaix, M. L. (2006). CD4-guided structured antiretroviral treatment interruption strategy in HIV-infected adults in west Africa (Trivacan ANRS 1269 trial): a randomised trial. The Lancet, 367(9527), 1981-1989.

Depas, G., Chiron, C., Tardieu, M., Nuttin, C., Blanche, S., Raynaud, C., & Syrota, A. (1995). Functional brain imaging in HIV-1-infected children born to seropositive mothers. *Journal of nuclear medicine: official publication, Society of Nuclear Medicine*, *36*(12), 2169-2174.

Despotović, I., Goossens, B., Philips, W. (2015). MRI segmentation of the human brain: challenges, methods, and applications. *Computational and mathematical methods in medicine, 2015*.

Dewey, J., Hana, G., Russell, T., Price, J., McCaffrey, D., Harezlak, J., Sem, E., Anyanwu, J.C., Guttmann, C.R., Navia, B., Cohen, R. (2010). Reliability and validity of MRI-based automated volumetry software relative to auto-assisted manual measurement of subcortical structures in HIV-infected patients from a multisite study. Neuroimage, 51(4), 1334-1344.

Diamond, A. (2002). Normal development of prefrontal cortex from birth to young adulthood: Cognitive functions, anatomy, and biochemistry. *Principles of frontal lobe function*, 466-503.

Di sclafani, V., Mackay, R. S., Meyerhoff, D. J., Norman, D., Weiner, M. W., Fein, G. (1997). Brain atrophy in HIV infection is more strongly associated with CDC clinical stage than with cognitive impairment. *Journal of the International Neuropsychological Society*, *3*(03), 276-287

Donald, K. A., Hoare, J., Eley, B., & Wilmshurst, J. M. (2014). Neurologic complications of pediatric human immunodeficiency virus: implications for clinical practice and management challenges in the African setting. In *Seminars in pediatric neurology* (Vol. 21, No. 1, pp. 3-11). WB Saunders.
Driemeyer, J., Boyke, J., Gaser, C., Büchel, C., May, A. (2008). Changes in gray matter induced by learning—revisited. *PLoS One*, *3*(7), e2669.

Du, H., Wu, Y., Ochs, R., Edelman, R. R., Epstein, L. G., McArthur, J., &Ragin, A. B. (2012). A comparative evaluation of quantitative neuroimaging measurements of brain status in HIV infection. *Psychiatry Research*, *203*(1), 95-99. doi:10.1016/j.pscychresns.2011.08.014

Dubois, J., Benders, M., Borradori-Tolsa, C., Cachia, A., Lazeyras, F., Leuchter, R. H. V., Sizonenko, S.V., Warfield, S.K., Mangin, J.F., Hüppi, P. S. (2008). Primary cortical folding in the human newborn: an early marker of later functional development. *Brain*,*131*(8), 2028-2041.

Dubrocq, G., Rakhmanina, N. (2018). Antiretroviral therapy interruptions: impact on HIV treatment and transmission. *HIV/AIDS (Auckland, NZ)*, *10*, 91.

Dyda, F., Hickman, A. B., Jenkins, T. M., Engelman, A., Craigie, R., Davies, D. R. (1994). Crystal structure of the catalytic domain of HIV-1 integrase: similarity to other polynucleotidyl transferases. *Science*, *266*(5193), 1981-1986.

Ebonyi, A. O., Ejeliogu, E. U., Okpe, S. E., Shwe, D. D., Yiltok, E. S., Ochoga, M. O., Oguche, S. (2015). Factors associated with antiretroviral treatment interruption in human immunodeficiency virus (HIV)-1-infected children attending the Jos University Teaching Hospital, Jos, Nigeria. *Nigerian medical journal: journal of the Nigeria Medical Association*, *56*(1), 43.

Ecker, C., Andrews, D., Dell'Acqua, F., Daly, E., Murphy, C., Catani, M., Thiebaut de Schotten, M., Baron-Cohen, S., Lai, M.C., Lombardo, M.V., Bullmore, E. T. (2016). Relationship between cortical gyrification, white matter connectivity, and autism spectrum disorder. *Cerebral Cortex*, *26*(7), 3297-3309.

Egger, C., Opfer, R., Wang, C., Kepp, T., Sormani, M. P., Spies, L., Barnett, M., Schippling, S. (2017). MRI FLAIR lesion segmentation in multiple sclerosis: Does automated segmentation hold up with manual annotation? *NeuroImage: Clinical*, *13*, 264-270.

Ellis, R (2010). HIV and antiretroviral therapy: Impact on the central nervous system. Progress in Neurobiology, 91. pp. 185 – 187

Elnakib, A. A. E. (2013). Developing advanced mathematical models for detecting abnormalities in 2D/3D medical structures.

Epstein, H. T. (1986). Stages in human brain development. *Developmental Brain Research*, *30*(1), 114-119.

Epstein, L. G., Sharer, L. R., Oleske, J. M., Connor, E. M., Goudsmit, J., Bagdon, L., Koenigsberger, M. R. (1986). Neurologic manifestations of human immunodeficiency virus infection in children. *Pediatrics*, *78*(4), 678-687.

Fennema-Notestine, C., Gamst, A. C., Quinn, B. T., Pacheco, J., Jernigan, T. L., Thal, L., Buckner, R., Killiany, R., Blacker, D., Dale, A.M., Fischl, B. (2007). Feasibility of multi-site clinical structural neuroimaging studies of aging using legacy data. *Neuroinformatics*, *5*(4), 235-245.

Fennema-Notestine, C., Ellis, R. J., Archibald, S. L., Jernigan, T. L., Letendre, S. L., Notestine, R. J., Taylor, M.J., Theilmann, R.J., Julaton, M.D., Croteau, D.J., Wolfson, T., Heaton, R.K., Gamst, A.C., Franklin Jr., D.R., Clifford, D.B., Collier, A.C., Gelman, B.B., Marra, C., McArthur, J.C., McCutchan, J.A., Morgello, S., Simpson, D.M., Grant, I. and CHARTER group (2013). Increases in brain white matter abnormalities and subcortical gray matter are linked to CD4 recovery in HIV infection. *Journal of neurovirology*, *19*(4), 393-401.

Fettiplace, A., Stainsby, C., Winston, A., Givens, N., Puccini, S., Vannappagari, V., Hsu, R., Fusco, J., Quercia, R., Aboud, M., Curtis, L. (2017). Psychiatric symptoms in patients receiving dolutegravir. *Journal of acquired immune deficiency syndromes (1999)*, *74*(4), 423.

Filippi, C. G., Uluğ, A. M., Ryan, E., Ferrando, S. J., & van Gorp, W. (2001). Diffusion tensor imaging of patients with HIV and normal-appearing white matter on MR images of the brain. *American Journal of Neuroradiology*,*22*(2), 277-283.

Fischl, B. (2012). Freesurfer. *Neuroimage*,*62*(2), 774-781. doi:10.1016/j.neuroimage.2012.01.021.

Fischl, B., Dale, A. M. (2000). Measuring the thickness of the human cerebral cortex from magnetic resonance images. *Proceedings of the National Academy of Sciences*, *97*(20), 11050-11055.

Fischl B, Sereno M.I, Tootell R.B, Dale A.M. (1999) High-resolution intersubject averaging and a coordinate system for the cortical surface. Hum. Brain Mapp.; 8:272–284. [PubMed: 10619420]

Fischl, B, Salat D.H., Busa E, Albert M, Dieterich M, Haselgrove C, van der Kouwe A, Killiany R, Kennedy D, Klaveness S, Montillo A, Makris N, Rosen B, Dale A.M. (2002). Whole brain segmentation: automated labeling of neuroanatomical structures in the human brain. Neuron. 33:341–355.

Fischl B, Salat D.H, van der Kouwe A.J, Makris N, Segonne F, Quinn B.T, Dale A.M. (2004a) Sequence independent segmentation of magnetic resonance images. Neuroimage; 23(Suppl. 1): S69–S84. [PubMed: 15501102].

Fischl B, van der Kouwe A, Destrieux C, Halgren E, Segonne F, Salat D.H, Busa E, Seidman L.J, Goldstein J, Kennedy D, Caviness V, Makris N, Rosen B, Dale A.M. (2004b). Automatically parcellating the human cerebral cortex. Cereb. Cortex. ; 14:11–22.

Fischl B, Rajendran N, Busa E, Augustinack J, Hinds O, Yeo B.T.T, Mohlberg H, Amunts K, Zilles K. (2008). Cortical folding patterns and predicting cytoarchitecture. Cereb. Cortex. ; 18:1973–1980. [PubMed: 18079129]

Fischl B, Stevens A.A, Rajendran N, Yeo B.T.T, Greve D.N, Van Leemput K, Polimeni J.R, Kakunoori S, Buckner R.L, Pacheco J, Salat D.H, Melcher J, Frosch M.P, Hyman B.T, Grant P.E, Rosen B.R, van der Kouwe A.J.W, Wiggins G.C, Wald L.L, Augustinack J.C. (2009). Predicting the location of entorhinal cortex from MRI. Neuroimage; 47:8–17. [PubMed: 19376238].

Fisher A.M, Cachia A, Fischer C, Mankiw C, Reardon P.K, Clasen L.S, Blumenthal J.D, Greenstein D, Giedd J.N, Mangin J.F, Raznahan A (2016) Influences of brain size, sex, and sex chromosome complement on the architecture of human cortical folding. Cereb Cortex. https://doi.org/10.1093/cercor/bhw323

Fjell, A. M., Westlye, L. T., Grydeland, H., Amlien, I., Espeseth, T., Reinvang, I., Raz, N., Dale, A.M., Walhovd, K.B., Alzheimer Disease Neuroimaging Initiative. (2012). Accelerating cortical thinning: unique to dementia or universal in aging? *Cerebral cortex*, *24*(4), 919-934.

Foster, C. J., Biggs, R. L., Melvin, D., Walters, M. D. S., Tudor-Williams, G., & Lyall, E. G. H. (2006). Neurodevelopmental outcomes in children with HIV infection under 3 years of age. *Developmental medicine and child neurology*, *48*(8), 677-682.

Fraser, M. A., Shaw, M. E., Anstey, K. J., Cherbuin, N. (2018). Longitudinal Assessment of Hippocampal Atrophy in Midlife and Early Old Age: Contrasting Manual Tracing and Semi-automated Segmentation (FreeSurfer). *Brain topography*, *31*(6), 949-962.

Friedman, L. A., Rapoport, J. L. (2015). Brain development in ADHD. *Current opinion in neurobiology*, *30*, 106-111.

Gaser, C., Luders, E., Thompson, P. M., Lee, A. D., Dutton, R. A., Geaga, J. A., Hayashi, K.M., Bellugi, U., Galaburda, A.M., Korenberg, J.R., Mills, D. L. (2006). Increased local gyrification mapped in Williams syndrome. *Neuroimage*, *33*(1), 46-54.

German, P., Liu, H. C., Szwarcberg, J., Hepner, M., Andrews, J., Kearney, B. P., & Mathias, A. (2012). Effect of cobicistat on glomerular filtration rate in subjects with normal and impaired renal function. *JAIDS Journal of Acquired Immune Deficiency Syndromes*, *61*(1), 32-40.

George, R., Andronikou, S., du Plessis, J., du Plessis, A., Van Toorn, R., &Maydell, A. (2009). Central nervous system manifestations of HIV infection in children. *Pediatric Radiology*, *39*(6), 575-585.

Giedd, J. N., Blumenthal, J., Jeffries, N. O., Castellanos, F. X., Liu, H., Zijdenbos, A., Paus, T., Evans, A.C., Rapoport, J. L. (1999). Brain development during childhood and adolescence: a longitudinal MRI study. *Nature neuroscience*,*2* (10), 861-863.

Giedd, J. N. (2004). Structural magnetic resonance imaging of the adolescent brain. *Annals of the New York Academy of Sciences*, *1021*(1), 77-85.

Giedd, J. N., & Rapoport, J. L. (2010). Structural MRI of pediatric brain development: what have we learned and where are we going? *Neuron*, *67*(5), 728-734.

Gogtay, N., Giedd, J. N., Lusk, L., Hayashi, K. M., Greenstein, D., Vaituzis, A. C., Nugent III, T.F., Herman, D.H., Clasen, L.S., Toga, A.W., Rapoport, J. L., Thompson, P.M. (2004). Dynamic mapping of human cortical development during childhood through early adulthood. *Proceedings of the National Academy of sciences of the United States of America*, *101*(21), 8174-8179.

Govender, R., Eley, B., Walker, K., Petersen, R., Wilmshurst, J. M. (2011). Neurologic and neurobehavioral sequelae in children with human immunodeficiency virus (HIV-1) infection. *Journal of child neurology*, *26*(11), 1355-1364.

Granato, A., Dering, B. (2018). Alcohol and the developing brain: why neurons die and how survivors change. *International journal of molecular sciences*, *19*(10), 2992.

Grimm, O., Pohlack, S., Cacciaglia, R., Winkelmann, T., Plichta, M. M., Demirakca, T., Flor, H. (2015). Amygdalar and hippocampal volume: A comparison between manual segmentation, Freesurfer and VBM. *Journal of neuroscience methods*, *253*, 254-261.

Haier, R. J., Jung, R. E., Yeo, R. A., Head, K., & Alkire, M. T. (2004). Structural brain variation and general intelligence. *Neuroimage*, *23*(1), 425-433.

Hall, M., Whaley, R., Robertson, K., Hamby, S., Wilkins, J., & Hall, C. (1996). The correlation between neuropsychological and neuroanatomic changes over time in asymptomatic and symptomatic HIV-1-infected individuals. *Neurology*, *46*(6), 1697-1702.

Hall, J. E. (2015). *Guyton and Hall textbook of medical physiology e-Book*. Elsevier Health Sciences.

Harrach, M. A., Rousseau, F., Groeschel, S., Wang, X., Hertz-pannier, L., Chabrier, S., Chabrier, S., Bohi, A., Lefevre, J., Dinomais, M., AVCnn group. (2019). Alterations in Cortical Morphology after Neonatal Stroke: Compensation in the Contralesional Hemisphere? *Developmental neurobiology*.

Hazuda, D. J., Felock, P., Witmer, M., Wolfe, A., Stillmock, K., Grobler, J. A., Espeseth, A., Gabryelski, L., Schleif, W., Blau, C., Miller, M. D. (2000). Inhibitors of strand transfer that prevent integration and inhibit HIV-1 replication in cells. *Science*, *287*(5453), 646-650.

Herron, T. J., Kang, X., & Woods, D. L. (2012). Automated measurement of the human corpus callosum using MRI. *Frontiers in neuroinformatics*, *6*, 25.

Hinkley, L. B., Marco, E. J., Findlay, A. M., Honma, S., Jeremy, R. J., Strominger, Z., Bukshpun, P., Wakahiro, M., Brown, W.S., Paul, L.K. Barkovich, A. J. (2012). The role of corpus callosum development in functional connectivity and cognitive processing. *PLoS One*, *7*(8), e39804.

Hisatomi, T., Nakazawa, T., Noda, K., Almulki, L., Miyahara, S., Nakao, S., Ito, Y., She, H., Kohno, R., Michaud, N., Ishibashi, T., Hafezi-Moghadam, A., Badley, A.D., Kroemer, G., Miller, J.W. (2008). HIV protease inhibitors provide neuroprotection through inhibition of mitochondrial apoptosis in mice. *The Journal of clinical investigation*, *118*(6), 2025-2038

Hoare, J., Fouche, J. P., Phillips, N., Joska, J. A., Donald, K. A., Thomas, K., & Stein, D. J. (2015). Clinical associations of white matter damage in cART-treated HIV-positive children in South Africa. *Journal of neurovirology*, *21*(2), 120-128.

Hoare, J., Fouche, J. P., Spottiswoode, B., Sorsdahl, K., Combrinck, M., Stein, D. J., Robert, H.P., & Joska, J. A. (2014). White-matter damage in clade C HIV-positive subjects: a diffusion tensor imaging study

Hoare, J., Fouche, J. P., Phillips, N., Joska, J. A., Myer, L., Zar, H. J., Stein, D. J. (2018). Structural brain changes in perinatally HIV-infected young adolescents in South Africa. *Aids*, *32*(18), 2707-2718.

Holt, J. L., Kraft-Terry, S., & Chang, L. (2012). Neuroimaging studies of the aging HIV-1-infected brain. *Journal of Neurovirology*, *18*(4), 291-302. doi:10.1007/s13365-012-0114-1.

Hong, S., Dissing-Olesen, L., & Stevens, B. (2016). New insights on the role of microglia in synaptic pruning in health and disease. *Current opinion in neurobiology*, *36*, 128-134.

Horowitz, A. L. (1989). Overview. In *MRI Physics for Physicians* (pp. 1). Springer US.

Horvath, S., Stein, D. J., Phillips, N., Heany, S. J., Kobor, M. S., Lin, D. T., Myer, L., Zar, H.J., Levine, A.J., Hoare, J. (2018). Perinatally acquired HIV infection accelerates epigenetic aging in South African adolescents. *Aids*, *32*(11), 1465-1474.

Huizinga, M., Dolan, C. V., van der Molen, M. W. (2006). Age-related change in executive function: Developmental trends and a latent variable analysis. *Neuropsychologia*, *44*(11), 2017-2036.

Huttenlocher, P. R., Dabholkar, A. S. (1997). Regional differences in synaptogenesis in human cerebral cortex. Journal of comparative Neurology, 387(2), 167-178.

Ibrahim, A., Nwosu, E., Robertson, F., Little, F., Cotton, M., Laughton, B., van der Kouwe, A., Meintjes, E., Holmes, M. (2019). Cortical thickness and neuropsychological outcomes in HIV infected and uninfected children at 5 years. 25th annual meeting of Organization of Human Brain Mapping (OHBM), Rome, Italy. Poster #: Th679

Jankiewicz, M., Holmes, M. J., Taylor, P. A., Cotton, M. F., Laughton, B., van der Kouwe, A. J., Meintjes, E. M. (2017). White Matter Abnormalities in Children with HIV Infection and Exposure. Frontiers in neuroanatomy, 11, 88.

Jenkinson, M., Beckmann, C. F., Behrens, T. E., Woolrich, M. W., & Smith, S. M. (2012). Fsl. *Neuroimage*, *62*(2), 782-790.

Jernigan, T. L., Archibald, S., Hesselink, J. R., Atkinson, J. H., Velin, R. A., McCutchan, J. A., Chandler, J., Grant, I. (1993). Magnetic resonance imaging morphometric analysis of cerebral volume loss in human immunodeficiency virus infection. *Archives of neurology*, *50*(3), 250-255.

Joint United Nations Programme on HIV/AIDS - UNAIDS (2014). HIV and AIDS estimate (2014). Retrieved on 11 April, 2016 fromhttp://www.unaids.org/en/regionscountries/countries/southafrica#

Jou, R. J., Minshew, N. J., Keshavan, M. S., & Hardan, A. Y. (2010). Cortical gyrification in autistic and Asperger disorders: a preliminary magnetic resonance imaging study. *Journal of child neurology*, *25*(12), 1462-1467.

Jung, R. E., Ryman, S. G., Vakhtin, A. A., Carrasco, J., Wertz, C., & Flores, R. A. (2014). Subcortical correlates of individual differences in aptitude. *PloS one*, *9*(2), e89425.

Kakuda, T. N. (2000). Pharmacology of nucleoside and nucleotide reverse transcriptase inhibitor-induced mitochondrial toxicity. *Clinical therapeutics*,*22*(6), 685-708.

Kallianpur, K. J., Kirk, G. R., Sailasuta, N., Valcour, V., Shiramizu, B., Nakamoto, B. K., & Shikuma, C. (2011). Regional cortical thinning associated with detectable levels of HIV DNA. *Cerebral Cortex*, bhr285.

Kallianpur, K. J., Shikuma, C., Kirk, G. R., Shiramizu, B., Valcour, V., Chow, D., & Sailasuta, N. (2013). Peripheral blood HIV DNA is associated with atrophy of cerebellar and subcortical gray matter. *Neurology*, *80*(19), 1792-1799.

Kallianpur, K. J., Gerschenson, M., Mitchell, B. I., LiButti, D. E., Umaki, T. M., Ndhlovu, L. C., Nakamoto, B.K., Chow, D.C., Shikuma, C. M. (2016). Oxidative mitochondrial DNA damage in peripheral blood mononuclear cells is associated with reduced volumes of hippocampus and subcortical gray matter in chronically HIV-infected patients. *Mitochondrion*, *28*, 8-15.

Kaul, M., Garden, G. A., & Lipton, S. A. (2001). Pathways to neuronal injury and apoptosis in HIV-associated dementia. *Nature*, *410*(6831), 988-994.

Kersbergen, K. J., Leroy, F., Išgum, I., Groenendaal, F., de Vries, L. S., Claessens, N. H., van Haastert, I.C., Moeskops, P., Fischer, C., Mangin, J.F., Viergever, M. A. (2016). Relation between

clinical risk factors, early cortical changes, and neurodevelopmental outcome in preterm infants. *Neuroimage*, *142*, 301-310.

Kesler, S. R., Vohr, B., Schneider, K. C., Katz, K. H., Makuch, R. W., Reiss, A. L., Ment, L. R. (2006). Increased temporal lobe gyrification in preterm children. *Neuropsychologia*, *44*(3), 445-453.

Kfutwah, A. K., Ngoupo, P. A. T., Sofeu, C. L., Ndongo, F. A., Guemkam, G., Ndiang, S. T., Owona, F., Penda, I.C., Tchendjou, P., Rouzioux, C., Warszawski, J. (2017). Cytomegalovirus infection in HIV-infected versus non-infected infants and HIV disease progression in Cytomegalovirus infected versus non infected infants early treated with cART in the ANRS 12140—Pediacam study in Cameroon. *BMC infectious diseases*, *17*(1), 224.

Khan, A. M. (2013). Physics of MRI. *Principles and Practice of Urology*, 92.

Kieck, J., Andronikou, S. (2008). Usefulness of neuro-imaging for the diagnosis of HIV encephalopathy in children. *South African Medical Journal*, *94*(8), 628.

Klein, D., Rotarska-Jagiela, A., Genc, E., Sritharan, S., Mohr, H., Roux, F., Han, C.E., Kaiser, M., Singer, W., Uhlhaas, P. J. (2014). Adolescent brain maturation and cortical folding: evidence for reductions in gyrification. *PloS one*, *9*(1), e84914.

Lanciego, J. L., Luquin, N., & Obeso, J. A. (2012). Functional neuroanatomy of the basal ganglia. *Cold Spring Harbor perspectives in medicine*, a009621.

Langerak, N. G., du Toit, J., Burger, M., Cotton, M. F., Springer, P. E., Laughton, B. (2014). Spastic diplegia in children with HIV encephalopathy: first description of gait and physical status. *Developmental Medicine & Child Neurology*, *56*(7), 686-694.

Laughton, B., Cornell, M., Grove, D., Kidd, M., Springer, P. E., Dobbels, E., Janse van Rensburg, A., Violari, A., Babiker, A.,Madhi, S.A., Jean-Philippe, P., Gibb, D.M., Cotton, M. F. (2012). Early antiretroviral therapy improves neurodevelopmental outcomes in infants. *AIDS (London, England)*, *26*(13), 1685.

Laughton B, Cornell M, Boivin M, Van Rie A (2013) Neurodevelopment in perinatally HIV-infected children: a concern for adolescence. J Int AIDS Soc 16(1):18603Cameroon. *BMC infectious diseases*, *17*(1), 224.

Laughton, B., Cornell, M., Kidd, M., Springer, P. E., Dobbels, E. F. M. T., Rensburg, A. J. V., Otwombe, K., Babiker, A., Gibb, D.M., Violari, A., Kruger, M., Cotton, M.F. (2018). Five-year neurodevelopment outcomes of perinatally HIV-infected children on early limited or deferred continuous antiretroviral therapy. Journal of the International AIDS Society, 21(5), e25106.

Lebel, C., Beaulieu, C. (2011). Longitudinal development of human brain wiring continues from childhood into adulthood. Journal of Neuroscience, 31(30), 10937-10947.

Le Doaré, K., Bland, R., & Newell, M. (2012). Neurodevelopment in children born to HIV-infected mothers by infection and treatment status.*Pediatrics*, *130*(5), e1326-e1344. doi:10.1542/peds.2012-0405.

Lenroot, R. K., Gogtay, N., Greenstein, D. K., Wells, E. M., Wallace, G. L., Clasen, L. S, Blumenthal, J.D., Lerch, J., Zijdenbos, A.P., Evans, A.C., Thompson, P. M. (2007). Sexual dimorphism of brain developmental trajectories during childhood and adolescence. *Neuroimage*, *36*(4), 1065-1073.

Lewis, J., Payne, H., Walker, A. S., Otwombe, K., Gibb, D. M., Babiker, A. G., Panchia, R., Cotton, M.F., Violari, A., Klein, N., Callard, R. E. (2017). Thymic output and CD4 T-cell reconstitution in HIV-infected children on early and interrupted antiretroviral treatment: Evidence from the children with HIV early antiretroviral therapy trial. *Frontiers in immunology*, *8*, 1162.

Lewis-de los Angeles, C.P. (2017). Altered Neurodevelopment in Youth with Perinatally-Acquired HIV: Analyses of Grey Matter Spatial Distribution Patterns Using Structural Magnetic Resonance Imaging. Doctoral dissertation. Northwestern University

Lewis-de los Angeles, C. P., Alpert, K. I., Williams, P. L., Malee, K., Huo, Y., Csernansky, J. G., Yogev, R., Van Dyke, R.B., Sowell, E.R., Wang, L. (2016). Deformed subcortical structures are related to past HIV disease severity in youth with perinatally acquired HIV infection. Journal of the Pediatric Infectious Diseases Society, 5(suppl_1), S6-S14.

Lewis-de los Angeles, C. P., Williams, P. L., Huo, Y., Wang, S. D., Uban, K. A., Herting, M. M, Malee, K., Yogev, R., Csernansky, J.G., Nichols, S., Van Dyke, R. B. (2017). Lower total and regional grey matter brain volumes in youth with perinatally-acquired HIV infection: associations with HIV disease severity, substance use, and cognition. *Brain, behavior, and immunity*, *62*, 100-109.

Li, G., Wang, L., Shi, F., Lyall, A. E., Lin, W., Gilmore, J. H., & Shen, D. (2014). Mapping longitudinal development of local cortical gyrification in infants from birth to 2 years of age. *Journal of Neuroscience*, *34*(12), 4228-4238.

Li, J. Z., Smith, D. M., Mellors, J. W. (2015). The critical roles of treatment interruption studies and biomarker identification in the search for an HIV cure. *AIDS (London, England)*, *29*(12), 1429.

Lindsey.J.C, Malee.K.M, Brouwers.P, Hughes.M.D (2007). Neurodevelopmental functioning in HIV-infected infants and young children before and after the introduction of protease inhibitor-based highly active antiretroviral therapy. PEDIATRICS. DOI: 10.1542/peds.2006-1145.

Lobato, M. N., Caldwell, M. B., Ng, P., Oxtoby, M. J., & Pediatric Spectrum of Disease Clinical Consortium. (1995). Encephalopathy in children with perinatally acquired human immunodeficiency virus infection. *The Journal of pediatrics*, *126*(5), 710-715.

Loh, W. Y., Connelly, A., Cheong, J. L., Spittle, A. J., Chen, J., Adamson, C., Ahmadzai, Z.M., Fam, L.G., Rees, S., Lee, K.J., Doyle, L. W. (2016). A new MRI-based pediatric subcortical segmentation technique (PSST). *Neuroinformatics*, *14*(1), 69-81.

Luders, E., Narr, K. L., Thompson, P. M., Rex, D. E., Jancke, L., Steinmetz, H., Toga, A. W. (2004). Gender differences in cortical complexity. *Nature neuroscience*, *7*(8), 799-800.
Lyden, H., Gimbel, S. I., Del Piero, L., Tsai, A. B., Sachs, M. E., Kaplan, J. T., Margolin, G., Saxbe, D. (2016). Associations between family adversity and brain volume in adolescence: Manual vs. automated brain segmentation yields different results. *Frontiers in neuroscience*, *10*, 398

Lyall, A. E., Shi, F., Geng, X., Woolson, S., Li, G., Wang, L., Hamer, R.M., Shen, D., Gilmore, J. H. (2015). Dynamic development of regional cortical thickness and surface area in early childhood. *Cerebral cortex*, *25*(8), 2204-2212.

Lyden, H., Gimbel, S. I., Del Piero, L., Tsai, A. B., Sachs, M. E., Kaplan, J. T., Margolin, G., Saxbe, D. (2016). Associations between family adversity and brain volume in adolescence: Manual vs. automated brain segmentation yields different results. *Frontiers in neuroscience*, *10*, 398.

Madhi, S. A., Adrian, P., Cotton, M. F., McIntyre, J. A., Jean-Philippe, P., Meadows, S., Nachman, S., Käyhty, H., Klugman, K.P., Violari, A. (2010). Effect of HIV infection status and anti-retroviral treatment on quantitative and qualitative antibody responses to pneumococcal conjugate vaccine in infants. *The Journal of infectious diseases*, *202*(3), 355-361.

Magnotta, V. A., Andreasen, N. C., Schultz, S. K., Harris, G., Cizadlo, T., Heckel, D., Nopoulos, P., Flaum, M. (1999). Quantitative in vivo measurement of gyrification in the human brain: changes associated with aging. *Cerebral Cortex*, *9*(2), 151-160.

Makowski, C., Béland, S., Kostopoulos, P., Bhagwat, N., Devenyi, G. A., Malla, A. K., Joober, R., Lepage, M., Chakravarty, M. M. (2018). Evaluating accuracy of striatal, pallidal, and thalamic segmentation methods: Comparing automated approaches to manual delineation. *NeuroImage*, *170*, 182-198.

Makris, N., Kennedy, D. N., Meyer, J., Worth, A., Caviness, V. S., Seidman, L., Goldstein, J., Goodman, J., Hoge, E., Macpherson, C., Tourville, J. (2004). General brain segmentation: Method and utilization. *Center for morphometric analysis*.

Maltbie, E., Bhatt, K., Paniagua, B., Smith, R. G., Graves, M. M., Mosconi, M. W., Peterson, S., White, S., Blocher, J., El-Sayed, M., Hazlett, H. C. (2012). Asymmetric bias in user guided segmentations of brain structures. *Neuroimage*, *59*(2), 1315-1323.

Mangin, J. F., Jouvent, E., & Cachia, A. (2010). In-vivo measurement of cortical morphology: means and meanings. *Current opinion in neurology*,*23*(4), 359-367.

Manicklal S, Emery VC, Lazzarotto T, Boppana SB, Gupta RK. (2013). The “silent” global burden of congenital cytomegalovirus. *Clinical microbiology reviews*, *26*(1), 86-102.

Mattson, M. P., Haughey, N. J., & Nath, A. (2005). Cell death in HIV dementia. *Cell Death & Differentiation*, *12*, 893-904.

May, A., Hajak, G., Gänssbauer, S., Steffens, T., Langguth, B., Kleinjung, T., & Eichhammer, P. (2007). Structural brain alterations following 5 days of intervention: dynamic aspects of neuroplasticity. *Cerebral Cortex*, *17*(1), 205-210.

Masuah, E., Achim, C. L., Hansen, L. A., & Wiley, C. A. (1992). Selective neuronal vulnerability in HIV encephalitis. *Journal of Neuropathology & Experimental Neurology*, *51*(6), 585-593.

Mbugua, K.K, Holmes, M.J, Cotton, M.F, Ratai, E.M, Little, F, Hess, A.T, Dobbels, E, Van der Kouwe, A.J, Laughton, B, Meintjes, E.M. (2016). HIV-associated CD4/8 depletion in infancy is associated with neurometabolic reductions in the basal ganglia at age 5 years despite early antiretroviral therapy. *AIDS (London, England)*, *30*(9), 1353.

McCoig.C, Castrejon.M.M, Castano.E, Onix de Suman, Baez.C, Redondo.W, McClernon.D, Danebower.S, Lanier Randall.E, Richardson.C, Keller.A, Hetherington.S, Saez-Llorens.X, Ramilo.O (2002). Effect of combination antiretroviral therapy on cerebrospinal fluid HIV RNA, HIV resistance, and clinical manifestations of encephalopathy. The Journal of Pediatrics. Vol. 141, Number1. pp.36-44.

McGraw, K. O., & Wong, S. P. (1996). Forming inferences about some intraclass correlation coefficients. *Psychological methods*, *1*(1), 30.

McIntosh, R. C., Rosselli, M., Uddin, L. Q., & Antoni, M. (2015). Neuropathological sequelae of human immunodeficiency virus and apathy: a review of neuropsychological and neuroimaging studies. *Neuroscience & Biobehavioral Reviews*, *55*, 147-164.

Mills, K. L., Tamnes, C. K. (2014). Methods and considerations for longitudinal structural brain imaging analysis across development. Developmental cognitive neuroscience, 9, 172-190.

Mitchell, W. (2001). Neurological and developmental effects of HIV and AIDS in children and adolescents. *Mental Retardation and Developmental Disabilities Research Reviews, 7*(3), 211-216.

Mitchell, C. D. (2006). HIV-1 encephalopathy among perinatally infected children: Neuropathogenesis and response to highly active antiretroviral therapy. *Mental retardation and developmental disabilities research reviews*, *12*(3), 216-222.

Moeskops, P., Benders, M. J., Kersbergen, K. J., Groenendaal, F., de Vries, L. S., Viergever, M. A., Išgum, I. (2015). Development of cortical morphology evaluated with longitudinal MR brain images of preterm infants. PloS one, 10(7), e0131552.

Montserrat, M., Plana, M., Guardo, A. C., Andrés, C., Climent, N., Gallart, T., Leal, L., Gatell, J.M., Sanchez-Palomino, S., García, F. (2017). Impact of long-term antiretroviral therapy interruption and resumption on viral reservoir in HIV-1 infected patients. *Aids*, *31*(13), 1895-1897.

Mooshagian, E. (2008). Anatomy of the corpus callosum reveals its function. *Journal of Neuroscience*, *28*(7), 1535-1536.

Morey, R. A., Petty, C. M., Xu, Y., Hayes, J. P., Wagner, H. R., Lewis, D. V., LaBar, K.S., Styner, M., McCarthy, G. (2009). A comparison of automated segmentation and manual tracing for quantifying hippocampal and amygdala volumes. *Neuroimage*, *45*(3), 855-866.

Musielak, K. A., & Fine, J. G. (2015). An Updated Systematic Review of Neuroimaging Studies of Children and Adolescents with Perinatally Acquired HIV. *Journal of Pediatric Neuropsychology*, 1-16.

Mutlu, A. K., Schneider, M., Debbané, M., Badoud, D., Eliez, S., Schaer, M. (2013). Sex differences in thickness, and folding developments throughout the cortex. *Neuroimage*, *82*, 200-207.

Narr, K. L., Bilder, R. M., Kim, S., Thompson, P. M., Szeszko, P., Robinson, D., Luders, E., Toga, A. W. (2004). Abnormal gyral complexity in first-episode schizophrenia. *Biological psychiatry*, *55*(8), 859-867.

Nasi, A., Chiodi, F. (2018). Mechanisms regulating expansion of CD8+ T cells during HIV-1 infection. *Journal of internal medicine*.

Navia, B. A., & Price, R. W. (1987). The acquired immunodeficiency syndrome dementia complex as the presenting or sole manifestation of human immunodeficiency virus infection.*Archives of Neurology*, *44*(1), 65.

Ndongo, F. A., Texier, G., Penda, C. I., Tejiokem, M. C., Ndiang, S. T., Ndongo, J. A., Guemkam, G., Sofeu, C.L., Kfutwah, A., Faye, A., Msellati, P. (2018). Virologic Response to Early Antiretroviral Therapy in Hiv-infected Infants: Evaluation After 2 Years of Treatment in the Pediacam Study, Cameroon. *The Pediatric infectious disease journal*, *37*(1), 78-84.

Nie, J., Li, G., & Shen, D. (2013). Development of cortical anatomical properties from early childhood to early adulthood. *Neuroimage*, *76*, 216-224.

NIH U.S National Library of Medicine (NUNLM) (2019). Guidelines for the Use of Antiretroviral Agents in Pediatric HIV Infection. Retrieved from https://aidsinfo.nih.gov/guidelines/html/2/pediatric-arv/70/when-to-initiate-therapy-in-antiretroviral-naive-children. Accessed 21 June 2019

Nugent, A. C., Luckenbaugh, D. A., Wood, S. E., Bogers, W., Zarate Jr, C. A., Drevets, W. C. (2013). Automated subcortical segmentation using FIRST: test–retest reliability, interscanner reliability, and comparison to manual segmentation. *Human brain mapping*, *34*(9), 2313-2329.

Nwosu, E.C. (2015). Effects of HIV and different Antiretroviral therapy regimens on brain morphometry in HIV-infected children at age 7. (master's in medicine thesis, University of Cape Town, South Africa). https://open.uct.ac.za/bitstream/handle/11427/16696/thesis_hsf_2015_nwosu_emmanuel_chukwubuikem.pdf?sequence=1&isAllowed=y

[a]Nwosu E.C, Robertson F.C, Holmes M.J, Cotton M.F, Dobbels E, Little F, Laughton B, van der Kouwe A, Meintjes E.M. (2018). Altered brain morphometry in 7-year old HIV-infected children on early ART. *Metabolic brain disease*, *33*(2), 523-535.

[b]Nwosu, E.C., Holmes, M.J., Cotton, M.F., Dobbels, E., Little, F., Laughton, B., van der Kouwe, A.J.W., Meintjes, E.M., Robertson, F.C. (2018)**.** Antiretroviral therapy (ART) interruption is associated with reduced cortical structures at age 5 years compared to uninterrupted. Proceedings at 10th International workshop on HIV PEDIATRICS, Amsterdam, Netherlands Abstract number: #68

O'connor, E. E., Zeffiro, T. A., & Zeffiro, T. A. (2018). Brain structural changes following HIV infection: meta-analysis. *American Journal of Neuroradiology*, *39*(1), 54-62.

Oh, S. W., Shin, N. Y., Choi, J. Y., Lee, S. K., & Bang, M. R. (2018). Altered White Matter Integrity in Human Immunodeficiency Virus-Associated Neurocognitive Disorder: A Tract-Based Spatial Statistics Study. *Korean journal of radiology*, *19*(3), 431-442.

Paediatric European Network for Treatment of AIDS (PENTA) Steering Committee: PENTA (2009) guidelines for the use of antiretroviral therapy in paediatric HIV-1 infection (2009). HIV Med 10(10):591–613. https://doi.org/10.1111/j.1468-1293.2009.00759.x

Paediatric European Network for Treatment of AIDS (PENTA). (2010). Response to planned treatment interruptions in HIV infection varies across childhood. *AIDS*, *24*(2), 231-241.

Palaniyappan, L., & Liddle, P. F. (2012). Aberrant cortical gyrification in schizophrenia: a surface-based morphometry study. *Journal of psychiatry & neuroscience: JPN*, *37*(6), 399.

Pardoe, H. R., Pell, G. S., Abbott, D. F., & Jackson, G. D. (2009). Hippocampal volume assessment in temporal lobe epilepsy: how good is automated segmentation? *Epilepsia*, *50*(12), 2586-2592.

Paul, R., Cohen, R., Navia, B., Tashima, K. (2002). Relationships between cognition and structural neuroimaging findings in adults with human immunodeficiency virus type-1. *Neuroscience &Biobehavioral Reviews*, *26*(3), 353-359. doi: http://dx.doi.org/10.1016/S0149-7634(02)00006-4.

Paul, R., Prasitsuebsai, W., Jahanshad, N., Puthanakit, T., Thompson, P., Aurpibul, L., Hansudewechakul, R., Kosalaraksa, P., Kanjanavanit, S., Ngampiyaskul, C., Luesomboon, W. (2018). Structural Neuroimaging and Neuropsychologic Signatures in Children With Vertically Acquired HIV. *The Pediatric infectious disease journal*, *37*(7), 662-668.

Paus, T. (2005). Mapping brain maturation and cognitive development during adolescence. *Trends in cognitive sciences*, *9*(2), 60-68.

Peelen, M. V., Caramazza, A. (2012). Conceptual object representations in human anterior temporal cortex. *Journal of Neuroscience*, *32*(45), 15728-15736.

Perlaki, G., Horvath, R., Nagy, S. A., Bogner, P., Doczi, T., Janszky, J., & Orsi, G. (2017). Comparison of accuracy between FSL's FIRST and Freesurfer for caudate nucleus and putamen segmentation. *Scientific reports*, *7*(1), 2418.

Persidsky, Y., Ramirez, S. H., Haorah, J., & Kanmogne, G. D. (2006). Blood–brain barrier: Structural components and function under physiologic and pathologic conditions. *Journal of Neuroimmune Pharmacology*, *1*(3), 223-236.

Phongsamart W, Hansudewechakul R, Bunupuradah T, Klinbuayaem V, Teeraananchai S, Prasithsirikul W, Kerr SJ, Akarathum N, Denjunta S, Ananworanich J, Chokephaibulkit K (2014) Long-term outcomes of HIV-infected children in Thailand: the Thailand Pediatric HIV Observational Database. Int J Infect Dis 22:19–24. https://doi.org/10.1016/j.ijid.2013.12.011

Pipitone, J., Park, M. T. M., Winterburn, J., Lett, T. A., Lerch, J. P., Pruessner, J. C., Lepage, M., Voineskos, A.N., Chakravarty, M.M. and Alzheimer's Disease Neuroimaging Initiative. (2014). Multi-atlas segmentation of the whole hippocampus and subfields using multiple automatically generated templates. *Neuroimage*, *101*, 494-512.

Plewes, D. B., & Kucharczyk, W. (2012). Physics of MRI: a primer. *Journal of Magnetic Resonance Imaging*, *35*(5), 1038-1054.

Puthanakit, T., Saphonn, V., Ananworanich, J., Kosalaraksa, P., Hansudewechakul, R., Vibol, U., Kerr, S.J., Kanjanavanit, S., Ngampiyaskul, C., Wongsawat, J., Luesomboon, W. (2012). Early versus deferred antiretroviral therapy for children older than 1 year infected with HIV (PREDICT): a multicentre, randomised, open-label trial. *The Lancet infectious diseases*, *12*(12), 933-941.

Puthanakit, T., Ananworanich, J., Vonthanak, S., Kosalaraksa, P., Hansudewechakul, R., van der Lugt, J., Kerr, S.J., Kanjanavanit, S., Ngampiyaskul, C., Wongsawat, J., Luesomboon, W. (2013). Cognitive function and neurodevelopmental outcomes in HIV-infected children older than 1 year of age randomized to early versus deferred antiretroviral therapy: the PREDICT neurodevelopmental study. *The Pediatric infectious disease journal*, *32*(5), 501.

Ragin, A. B., Storey, P., Cohen, B. A., Epstein, L. G., & Edelman, R. R. (2004). Whole brain diffusion tensor imaging in HIV-associated cognitive impairment. *American Journal of Neuroradiology*, *25*(2), 195-200.

Raininko, R., Elovaara, I., Virta, A., Valanne, L., Haltia, M., & Valle, S. L. (1992). Radiological study of the brain at various stages of human immunodeficiency virus infection: early development of brain atrophy.*Neuroradiology*, *34*(3), 190-196.

Rakic, P., Bourgeois, J. P., & Goldman-Rakic, P. S. (1994). Synaptic development of the cerebral cortex: implications for learning, memory, and mental illness. In *Progress in brain research* (Vol. 102, pp. 227-243). Elsevier.

Randall, S. R. (2015). The effects of HIV-1 infection on subcortical brain structures in children receiving ART: a structural MRI study (Masters dissertation, University of Cape Town).

Randall, S. R., Warton, C. M., Holmes, M. J., Cotton, M. F., Laughton, B., van der Kouwe, A. J., & Meintjes, E. M. (2017). Larger Subcortical Gray Matter Structures and Smaller Corpora Callosa at Age 5 Years in HIV Infected Children on Early ART. Frontiers in neuroanatomy, 11, 95.

Rausch, D. M., & Stover, E. S. (2001). Neuroscience research in AIDS. *Progress in Neuro-Psychopharmacology and Biological Psychiatry, 25*(1), 231-257.

Raznahan, A., Shaw, P., Lalonde, F., Stockman, M., Wallace, G. L., Greenstein, D., Clasen, L., Gogtay, N., Giedd, J. N. (2011). How does your cortex grow? *The Journal of Neuroscience, 31*(19), 7174-7177.

Remer, J., Croteau-Chonka, E., Dean III, D. C., D'Arpino, S., Dirks, H., Whiley, D., & Deoni, S. C. (2017). Quantifying cortical development in typically developing toddlers and young children, 1–6 years of age. *Neuroimage*, *153*, 246-261.

Reuter, M., Rosas, H. D., & Fischl, B. (2010). Highly accurate inverse consistent registration: a robust approach. *Neuroimage*, *53*(4), 1181-1196.

Reuter, M., & Fischl, B. (2011). Avoiding asymmetry-induced bias in longitudinal image processing. *Neuroimage*, *57*(1), 19-21.

Reuter, M., Schmansky, N. J., Rosas, H. D., & Fischl, B. (2012). Within-subject template estimation for unbiased longitudinal image analysis.*Neuroimage, 61*(4), 1402-1418.

Rice, D., Barone Jr, S. (2000). Critical periods of vulnerability for the developing nervous system: evidence from humans and animal models. *Environmental health perspectives*, *108*(suppl 3), 511-533.

Richards, C. L., Malouin, F. (2013). Cerebral palsy: definition, assessment and rehabilitation. In *Handbook of clinical neurology* (Vol. 111, pp. 183-195). Elsevier.

Richman, D. P., Stewart, R. M., Hutchinson, J. W., Caviness, V. S. (1975). Mechanical model of brain convolutional development. *Science*, *189*(4196), 18-21

Robb, R. A., & Hanson, D. P. (1991). A software system for interactive and quantitative visualization of multidimensional biomedical images. Australasian physical & engineering sciences in medicine/supported by the Australasian College of Physical Scientists in Medicine and the Australasian Association of Physical Sciences in Medicine, 14(1), 9-30.

Robertson, K., Liner, J., & Meeker, R. B. (2012). Antiretroviral neurotoxicity. *Journal of neurovirology*, *18*(5), 388-399.

Robertson, F. C., Holmes, M. J., Cotton, M. F., Dobbels, E., Little, F., Laughton, B., Van Der Kouwe, A.J., Meintjes, E. M. (2018). Perinatal HIV Infection or Exposure is Associated with Low N-acetylaspartate and Glutamate in Basal Ganglia at age 9 but not 7 Years. *Frontiers in human neuroscience*, *12*, 145.

Rodionov, R., Chupin, M., Williams, E., Hammers, A., Kesavadas, C., & Lemieux, L. (2009). Evaluation of atlas-based segmentation of hippocampi in healthy humans. *Magnetic resonance imaging*, *27*(8), 1104-1109.

Rogers, B. P., Sheffield, J. M., Luksik, A. S., Heckers, S. (2012). Systematic error in hippocampal volume asymmetry measurement is minimal with a manual segmentation protocol. *Frontiers in neuroscience*, *6*, 179.

RStudio Team (2016). RStudio: Integrated Development for R. RStudio, Inc., Boston, MA URL http://www.rstudio.com/.

Sabuncu, M. R., Yeo, B. T., Van Leemput, K., Fischl, B., Golland, P. (2010). A generative model for image segmentation based on label fusion. *IEEE transactions on medical imaging*, *29*(10), 1714-1729.

Sainz, T., Serrano-Villar, S., Díaz, L., Tomé, M. I. G., Gurbindo, M. D., de José, M. I., Mellado, M.J., Ramos, J.T., Zamora, J., Moreno, S., Muñoz-Fernández, M. Á. (2013). The CD4/CD8 ratio as a marker T-cell activation, senescence and activation/exhaustion in treated HIV-infected children and young adults. *Aids*, *27*(9), 1513-1516.

Sánchez-Benavides, G., Gómez-Ansón, B., Sainz, A., Vives, Y., Delfino, M., & Peña-Casanova, J. (2010). Manual validation of FreeSurfer's automated hippocampal segmentation in normal aging, mild cognitive impairment, and Alzheimer Disease subjects. *Psychiatry Research: Neuroimaging*, *181*(3), 219-225.

Santos E., Noggle C.A. (2011) Synaptic Pruning. In: Goldstein S., Naglieri J.A. (eds) Encyclopedia of Child Behavior and Development. Springer, Boston, MA.

Sarma, M. K., Nagarajan, R., Keller, M. A., Kumar, R., Nielsen-Saines, K., Michalik, D. E., Deville, J., Church, J.A., Thomas, M. A. (2014). Regional brain gray and white matter changes in perinatally HIV-infected adolescents. *NeuroImage: Clinical*, *4*, 29-34.

Sasabayashi, D., Takayanagi, Y., Nishiyama, S., Takahashi, T., Furuichi, A., Kido, M., Nishikawa, Y., Nakamura, M., Noguchi, K., Suzuki, M. (2017). Increased frontal gyrification negatively correlates with executive function in patients with first-episode schizophrenia. *Cerebral Cortex*, *27*(4), 2686-2694.

Schaer, M., Schmitt, J. E., Glaser, B., Lazeyras, F., Delavelle, J., & Eliez, S. (2006). Abnormal patterns of cortical gyrification in velo-cardio-facial syndrome (deletion 22q11. 2): an MRI study. *Psychiatry Research: Neuroimaging*, *146*(1), 1-11.

Schaer, M., Cuadra, M. B., Tamarit, L., Lazeyras, F., Eliez, S., & Thiran, J. (2008). A surface-based approach to quantify local cortical gyrification. *Medical Imaging, IEEE Transactions on*, *27*(2), 161-170.

Schaer M, Cuadra MB, Schmansky N, Fischl B, Thiran JP, Eliez S. (2012). How to Measure Cortical Folding from MR Images: a Step-by-Step Tutorial to Compute Local Gyrification Index. Journal of Visualized Experiments : JoVE, (59):3417. https://doi.org/10.3791/3417

Schafer, D. P., Lehrman, E. K., Kautzman, A. G., Koyama, R., Mardinly, A. R., Yamasaki, R., Ransohoff, R.M, Greenberg, M.E, Barres, B.A, Stevens, B. (2012). Microglia sculpt postnatal neural circuits in an activity and complement-dependent manner. *Neuron*, *74*(4), 691-705.

Schoemaker, D., Buss, C., Head, K., Sandman, C. A., Davis, E. P., Chakravarty, M. M., Gauthier, S., Pruessner, J. C. (2016). Hippocampus and amygdala volumes from magnetic resonance images in children: Assessing accuracy of FreeSurfer and FSL against manual segmentation. *NeuroImage*, *129*, 1-14.

Shah, A., Gangwani, M. R., Chaudhari, N. S., Glazyrin, A., Bhat, H. K., & Kumar, A. (2016). Neurotoxicity in the post-HAART era: caution for the antiretroviral therapeutics. *Neurotoxicity research*, *30*(4), 677-697.

Sharland, M., &Handforth, J. (2005). Pediatric HIV infection. *Medicine*, *33*(6), 28-29. doi: http://dx.doi.org/10.1383/medc.33.6.28.66013.

Shaw, P., Greenstein, D., Lerch, J., Clasen, L., Lenroot, R., Gogtay, N., Evans, A., Rapoport, J., Giedd, J. (2006). Intellectual ability and cortical development in children and adolescents. *Nature*, *440*(7084), 676-679.

Shaw, P., Kabani, N. J., Lerch, J. P., Eckstrand, K., Lenroot, R., Gogtay, N., Greenstein, D., Clasen, L., Evans, A., Rapoport, J.L., Giedd, J. N., Wise, S.P. (2008). Neurodevelopmental trajectories of the human cerebral cortex. *The Journal of Neuroscience*, *28*(14), 3586-3594.

Shaw, M. E., Sachdev, P. S., Anstey, K. J., & Cherbuin, N. (2016). Age-related cortical thinning in cognitively healthy individuals in their 60s: the PATH Through Life study. *Neurobiology of aging*, *39*, 202-209.

Sherr, L., Croome, N., Castaneda, K. P., Bradshaw, K., & Romero, R. H. (2014). Developmental challenges in HIV infected children—An updated systematic review. *Children and Youth Services Review*, *45*, 74-89.

Shiohama. T, Levman .J, Baumer .N, Takahashi .E. (2019). Structural Magnetic Resonance Imaging-Based Brain Morphology Study in Infants and Toddlers with Down Syndrome: The Effect of Comorbidities. Pediatric Neurology ISSN 0887-8994, https://doi.org/10.1016/j.pediatrneurol.2019.03.015.

Shrout, P. E., & Fleiss, J. L. (1979). Intraclass correlations: uses in assessing rater reliability. *Psychological bulletin*, *86*(2), 420.

Slyker, J. A., Lohman-Payne, B. L., John-Stewart, G. C., Maleche-Obimboc, E., Emery, S., Richardson, B., Dong, T., Iversen, A.K., Mbori-Ngacha, D., Overbaugh, J, Emery, V. C. (2009). Acute cytomegalovirus infection in Kenyan HIV-infected infants. *AIDS (London, England)*, *23*(16), 2173.

Smith, H. (2014). Paediatric antiretroviral guidelines at a glance. *SA Pharmaceutical Journal*, *81*(2), 22-25

Sowell, E. R., Trauner, D. A., Gamst, A., & Jernigan, T. L. (2002). Development of cortical and subcortical brain structures in childhood and adolescence: a structural MRI study. *Developmental Medicine & Child Neurology*, *44*(01), 4-16.

Sowell, E. R., Peterson, B. S., Thompson, P. M., Welcome, S. E., Henkenius, A. L., Toga, A. W. (2003). Mapping cortical change across the human life span. *Nature neuroscience*, *6*(3), 309.

Sowell, E. R., Thompson, P. M., Leonard, C. M., Welcome, S. E., Kan, E., Toga, A. W. (2004). Longitudinal mapping of cortical thickness and brain growth in normal children. *Journal of Neuroscience*, *24*(38), 8223-8231.

Spies, G., Ahmed-Leitao, F., Fennema-Notestine, C., Cherner, M., & Seedat, S. (2015). Effects of HIV and childhood trauma on brain morphometry and neurocognitive function. *Journal of neurovirology*, 1-10.

Spudich, S. S., &Ances, B. M. (2012). Neurologic complications of HIV infection. *TopAntiviral Med*, *20*, 41-47.

Steinbrink, F., Evers, S., Buerke, B., Young, P., Arendt, G., Koutsilieri, E.,Husstedt, I. (2013). Cognitive impairment in HIV infection is associated with MRI and CSF pattern of neurodegeneration. *European Journal of Neurology: The Official Journal of the European Federation of Neurological Societies, 20*(3), 420-428. doi:10.1111/ene.12006.

Su, S., White, T., Schmidt, M., Kao, C. Y., Sapiro, G. (2013). Geometric computation of human gyrification indexes from magnetic resonance images. *Human brain mapping*, *34*(5), 1230-1244.

Szekely, G., Kelemen, A., Brechbuhler, C., & Gerig, G. (1996). Segmentation of 2-D and 3-D objects from MRI volume data using constrained elastic deformations of flexible Fourier contour and surface models. *Medical Image Analysis*, *1*(1), 19-34.

Tamnes, C. K., Walhovd, K. B., Dale, A. M., Østby, Y., Grydeland, H., Richardson, G., Westlye, L.T., Roddey, J.C., Hagler Jr, D.J., Due-Tønnessen, P., Holland, D. (2013). Brain development and aging: overlapping and unique patterns of change. Neuroimage, 68, 63-74.

Tamnes, C. K., Herting, M. M., Goddings, A. L., Meuwese, R., Blakemore, S. J., Dahl, R. E., Güroğlu, B., Raznahan, A., Sowell, E.R., Crone, E.A. Mills, K. L. (2017). Development of the cerebral cortex across adolescence: a multisample study of inter-related longitudinal changes in cortical volume, surface area, and thickness. *Journal of Neuroscience*, *37*(12), 3402-3412.

Tardieu, M., Le Chenadec, J., Persoz, A., Meyer, L., Blanche, S., &Mayaux, M. J. (2000). HIV-1-related encephalopathy in infants compared with children and adults. french pediatric HIV infection study and the SEROCO group. *Neurology*, *54*(5), 1089-1095.

[a]Thompson, P. M., Dutton, R. A., Hayashi, K. M., Toga, A. W., Lopez, O. L., Aizenstein, H. J., & Becker, J. T. (2005). Thinning of the cerebral cortex visualized in HIV/AIDS reflects CD4+ T lymphocyte decline. *Proceedings of the National Academy of Sciences*, *102*(43), 15647-15652

[b]Thompson, P. M., Lee, A. D., Dutton, R. A., Geaga, J. A., Hayashi, K. M., Eckert, M. A., Bellugi, U., Galaburda, A.M., Korenberg, J.R., Mills, D.L., Toga, A. W., Reiss, A.L. (2005). Abnormal cortical complexity and thickness profiles mapped in Williams syndrome. *The Journal of Neuroscience*, *25*(16), 4146-4158

Thompson, P. M., Dutton, R. A., Hayashi, K. M., Lu, A., Lee, S. E., Lee, J. Y., Lopez, O.L., Aizenstein, H.J., Toga, A.W., Becker, J. T. (2006). 3D mapping of ventricular and corpus callosum abnormalities in HIV/AIDS. *Neuroimage*, *31*(1), 12-23.

Thurnher, M. M., Schindler, E. G., Thurnher, S. A., Pernerstorfer-Schön, H., Kleibl-Popov, C., &Rieger, A. (2000). Highly active antiretroviral therapy for patients with AIDS dementia complex: Effect on MR imaging findings and clinical course. *American Journal of Neuroradiology*, *21*(4), 670-678.

Toich, J. T., Taylor, P. A., Holmes, M. J., Gohel, S., Cotton, M. F., Dobbels, E., Laughton, B., Little, F., Van Der Kouwe, A.J., Biswal, B., Meintjes, E. M. (2018). Functional Connectivity Alterations between Networks and Associations with Infant Immune Health within Networks in HIV Infected Children on Early Treatment: A Study at 7 Years. Frontiers in human neuroscience, 11, 635.

Treble. A, Juranek.J, Stuebing.K.K, Dennis.M, Fletcher.J.M (2013). Functional Significance of A typical Cortical Organization in Spina Bifida Myelomeningocele: Relations of Cortical Thickness and Gyrification with IQ and Fine Motor Dexterity. Cerebral Cortex Vol. 23 No. 10 pp.2357–2369.

Trickey, A., May, M. T., Schommers, P., Tate, J., Ingle, S. M., Guest, J. L., Gill, M.J., Zangerle, R., Saag, M., Reiss, P., Monforte, A. D. A. (2017). CD4: CD8 Ratio and CD8 Count as Prognostic Markers for Mortality in Human Immunodeficiency Virus–Infected Patients on Antiretroviral Therapy: The Antiretroviral Therapy Cohort Collaboration (ART-CC). *Clinical Infectious Diseases*, *65*(6), 959-966.

Tubiana, R., Ghosn, J., De-Sa, M., Wirden, M., Gautheret-Dejean, A., Bricaire, F., Katlama, C. (2002). Warning: antiretroviral treatment interruption could lead to an increased risk of HIV transmission. *Aids*, *16*(7), 1083-1084.

Tucker, K. A., Robertson, K. R., Lin, W., Smith, J. K., An, H., Chen, Y., Hall, C. D. (2004). Neuroimaging in human immunodeficiency virus infection. *Journal of Neuroimmunology, 157*(1–2), 153-162. Doi : http://dx.doi.org/10.1016/j.jneuroim.2004.08.036.

Uban, K. A., Herting, M. M., Williams, P. L., Ajmera, T., Gautam, P., Yanling, H., Nichols, S. L. (2015). White matter microstructure among youth with perinatally acquired HIV is associated with disease severity. *AIDS (London, England), 29*(9), 1035.

Uban, K. A., Herting, M. M., Williams, P. L., Ajmera, T., Gautam, P., Yanling, H., Malee, K.M., Yogev, R., Csernansky, J.G., Wang, L., Nichols, S. L. (2015). White matter microstructure among youth with perinatally acquired HIV is associated with disease severity. *AIDS (London, England)*, *29*(9), 1035.

UNAIDS (2017). UNAIDS data 2017 – Retrieved from http://www.unaids.org/sites/default/files/media_asset/20170720_Data_book_2017_en.pdf Accessed 14 September, 2018

UNAIDS (2018). Global HIV & AIDS statistics – 2018 fact sheet. Retrieved from http://www.unaids.org/en/resources/fact-sheet. Accessed 14 September 2018

Underwood, J., Cole, J. H., Caan, M., De Francesco, D., Leech, R., van Zoest, R. A., Su, T., Geurtsen, G.J., Schmand, B.A., Portegies, P, Prins, M. (2017). Gray and white matter abnormalities in treated human immunodeficiency virus disease and their relationship to cognitive function. *Clinical Infectious Diseases, 65*(3), 422-432.

U.S Department of Health and Human Services (USDHHS) (2017). The Global HIV/AIDS epidemic. Retrieved from https://www.hiv.gov/hiv-basics/overview/data-and-trends/global-statistics. Accessed 14 September 2018

Van Arnhem, L. A., Bunders, M. J., Scherpbier, H. J., Majoie, C. B., Reneman, L., Frinking, O., Kuijpers, T.W., Pajkrt, D. (2013). Neurologic abnormalities in HIV-1 infected children in the era of combination antiretroviral therapy. *PLoS One*, *8*(5), e64398.

Vance, D. E., Fazeli, P. L., & Gakumo, C. A. (2013). The impact of neuropsychological performance on everyday functioning between older and younger adults with and without HIV. *Journal of the Association of Nurses in AIDS Care*, *24*(2), 112-125.

Van den Hof, M., ter Haar, A. M., Scherpbier, H. J., van der Lee, J. H., Reiss, P., Wit, F. W., Oostrom, K.J., Pajkrt, D. (2019). Neurocognitive development in perinatally HIV-infected adolescents on long-term treatment compared to healthy matched controls: a longitudinal study. *Clinical Infectious Diseases*.

Van der Kouwe, A.J., Benner, T., Salat, D.H., Fischl, B. (2008). Brain morphometry with multiecho MPRAGE. Neuroimage 40(2):559-569.

Van Essen, D. C. (1997). A tension-based theory of morphogenesis and compact wiring in the central nervous system. *Nature, 385*(6614), 313.

Van Rie, A., Harrington, P. R., Dow, A., & Robertson, K. (2007). Neurologic and neurodevelopmental manifestations of pediatric HIV/AIDS: A global perspective. *European Journal of Pediatric Neurology, 11*(1), 1-9. doi: http://dx.doi.org/10.1016/j.ejpn.2006.10.006.

Violari, A., Cotton, M. F., Gibb, D. M., Babiker, A. G., Steyn, J., Madhi, S. A., Jean-Philippe, P., McIntyre, J. A. (2008). Early antiretroviral therapy and mortality among HIV-infected infants. *New England Journal of Medicine*, *359*(21), 2233-2244.

Wachsler-Felder, J., & Golden, C. J. (2002). Neuropsychological consequences of HIV in children: A review of current literature. *Clinical Psychology Review*, *22*(3), 443-464.

Wade, B. S., Valcour, V. G., Puthanakit, T., Saremi, A., Gutman, B. A., Nir, T. M., Watson C, Aurpibul L, Kosalaraksa P, Ounchanum P, Kerr, S. (2019). Mapping abnormal subcortical neurodevelopment in a cohort of Thai children with HIV. *NeuroImage: Clinical*, *23*, 101810.
Wallace, G. L., Robustelli, B., Dankner, N., Kenworthy, L., Giedd, J. N., & Martin, A. (2013). Increased gyrification, but comparable surface area in adolescents with autism spectrum disorders. *Brain*, *136*(6), 1956-1967.

Wamalwa, D., Benki-Nugent, S., Langat, A., Tapia, K., Ngugi, E., Moraa, H., Maleche-Obimbo E, Otieno V, Inwani I, Richardson BA, Chohan B. (2016). Treatment interruption after 2-year antiretroviral treatment initiated during acute/early HIV in infancy. *AIDS*, *30*(15), 2303-2313.

Weber, V., Radeloff, D., Reimers, B., Salzmann-Manrique, E., Bader, P., Schwabe, D., Königs, C. (2017). Neurocognitive development in HIV-positive children is correlated with plasma viral loads in early childhood. *Medicine*, *96*(23).

Weishaupt, D., Froehlich, J. M., Nanz, D., Köchli, V. D., Pruessmann, K. P., & Marincek, B. (2008). *How does MRI work?: an introduction to the physics and function of magnetic resonance imaging*. Springer.

Weiss, B., & Landrigan, P. J. (2000). The developing brain and the environment: an introduction. *Environmental health perspectives*, *108*(Suppl 3), 373.

Weissenhorn, W., Dessen, A., Harrison, S. C., Skehel, J. J., & Wiley, D. C. (1997). Atomic structure of the ectodomain from HIV-1 gp41. *Nature*, *387*(6631), 426.

Weller, I. V., & Williams, I. G. (2001). ABC of AIDS: Antiretroviral drugs. *BMJ: British Medical Journal*, *322*(7299), 1410.

Wenger, E., Mårtensson, J., Noack, H., Bodammer, N. C., Kühn, S., Schaefer, S., Heinze, H,J., Duzel, E., Backman, L., Lindenberger, U., Lövdén, M. (2014). Comparing manual and automatic segmentation of hippocampal volumes: reliability and validity issues in younger and older brains. *Human brain mapping*, *35*(8), 4236-4248.

White, T., Andreasen, N. C., Nopoulos, P., & Magnotta, V. (2003). Gyrification abnormalities in childhood-and adolescent-onset schizophrenia. *Biological psychiatry*, *54*(4), 418-426.

White, T., Su, S., Schmidt, M., Kao, C. Y., & Sapiro, G. (2010). The development of gyrification in childhood and adolescence. *Brain and cognition*, *72*(1), 36-45.

Wierenga, L., Langen, M., Ambrosino, S., van Dijk, S., Oranje, B., & Durston, S. (2014). Typical development of basal ganglia, hippocampus, amygdala and cerebellum from age 7 to 24. *Neuroimage*, *96*, 67-72.

Wierenga, L. M., Sexton, J. A., Laake, P., Giedd, J. N., & Tamnes, C. K. (2017). A key characteristic of sex differences in the developing brain: greater variability in brain structure of boys than girls. *Cerebral Cortex*, 1-11.

Wiley, C. A., Masliah, E., Morey, M., Lemere, C., DeTeresa, R., Grafe, M., Hansen, L., Terry, R. (1991). Neocortical damage during HIV infection. *Annals of neurology*, *29*(6), 651-657.

Wilke, M., Sohn, J. H., Byars, A. W., & Holland, S. K. (2003). Bright spots: correlations of gray matter volume with IQ in a normal pediatric population.*Neuroimage*, *20*(1), 202-215.

Woods, R. P. (2003). Multitracer: a Java-based tool for anatomic delineation of grayscale volumetric images. *Neuroimage*, *19*(4), 1829-1834.

World Health Organization (WHO) 2006 Antiretroviral therapy of HIV infection in infants and children in resource-limited settings: towards universal access. Recommendations for a public health approach. Retrieved from http://www.who.int/hiv/pub/guidelines/WHOpaediatric.pdf. Accessed 12 October, 2017

World Health Organization (WHO) (2008) Report of the WHO Technical Reference Group. Paediatric HIV/ART Care Guideline Group Meeting In, WHO Headquarter, Geneva, Switzerland

World Health Organization. (2013). Consolidated guidelines on the use of antiretroviral drugs for treating and preventing HIV infection. Retrieved from http://www.who.int/hiv/pub/guidelines/ arv2013/download/en/

World Health Organization. (2015a). Antiretroviral therapy. Retrieved from http://www.who.int/ topics/antiretroviral_therapy/en/

World Health Organization. (2015b). Treatment of children living with HIV. Retrieved from http:// www.who.int/hiv/topics/paediatric/hiv-paediatric-infopage/en/

World Health Organization (WHO) (2018). HIV/AIDS. Retrieved from http://www.who.int/en/news-room/fact-sheets/detail/hiv-aids. Accessed 14 September, 2018

Working Group on Antiretroviral Therapy and Medical Management of HIV-Infected Children: 2008 Guidelines for the Use of Antiretroviral Agents in Paediatric HIV Infection (ART Guideline 2008) pp. 1–126

Wright, P. W., Pyakurel, A., Vaida, F. F., Price, R. W., Lee, E., Peterson, J., Fuchs, D., Zetterberg, H., Robertson, K.R., Walter, R., Meyerhoff, D. J. (2016). Putamen volume and its clinical and neurological correlates in primary HIV infection. *AIDS (London, England)*, *30*(11), 1789.

Yadav, S. K., Gupta, R. K., Garg, R. K., Venkatesh, V., Gupta, P. K., Singh, A. K., Hashem, S., Al-Sulaiti, A., Kaura, D., Wang, E., Marincola, F. M. (2017). Altered structural brain changes and neurocognitive performance in pediatric HIV. NeuroImage: Clinical, 14, 316-322.

Yu, X., & Gao, L. (2019). Neuroanatomical Changes Underlying Vertical HIV Infection in Adolescents. *Frontiers in immunology*, *10*, 814.

Zhang, Y., Zhou, Y., Yu, C., Lin, L., Li, C., & Jiang, T. (2010). Reduced cortical folding in mental retardation. *American Journal of Neuroradiology*,*31*(6), 1063-1067.

Zilles, K., Armstrong, E., Schleicher, A., & Kretschmann, H. J. (1988). The human pattern of gyrification in the cerebral cortex. *Anatomy and embryology*, *179*(2), 173-179

Zhou, D., Lebel, C., Evans, A., Beaulieu, C. (2013). Cortical thickness asymmetry from childhood to older adulthood. *Neuroimage*, *83*, 66-74.